α-Synuclein Interaction with Membranes

Imola G. Zigoneanu

A dissertation submitted to the faculty of the University of North Carolina at Chapel Hill in partial fulfillment of the requirements for the degree of Doctorate of Philosophy in the Department of Chemistry.

Chapel Hill

2011

Approved by:

Professor Gary J. Pielak, Ph.D.

Professor Joseph M. DeSimone, Ph.D.

Professor Mathew M. Redinbo, Ph.D.

Professor Linda L. Spremulli, Ph.D.

Professor Nancy L. Thompson, Ph.D.

Abstract

IMOLA G. ZIGONEANU: α-Synuclein Interaction with Membranes
(Under the direction of Professor Gary J. Pielak, Ph.D.)

The association of α-synuclein with membranes appears to be an important factor in Parkinson's disease. My dissertation research was focused on understanding the interactions of the protein with artificial membranes, the extracellular plasma membrane, and intracellular membranes. Fluorescence and nuclear magnetic resonance spectroscopy were used to monitor these interactions. Large unillamelar vesicles with a composition similar to mitochondrial membranes were studied. Cardiolipin, present mainly in the inner mitochondrial membrane, is key for protein binding, and reducing the amount of cardiolipin decreases binding. The nature of cardiolipin's acyl chains is also important; cardiolipin with chains containing one double bond interact more strongly than those with chains having two double bonds or saturated acyl chains. This finding is physiologically relevant for Parkinson's disease because cardiolipin containing fatty acids with one double bond are the most abundant phospholipid in the brain. The affinity of α-synuclein for plasma membrane was tested, and only N-terminal region of the protein binds. Also, ^{19}F NMR proved useful for monitoring the interactions of proteins and fused peptide-proteins with the plasma membrane. Information on protein interactions with intracellular

membranes reveals that the N-terminal region may be cleaved in cells, but further studies are needed to confirm this idea.

Dedication

To my family:

Thank you for being near me when nobody else was.

Aknowledgements

Many people helped me on this pathway and I want to thank them. I want to thank to Dr. Gary Pielak for accepting me in his group and for giving me the opportunity to go to conferences where I had the chance to meet peers and discuss interesting ideas. My colleagues in the Pielak's lab were very good at giving feedback and sharing their knowledge with me, especially Drs. Lisa Charlton, Rebecca Ruf, and Kristin Slade who helped me at the beginning of my graduate school at UNC. I want to thank my two brilliant, hard-working, and smart undergraduate students, Ms.Yuri Yang and Mr. Alex Krois, for their help and challenging questions. Dr. Linda Spremulli, an outstanding faculty, a great instructor, and most of all she cares about the students. Thank you for being part of my PhD experience. I want to thank Dr. Mathew Redinbo for his feedback and for encouraging me to trust and try my ideas and Dr. Joseph DeSimone for his advice. I want to thank Dr. Nancy Thompson for her advice on fluorescence and binding experiments and for providing me a quiet and warm environment. Dr. Emdadul Haque and Punya Navaratnarajah helped me with preparation of lipid vesicles and data interpretation and Dr. Ashutosh Tripathy with data collection. I want to thank Dr. Marc ter Horst for teaching me NMR and Dr. Michael Chua for training me with confocal microscopy. I want to thank to my family for their unlimited moral support and encouragement.

TABLE OF CONTENTS

List of Tables

Chapter 2

List of Figures

Chapter 2

Chapter 3

Chapter 4

List of Abbreviations and Symbols

AF488	Alexa Fluor 488
amp	ampicillin
C	Celsius
CH	Cholesterol
CHO-K1	Chinese hamster ovary
CI2	chymotrypsin inhibitor 2
CL	Cardiolipin
cm	centimeter
CTP	cytoplasmic transduction peptide
Da	Dalton
DMEM	Dulbecco's Modified Eagle Medium
DOPC	1,2-dioleoyl-*sn*-glycero-3-phosphocholine
DOPE	1,2-dioleoyl-*sn*-glycero-3-phosphoethanolamine
DPH	1,6-diphenyl-1,3,5-hexatriene
DTT	dithiothreitol
E. coli	*Escherichia coli*
EDTA	ethylenediaminetetraacetic acid
FBS	fetal bovine serum

3FY	3-fluoro-*L*-tyrosine
g	standard gravity
GFP	green fluorescent protein
h	hour
HeLa	Human epithelial carcinoma cells
HSQC	heteronuclear single quantum correlation
IPTG	isopropyl β-D-1-thiogalactopyranoside
K_d	dissociation constant
kDa	kilodalton
L	liter
LB	Luria broth
LUV	large unilamellar vesicle
M	molar
MALDI/MS	matrix-assisted laser desorption/ionization mass spectrometry
MHz	megahertz
min	minute
mg	milligram
mL	milliliter
mM	millimolar
MWCO	molecular weight cut off
NAC	non amyloid component
nm	nanometer
NMR	nuclear magnetic resonance

OD	optical density
PAGE	polyacrylamide gel electrophoresis
PBS	phosphate buffer saline
PCR	polymerase chain reaction
PDI	polydispersity index
PMSF	phenylmethylsulphonyl fluoride
rpm	revolutions per minute
RT	room temperature
SDS	sodium dodecyl sulfate
SDS-PAGE	sodium dodecyl sulfate polyacrylamide gel electrophoresis
T	temperature
TAT	trans-acting activator of transcription
TM CL	1',3'-Bis[1,2-dimyristoyl-*sn*-glycero-3-phospho]-*sn*-glycerol
TO CL	1',3'-bis[1,2-dioleoyl-*sn*-glycero-3-phospho]-*sn*-glycerol
Tris	trishydroxymethylaminomethane
v/v	volume/volume
w/v	weight/volume
X. laevis	*Xenopus laevis*
α-syn	α-synuclein
µg	microgram
µL	microliter

CHAPTER 1

Introduction

1.1 Parkinson's Disease

Parkinson's disease is the second most common progressive neurological disorder [1, 2] affecting more than 500,000 people in United States with more than 50,000 new cases reported annually [3]. Its symptoms include rest tremor, bradykinesia, rigidity and loss of postural reflexes [4]. The disease is more prevalent in subjects older than 50, with the symptoms progressing more quickly in some individuals [3, 5].

Parkinson's disease is caused by the loss of dopaminergic neurons within the *substantia nigra pars compacta* [6-8]. The disease is also characterized by the presence of Lewy bodies in the cytoplasm of neurons in the *substantia nigra*. Lewy bodies are pathological inclusions of 5-25 μm in diameter [9] having α-synuclein as a primary component [9-12]. Parkinson's disease is diagnosed only based on clinical symptoms; no single laboratory test exists. The factors that are believed to cause the disease (because they induce Parkinson's symptoms in

animal models) are: environmental [13-18], genetic [19, 20], and age-related [5, 21].

1.2 α-Synuclein

α-Synuclein is an intrinsically-disordered protein found in the presynaptic nerve terminals [22-28]. The 140-residue protein comprises a positively-charged N-terminus, a hydrophobic middle region, and a negatively charged C-terminus [29-31]. In its monomeric form, α-synuclein is natively unfolded but can assume a β-sheet character or α-helical structure depending on the solution conditions [32-34]. Also, α-synuclein forms protofibrils [35, 36] and fibrils [37, 38] that are toxic for the neurons.

The N-terminal region of α-synuclein forms an α-helix upon interaction with vesicles of different lipid composition [39], phospholipid headgroups [40], sizes [41], and surfaces [42, 43]. It is known that the protein has a higher affinity for small unilamellar vesicles than for large unilamellar vesicles (LUVs), and that the protein binds more strongly to vesicles containing anionic phospholipids [39, 40, 44, 45].

Two α-synuclein variants, A30P and A53T, associated with Parkinson's disease have been identified [46]. *In vitro* studies confirm that fibrils form at an increased rate for these mutants compared to wild-type α-synuclein, revealing the importance of these α-synuclein mutations in protein aggregation [6]. α-Synuclein is suspected to have multiple functions including roles in neurotransmitter release [47], mitochondrial dysfunction [48-50], and aging [51].

A recent study shows that α-synuclein is implicated in SNARE-complex assembly at presynaptic vesicles via its C-terminal region while its N-terminal region is anchored to the vesicle [47]. The protein is involved in synaptic activity when the nerve terminals repeatedly release neurotransmitters necessary for assembly and disassembly of the complex. However, another recent study, shows that α-synuclein isolated under non-denaturing conditions from brain tissue and human cells is a partly-folded tetramer that is more resistant to aggregation as compared to monomeric α-synuclein [52]. These recent findings are important to gain insight into α-synuclein intracellular functions and represent steps forward in elucidating the biochemistry of Parkinson's disease. They also indicate that a complete understanding of α-synuclein structure and functions and how these properties relate to the disease need to be studied in the future.

1.3 Delivery Systems

Several peptides have been designed to cross the plasma membrane of different cell types. Among these, the PEP family of amphipathic carriers have been used to transport proteins and peptides [53, 54], antibodies [54], and nucleic acids [55-57] into higher eukaryotic cells. The main component of this class is the peptide, PEP-1 (Ac-KETWWETWWTEWSQPKKKRKV-Cya). This peptide comprises a hydrophobic tryptophan-rich domain that interacts with the cargo, a hydrophilic lysine-rich domain designed to improve intracellular delivery and increase the solubility of the peptide, and a linker between the two domains (SQP) [54]. The peptide has a cysteamine at its C-terminus, which improves the PEP-1 interaction with the lipid membrane [58]. PEP-1 forms a complex with the

cargo through non-covalent interactions. This complex is efficiently translocated in a large number of cell lines [54]. The mechanism of PEP-1 translocation with its cargo into higher eukaryotic cells is not well understood [59, 60]. Morris et al. proved, using scanning electron microscopy and dynamic light scattering, that PEP-1 forms nanoparticles with the cargo [61]. The particle's size and morphology is unaffected by the size of cargo, but the molar ratio of PEP-1 to cargo has an important role in defining these parameters. After translocation, the PEP-1/cargo complex rapidly dissociates in the cytoplasm, the peptide localizing mostly in the nucleus while the cargo's intracellular localization remains unaffected (if the cargo's function is in the cytosol than it remains there) [54]. PEP-1/cargo nanoparticles enter cells independently of the endosomal pathway and deliver the cargo efficiently in a fully biological active form to a wide range of cell lines [53, 54]. An important criterion for designing a delivery system is the toxicity of the carrier. PEP-1 was tested on different cell lines, and no toxicity was observed for concentrations of peptide of 100 μM [54].

Another common method of protein translocation involves making genes that fuse the peptide to the cargo protein and expressing the construct in *Escherichia coli*. One popular peptide is the trans-acting activator of transcription (TAT) from the human immunodeficiency virus (HIV-1). This peptide has been used to deliver proteins [62], oligonucleotides [63, 64], liposomes [65], and nanoparticles [66]. TAT targets the cargo to the nucleus [67]. A more efficient peptide developed by Kim et al. [68], is designed to translocate important amounts of cargo into the cytosol. A series of sequences were designed and

tested on live cells. The sequence YGR_2AR_6 proved to be the most efficient in translocating β-galactosidase into several cell lines. After transduction, the peptide is cleaved in the cells by cytoplasmic enzymes and the cargo is released [68]. PEP-1 and the YGR_2AR_6 peptide were selected to translocate α-synuclein into higher eukaryotic cells. These peptides were chosen because of their ability to translocate large amounts of cargo into the cells and because of their capability to release the cargo into the cytosol.

1.4 In-cell NMR

1.4.1 In-cell NMR in E. coli

1.4.1.1 Protein-Protein Interactions and Signal Transduction

In-cell NMR spectroscopy characterizes one protein at a time while a more interesting and valuable aspect would be to characterize the whole complex by enriching all the proteins in the complex with one of the NMR active nuclei. Unfortunately, the resulted spectra would be too complicated to analyze. Shekhtman et al. [69] developed a method to study a protein in a complex by NMR. STINT-NMR (structural interactions using NMR) works by enriching only one protein in a complex and expressing it using the orthogonal induction system. Shekhtman et al. [69] overexpressed ubiquitin in ^{15}N-enriched media by using the pBAD promoter. Next, the cells were collected by centrifugation and resuspended in unenriched media. The PT7/lac system was used to express the other protein in the complex. The interactions between the two proteins were noted by changes in the width or chemical shift of the resonances of the enriched protein.

Protein phosphorylation can be studied using NMR. Shekhtman's laboratory used STINT-NMR to understand signal transduction by simultaneously expressing three proteins: the target protein (ubiquitin), a large (>100 kDa) heterodimeric affector complex, and a specific kinase [70]. The ubiquitin was expressed under three conditions: alone, with coexpression of the affector complex, and with coexpression of the complex and kinase. They determined the interactions between ubiquitin and the complex and phosphorylation of ubiquitin induced by expression of the kinase. Changes induced by phosphorylation can be sensed by ubiquitin even though the complex is large.

1.4.1.2 Intrinsically Disordered Proteins

Intrinsically disordered proteins lack stable tertiary structure in dilute solution. Many members of this recently defined class play important roles in cell signaling, regulation, and control. Disordered proteins are associated with disease states, including amyloidoses and neurodegenerative disorders [71]. Although the properties of globular proteins do not change significantly over a wide range of solution conditions, the properties of intrinsically disordered proteins can vary [72]. This sensitivity to solution conditions should make them attractive targets for studies of physiologically relevant conditions. Despite this sensitivity, and the known relationships between protein disorder and disease, little is known about the intracellular structure of this protein class. Disordered proteins are easier to detect by in-cell NMR than are globular proteins of the same size. This increased sensitivity arises from differences in global and local motions for globular and disordered proteins [73]. Because of their rigidity, the

relaxation rates for globular proteins are most sensitive to global motion, which is described by a single rotational correlation time. Disordered proteins, on the other hand, are flexible. Their motions involve an ensemble of interconverting conformers where different residues have different effective correlation times. That is, the flexible nature of disordered proteins mitigates the deleterious effect of viscosity on their spectra.

The first in-cell NMR study of an intrinsically disordered protein was reported by Dedmon et al. [74]. The protein, FlgM, regulates flagellar synthesis upon binding a transcription factor. The intracellular environment in *E. coli* causes the C-terminal half of FlgM to gain structure while the N-terminal half remains unstructured. Similar characteristics were noted in vitro in solutions containing high levels of glucose, bovine serum albumin (BSA), and ovalbumin. These data show that it is important to study disordered proteins under physiologically relevant conditions. α-Synuclein, a 140-residue cytosolic eukaryotic protein, is the primary component of the intracellular protein aggregates called Lewy bodies [73]. These aggregates are present in substantia nigra neurons of patients with Parkinson's disease. Studying α-synuclein under crowded conditions may provide information related to its role in the disease. McNulty et al. [75] used in-cell NMR to investigate the structure of α-synuclein in *E. coli*. These authors first noticed a difference between ^{1}H-^{15}N HSQC spectra in dilute solution acquired at 10 and 35 ℃ [76]. Spectra collected at the higher temperature presented fewer cross-peaks (~35) compared to spectra collected at 10 ℃ (~70). Experiments using an α-synuclein comprising only the first 100

residues showed that cross-peaks in the spectrum acquired at 35 ℃ are from the C-terminal third of the protein. This temperature dependent behavior was associated with an increase in hydrodynamic radius and a gain in the level of secondary structure at 35 ℃. These changes were reversible when the temperature was decreased to 10 ℃. The authors concluded that the N-terminal two-thirds of the protein exchanges between a more structured extended state and more disordered but more compact state. Heating the protein increases the rate of exchange between these states, causing the crosspeaks to disappear.

The in-cell spectrum of α-synuclein at 35 ℃ looks like the spectrum recorded at 10 ℃ in dilute solution. In vitro experiments in 300 g/L BSA yield spectra similar to those acquired from *E. coli* at 35 ℃. These observations give rise to the idea that crowding in these cells or in vitro keeps α-synuclein in a disordered but more compact state. These conclusions, however, have been questioned. Croke et al. [77] suggest the difference between the in-cell and dilute solution results reflects a mismatch in pH between the samples, which results in higher amide proton exchange rates and a concomitant loss of resonances at 35 ℃.

1.4.1.3 The effect of intracellular crowding on proteins

Li et al. [78] studied globular and disordered proteins in *E. coli*. Globular ^{15}N-enriched proteins cannot be detected in bacteria by using NMR. While ^{1}H-^{15}N HSQC spectra are not resolved in intact cells, the ^{19}F spectra can provide good information about intracellular dynamics of globular and disordered proteins. Small globular proteins (~10 kDa) labeled with 3-fluoro-L-tyrosine give resolved

spectra while larger size proteins (up to ~100 kDa) provide good spectra only when labeled with trifluoromethyl-L-phenylalanine.

Schlesinger et al. [79] studied the effect of *E. coli* cytosol on a variant of Protein L. The globular protein, Protein L (~7 kDa), is folded in cells and in dilute solution but the variant having seven lysine residues replaced by glutamic acids is mostly unfolded in dilute solution at room temperature. The Protein L variant is unfolded in cells suggesting that nonspecific interactions between cytoplasmic components are more important than the excluded-volume effect.

1.4.1.4 Determination of protein structure in E. coli

The structure of the heavy-metal binding protein TTHA1718 from *Thermus thermophilus* HB8 was determined *de novo* in *E. coli* [80]. This study represents one of the most important breakthroughs of the in-cell NMR in prokaryotic cells. The 3D NMR spectra were collected and the calculated structure reveals that the protein structure in *E. coli* is similar with the structure of the protein *in vitro*.

1.4.2 In-cell NMR in Higher Eukaryotic Cells

In-cell studies in *E. coli* will continue to provide fundamental information about crowding effects, but the medical relevance of higher eukaryotic cells makes them attractive targets for in-cell NMR. In addition, in-cell NMR in higher eukaryotic cells may be easier because the cytosol of eukaryotic cells seems to have a lower apparent viscosity [81].

The first in-cell NMR study of isotopically enriched proteins in nucleated higher eukaryotic cells was conducted in *Xenopus laevis* oocytes [82]. Their large size (~1 mm diameter) allows microinjection of isotopically enriched protein into

the cytosol. The B1 domain of streptococcal protein G (GB1) was expressed and ^{15}N-enriched in *E. coli*, purified, and injected into 200 oocytes. The authors studied a range of intracellular GB1 concentrations between 50 and 500 μM. The positions of the GB1 resonances in the HSQC spectra remained the same in dilute solution, in oocytes, and in solutions containing 250-300 mg/mL BSA, showing that neither crowding nor the environment in the cell changes the structure of GB1. Different behavior was observed, however, in terms of cross-peak intensity. Resonances of amides involved in intramolecular hydrogen bonds showed diminished intensity in cells and in BSA compared to dilute solution. This observation is consistent with the idea that more dynamic parts of the protein are less affected by the increased viscosity in cells [73]. Sakai et al. [83] studied protein behavior after microinjection of ^{15}N-enriched ubiquitin and calmodulin into *Xenopus* oocytes. The in-cell spectrum of wild-type ubiquitin presented fewer resonances compared to its *in vitro* spectrum. Mutations in the hydrophobic patch on the β-sheet of ubiquitin confirmed that the loss of the resonances is associated with interactions between ubiquitin and other proteins. Calmodulin spectra in oocytes presented two patterns correlated with the presence or absence of extracellular calcium ions. When calcium ions were coinjected with the calcium-free protein, the in-cell spectrum was characteristic of calcium-bound calmodulin, while the spectrum was characteristic of the calcium-free form if calcium was not coinjected. These observations show that the physiological intracellular calcium concentration (~0.1 μM) does not affect calcium-free calmodulin. We end this section with a note of caution. Oocytes are fragile, so

conditions that preserve them will facilitate longer acquisition times, thereby decreasing the amount of protein required for detection by NMR. Bodart et al. [84] showed that oocytes can be preserved by embedding them in a 20% Ficoll solution. The embedded cells remained intact for 20 h, allowing the detection of 5 *μ*M intracellular protein. Nevertheless, care must be taken to monitor protein leakage. Sakai et al. [85], working with enriched calmodulin and ubiquitin, have developed an oocyte coinjection method involving GFP that is useful for detecting leaks.

1.4.2.1 Phosphorylation in Higher Eukaryotic Cells

Selenko et al. [86] used NMR to detect phosphorylation of the viral SV40 T antigen in intact *X. laevis* oocytes by endogenous casein kinase 2 (CK2). CK2 phosphorylates two serine residues in the regulatory region of the T antigen, altering the nuclear-import properties of the full-length protein. These investigators provide the first NMR observation of an in vivo protein substrate phosphorylation event inside living cells by an endogenous protein kinase. Time-resolved NMR spectra in oocytes show sequential phosphorylation of the substrate. The investigators conclude that CK2 phosphorylation occurs in a two-step reaction with intermediate release of the substrate and preference of the kinase for the unphosphorylated substrate. The results obtained in oocytes agree with NMR spectra acquired in dilute solution and in egg extracts, implying that the kinetics of phosphorylation are not affected by macromolecular crowding. Phosphorylation of the intrinsically disordered protein tau in *X. laevis* oocytes has also been studied with NMR [84].

Bodart et al. [84] detected novel signals in the *in vivo* spectrum that they assigned to phosphorylated residues of tau. Comparison of the in-cell spectrum to the in vitro spectrum containing two known oocyte kinases revealed shifts in resonance positions. These shifts suggest that unidentified kinases in oocytes may alter the positions of resonances observed *in vitro*. This study provides the first analysis of an intrinsically disordered protein in live eukaryotic cells by in-cell NMR.

1.4.2.2 In-cell NMR in human cells

In-cell NMR spectra of ^{15}N-enriched ubiquitin and the B1 domain of streptococcal protein G (GB1) were conducted in HeLa cells [87]. The proteins were either fussed to the cell-penetrating peptides or bound trough disulphide links. Upon translocation, the proteins are released in the cytosol by specific intracellular enzymes that cleave the covalent bond or by the reduced intracellular pH for the disulphide links. The intracellular structure of all the proteins tested is similar with their *in vitro* NMR structure indicating that intracellular crowding does not have an effect on these proteins. However, important information for drug screening was obtained for FKBP12 when the cells were treated with extracellular immunosuppressants.

1.4.3 Caveats of in-cell NMR

A series of caveats are associated with NMR spectroscopy in live cells and Ito and Selenko reviewed them recently [88]. These include: the insensitivity of NMR spectroscopy [89] which requires large amounts of ^{15}N-enriched or ^{19}F-labeled protein in the cells, the cells viability during spectra acquisition, binding of

the protein to other macromolecules or membranes in cells, protein leakage from the cells, degradation and instability of translocated proteins in cells, and sample inhomogeneity.

Studying α-synuclein in live cells and its interaction with the membranes using NMR provides atomic level information about this protein inside the cells and helps elucidate the function of α-synuclein in Lewy bodies formation in Parkinson's disease. This information may be relevant for prevention and treatment of this debilitating disease.

1.5 References

1. M. Martinez, A. Brice, J.R. Vaughan, A. Zimprich, M.M. Breteler, G. Meco, A. Filla, M.J. Farrer, C. Betard, J. Hardy, G. De Michele, V. Bonifati, B. Oostra, T. Gasser, N.W. Wood, A. Durr, Genome-wide scan linkage analysis for Parkinson's disease: the European genetic study of Parkinson's disease, Journal of medical genetics 41 (2004) 900-907.

2. C. Haass, P.J. Kahle, Parkinson's pathology in a fly, Nature 404 (2000) 341, 343.

3. http://www.ninds.nih.gov/disorders/parkinsons_disease/parkinsons_disease_backgrounder.htm, Parkinson's Disease Backgrounder, as of 2009.

4. J. Jankovic, M. Stacy, Medical management of levodopa-associated motor complications in patients with Parkinson's disease, CNS drugs 21 (2007) 677-692.

5. J.H. Bower, D.M. Maraganore, S.K. McDonnell, W.A. Rocca, Incidence and distribution of parkinsonism in Olmsted County, Minnesota, 1976-1990, Neurology 52 (1999) 1214-1220.

6. R.A. Fredenburg, C. Rospigliosi, R.K. Meray, J.C. Kessler, H.A. Lashuel, D. Eliezer, P.T. Lansbury, Jr., The impact of the E46K mutation on the properties of alpha-synuclein in its monomeric and oligomeric states, Biochemistry 46 (2007) 7107-7118.

7. R.G. Perez, T.G. Hastings, Could a loss of alpha-synuclein function put dopaminergic neurons at risk?, Journal of neurochemistry 89 (2004) 1318-1324.

8. M.F. Chesselet, Dopamine and Parkinson's disease: is the killer in the house?, Molecular psychiatry 8 (2003) 369-370.

9. M.G. Spillantini, R.A. Crowther, R. Jakes, M. Hasegawa, M. Goedert, alpha-Synuclein in filamentous inclusions of Lewy bodies from Parkinson's disease and dementia with lewy bodies, Proceedings of the national academy of sciences of the United States of America 95 (1998) 6469-6473.

10. M. Vila, S. Vukosavic, V. Jackson-Lewis, M. Neystat, M. Jakowec, S. Przedborski, Alpha-synuclein up-regulation in substantia nigra dopaminergic neurons following administration of the parkinsonian toxin MPTP, Journal of neurochemistry 74 (2000) 721-729.

11. P. Desplats, H.J. Lee, E.J. Bae, C. Patrick, E. Rockenstein, L. Crews, B. Spencer, E. Masliah, S.J. Lee, Inclusion formation and neuronal cell death through neuron-to-neuron transmission of alpha-synuclein, Proceedings of the national academy of sciences of the United States of America 106 (2009) 13010-13015.

12. M.S. Parihar, A. Parihar, M. Fujita, M. Hashimoto, P. Ghafourifar, Mitochondrial association of alpha-synuclein causes oxidative stress, Cellular and molecular life sciences 65 (2008) 1272-1284.

13. J.W. Langston, P. Ballard, J.W. Tetrud, I. Irwin, Chronic Parkinsonism in humans due to a product of meperidine-analog synthesis, Science (New York, N.Y 219 (1983) 979-980.

14. P.R. Castello, D.A. Drechsel, M. Patel, Mitochondria are a major source of paraquat-induced reactive oxygen species production in the brain, The Journal of biological chemistry 282 (2007) 14186-14193.

15. J.S. Bus, J.E. Gibson, Paraquat: model for oxidant-initiated toxicity, Environmental health perspectives 55 (1984) 37-46.

16. T.B. Sherer, R. Betarbet, C.M. Testa, B.B. Seo, J.R. Richardson, J.H. Kim, G.W. Miller, T. Yagi, A. Matsuno-Yagi, J.T. Greenamyre, Mechanism of toxicity in rotenone models of Parkinson's disease, Journal neuroscience 23 (2003) 10756-10764.

17. G. Meco, V. Bonifati, N. Vanacore, E. Fabrizio, Parkinsonism after chronic exposure to the fungicide maneb (manganese ethylene-bis-dithiocarbamate), Scandinavian journal of work, environment & health 20 (1994) 301-305.

18. J. Zhang, V.A. Fitsanakis, G. Gu, D. Jing, M. Ao, V. Amarnath, T.J. Montine, Manganese ethylene-bis-dithiocarbamate and selective dopaminergic neurodegeneration in rat: a link through mitochondrial dysfunction, Journal of neurochemistry 84 (2003) 336-346.

19. S. Lesage, A. Brice, Parkinson's disease: from monogenic forms to genetic susceptibility factors, Human molecular genetics 18 (2009) R48-59.

20. E.M. Valente, F. Brancati, A. Ferraris, E.A. Graham, M.B. Davis, M.M. Breteler, T. Gasser, V. Bonifati, A.R. Bentivoglio, G. De Michele, A. Durr, P. Cortelli, D. Wassilowsky, B.S. Harhangi, N. Rawal, V. Caputo, A. Filla, G. Meco, B.A. Oostra, A. Brice, A. Albanese, B. Dallapiccola, N.W. Wood, PARK6-linked parkinsonism occurs in several European families, Annals of neurology 51 (2002) 14-18.

21. A.E. Lang, A.M. Lozano, Parkinson's disease. First of two parts, The New England journal of medicine 339 (1998) 1044-1053.

22. S. Chandra, G. Gallardo, R. Fernandez-Chacon, O.M. Schluter, T.C. Sudhof, Alpha-synuclein cooperates with CSPalpha in preventing neurodegeneration, Cell 123 (2005) 383-396.

23. G. Di Rosa, D. Puzzo, A. Sant'Angelo, F. Trinchese, O. Arancio, Alpha-synuclein: between synaptic function and dysfunction, Histology and histopathology 18 (2003) 1257-1266.

24. S. Chandra, F. Fornai, H.B. Kwon, U. Yazdani, D. Atasoy, X. Liu, R.E. Hammer, G. Battaglia, D.C. German, P.E. Castillo, T.C. Sudhof, Double-knockout mice for alpha- and beta-synucleins: effect on synaptic functions, Proceedings of the national academy of sciences of the United States of America 101 (2004) 14966-14971.

25. P.H. Jensen, J.Y. Li, A. Dahlstrom, C.G. Dotti, Axonal transport of synucleins is mediated by all rate components, The European journal of neuroscience 11 (1999) 3369-3376.

26. L. Maroteaux, J.T. Campanelli, R.H. Scheller, Synuclein: a neuron-specific protein localized to the nucleus and presynaptic nerve terminal, Journal of Neuroscience 8 (1988) 2804-2815.

27. D.L. Fortin, M.D. Troyer, K. Nakamura, S. Kubo, M.D. Anthony, R.H. Edwards, Lipid rafts mediate the synaptic localization of alpha-synuclein, Journal of Neuroscience 24 (2004) 6715-6723.

28. V.N. Uversky, Neuropathology, biochemistry, and biophysics of alpha-synuclein aggregation, Journal of neurochemistry 103 (2007) 17-37.

29. V.N. Uversky, J. Li, A.L. Fink, Evidence for a partially folded intermediate in alpha-synuclein fibril formation, The Journal of biological chemistry 276 (2001) 10737-10744.

30. D.P. Hong, W. Xiong, J.Y. Chang, C. Jiang, The role of the C-terminus of human alpha-synuclein: intra-disulfide bonds between the C-terminus and other regions stabilize non-fibrillar monomeric isomers, FEBS letters 585 561-566.

31. A.J. Trexler, E. Rhoades, Single molecule characterization of alpha-synuclein in aggregation-prone states, Biophysical journal 99 (2010) 3048-3055.

32. J.C. Kessler, J.C. Rochet, P.T. Lansbury, Jr., The N-terminal repeat domain of alpha-synuclein inhibits beta-sheet and amyloid fibril formation, Biochemistry 42 (2003) 672-678.

33. L.C. Serpell, J. Berriman, R. Jakes, M. Goedert, R.A. Crowther, Fiber diffraction of synthetic alpha-synuclein filaments shows amyloid-like cross-beta conformation, Proceedings of the national academy of sciences of the United States of America 97 (2000) 4897-4902.

34. T. Antony, W. Hoyer, D. Cherny, G. Heim, T.M. Jovin, V. Subramaniam, Cellular polyamines promote the aggregation of alpha-synuclein, The journal of biological chemistry 278 (2003) 3235-3240.

35. M.J. Volles, P.T. Lansbury, Jr., Vesicle permeabilization by protofibrillar alpha-synuclein is sensitive to Parkinson's disease-linked mutations and occurs by a pore-like mechanism, Biochemistry 41 (2002) 4595-4602.

36. T.T. Ding, S.J. Lee, J.C. Rochet, P.T. Lansbury, Jr., Annular alpha-synuclein protofibrils are produced when spherical protofibrils are incubated in solution or bound to brain-derived membranes, Biochemistry 41 (2002) 10209-10217.

37. K.C. Luk, C. Song, P. O'Brien, A. Stieber, J.R. Branch, K.R. Brunden, J.Q. Trojanowski, V.M. Lee, Exogenous alpha-synuclein fibrils seed the formation of Lewy body-like intracellular inclusions in cultured cells, Proceedings of the national academy of sciences of the United States of America 106 (2009) 20051-20056.

38. M. Vilar, H.T. Chou, T. Luhrs, S.K. Maji, D. Riek-Loher, R. Verel, G. Manning, H. Stahlberg, R. Riek, The fold of alpha-synuclein fibrils, Proceedings of the national academy of sciences of the United States of America 105 (2008) 8637-8642.

39. G.F. Wang, C. Li, G.J. Pielak, ^{19}F NMR studies of alpha-synuclein-membrane interactions, Protein science 19 (2010) 1686-1691.

40. E. Rhoades, T.F. Ramlall, W.W. Webb, D. Eliezer, Quantification of alpha-synuclein binding to lipid vesicles using fluorescence correlation spectroscopy, Biophysical journal 90 (2006) 4692-4700.

41. L. Kjaer, L. Giehm, T. Heimburg, D. Otzen, The influence of vesicle size and composition on alpha-synuclein structure and stability, Biophysical journal 96 (2009) 2857-2870.

42. A.C. Ferreon, Y. Gambin, E.A. Lemke, A.A. Deniz, Interplay of alpha-synuclein binding and conformational switching probed by single-molecule

fluorescence, Proceedings of the national academy of sciences U S A 106 (2009) 5645-5650.

43. C.C. Jao, B.G. Hegde, J. Chen, I.S. Haworth, R. Langen, Structure of membrane-bound alpha-synuclein from site-directed spin labeling and computational refinement, Proceedings of the national academy of sciences U S A 105 (2008) 19666-19671.

44. W.S. Davidson, A. Jonas, D.F. Clayton, J.M. George, Stabilization of alpha-synuclein secondary structure upon binding to synthetic membranes, The journal of biological chemistry 273 (1998) 9443-9449.

45. M. Zhu, J. Li, A.L. Fink, The association of alpha-synuclein with membranes affects bilayer structure, stability, and fibril formation, The journal of biological chemistry 278 (2003) 40186-40197.

46. J. Li, V.N. Uversky, A.L. Fink, Effect of familial Parkinson's disease point mutations A30P and A53T on the structural properties, aggregation, and fibrillation of human alpha-synuclein, Biochemistry 40 (2001) 11604-11613.

47. J. Burre, M. Sharma, T. Tsetsenis, V. Buchman, M.R. Etherton, T.C. Sudhof, Alpha-synuclein promotes SNARE-complex assembly *in vivo* and *in vitro*, Science 329 1663-1667.

48. M. Vila, D. Ramonet, C. Perier, Mitochondrial alterations in Parkinson's disease: new clues, Journal of neurochemistry 107 (2008) 317-328.

49. L. Devi, H.K. Anandatheerthavarada, Mitochondrial trafficking of APP and alpha synuclein: Relevance to mitochondrial dysfunction in Alzheimer's and Parkinson's diseases, Biochimica et biophysica acta 1802 (2010) 11-19.

50. N.B. Cole, D. Dieuliis, P. Leo, D.C. Mitchell, R.L. Nussbaum, Mitochondrial translocation of alpha-synuclein is promoted by intracellular acidification, Experimental cell research 314 (2008) 2076-2089.

51. I. Mikolaenko, O. Pletnikova, C.H. Kawas, R. O'Brien, S.M. Resnick, B. Crain, J.C. Troncoso, Alpha-synuclein lesions in normal aging, Parkinson disease, and Alzheimer disease: evidence from the Baltimore Longitudinal Study of Aging (BLSA), Journal of neuropathology and experimental neurology 64 (2005) 156-162.

52. T. Bartels, J.G. Choi, D.J. Selkoe, Alpha-synuclein occurs physiologically as a helically folded tetramer that resists aggregation, Nature 477 (2011) 107-110.

53. S. Deshayes, M. Morris, F. Heitz, G. Divita, Delivery of proteins and nucleic acids using a non-covalent peptide-based strategy, Advenced drug delivery reviews 60 (2008) 537-547.

54. M.C. Morris, J. Depollier, J. Mery, F. Heitz, G. Divita, A peptide carrier for the delivery of biologically active proteins into mammalian cells, Nature biotechnology 19 (2001) 1173-1176.

55. L. Crombez, A. Charnet, M.C. Morris, G. Aldrian-Herrada, F. Heitz, G. Divita, A non-covalent peptide-based strategy for siRNA delivery, Biochemical society transaction 35 (2007) 44-46.

56. S. Deshayes, F. Simeoni, M.C. Morris, G. Divita, F. Heitz, Peptide-mediated delivery of nucleic acids into mammalian cells, Methods in molecular biology 386 (2007) 299-308.

57. M.C. Morris, E. Gros, G. Aldrian-Herrada, M. Choob, J. Archdeacon, F. Heitz, G. Divita, A non-covalent peptide-based carrier for in vivo delivery of DNA mimics, Nucleic acids research 35 (2007) e49.

58. K. Weller, S. Lauber, M. Lerch, A. Renaud, H.P. Merkle, O. Zerbe, Biophysical and biological studies of end-group-modified derivatives of Pep-1, Biochemistry 44 (2005) 15799-15811.

59. S. Deshayes, A. Heitz, M.C. Morris, P. Charnet, G. Divita, F. Heitz, Insight into the mechanism of internalization of the cell-penetrating carrier peptide Pep-1 through conformational analysis, Biochemistry 43 (2004) 1449-1457.

60. S.T. Henriques, J. Costa, M.A. Castanho, Translocation of beta-galactosidase mediated by the cell-penetrating peptide pep-1 into lipid vesicles and human HeLa cells is driven by membrane electrostatic potential, Biochemistry 44 (2005) 10189-10198.

61. M.A. Munoz-Morris, F. Heitz, G. Divita, M.C. Morris, The peptide carrier Pep-1 forms biologically efficient nanoparticle complexes, Biochemical and biophysical research communication 355 (2007) 877-882.

62. E. Kubo, N. Fatma, Y. Akagi, D.R. Beier, S.P. Singh, D.P. Singh, TAT-mediated PRDX6 protein transduction protects against eye lens epithelial cell death and delays lens opacity, American journal of physiology 294 (2008) C842-855.

63. A. Eguchi, T. Akuta, H. Okuyama, T. Senda, H. Yokoi, H. Inokuchi, S. Fujita, T. Hayakawa, K. Takeda, M. Hasegawa, M. Nakanishi, Protein

transduction domain of HIV-1 Tat protein promotes efficient delivery of DNA into mammalian cells, The Journal of biological chemistry 276 (2001) 26204-26210.

64. A. Ziegler, J. Seelig, High affinity of the cell-penetrating peptide HIV-1 Tat-PTD for DNA, Biochemistry 46 (2007) 8138-8145.

65. V.P. Torchilin, R. Rammohan, V. Weissig, T.S. Levchenko, TAT peptide on the surface of liposomes affords their efficient intracellular delivery even at low temperature and in the presence of metabolic inhibitors, Proceedings of the national academy of sciences of the United States of America 98 (2001) 8786-8791.

66. C.C. Berry, J.M. de la Fuente, M. Mullin, S.W. Chu, A.S. Curtis, Nuclear localization of HIV-1 tat functionalized gold nanoparticles, IEEE transactions on nanobioscience 6 (2007) 262-269.

67. E. Vives, P. Brodin, B. Lebleu, A truncated HIV-1 Tat protein basic domain rapidly translocates through the plasma membrane and accumulates in the cell nucleus, The Journal of biological chemistry 272 (1997) 16010-16017.

68. D. Kim, C. Jeon, J.H. Kim, M.S. Kim, C.H. Yoon, I.S. Choi, S.H. Kim, Y.S. Bae, Cytoplasmic transduction peptide (CTP): new approach for the delivery of biomolecules into cytoplasm in vitro and in vivo, Experimental cell research 312 (2006) 1277-1288.

69. D.S. Burz, K. Dutta, D. Cowburn, A. Shekhtman, Mapping structural interactions using in-cell NMR spectroscopy (STINT-NMR), Nature methods 3 (2006) 91-93.

70. D.S. Burz, A. Shekhtman, In-cell biochemistry using NMR spectroscopy, PloS one 3 (2008) e2571.

71. V.N. Uversky, A.L. Fink, Conformational constraints for amyloid fibrillation: the importance of being unfolded, Biochimica et biophysica acta 1698 (2004) 131-153.

72. G.W. Daughdrill, Pielak, G. J., Uversky, V. N., Cortese, M. S.,, A.K. and Dunker, Natively disordered proteins. In Protein folding handbook (Buchner, J., and Kiefhaber, T., Eds.), (2005) pp 275- 357, Wiley-VCH, Weinheim, Germany.

73. C. Li, L.M. Charlton, A. Lakkavaram, C. Seagle, G. Wang, G.B. Young, J.M. Macdonald, G.J. Pielak, Differential dynamical effects of macromolecular crowding on an intrinsically disordered protein and a

globular protein: implications for in-cell NMR spectroscopy, Journal of the American Chemical Society 130 (2008) 6310-6311.

74. M.M. Dedmon, C.N. Patel, G.B. Young, G.J. Pielak, FlgM gains structure in living cells, Proceedings of the National Academy of Sciences of the United States of America 99 (2002) 12681-12684.

75. B.C. McNulty, G.B. Young, G.J. Pielak, Macromolecular crowding in the Escherichia coli periplasm maintains alpha-synuclein disorder, Journal of molecular biology 355 (2006) 893-897.

76. B.C. McNulty, A. Tripathy, G.B. Young, L.M. Charlton, J. Orans, G.J. Pielak, Temperature-induced reversible conformational change in the first 100 residues of alpha-synuclein, Protein science 15 (2006) 602-608.

77. R.L. Croke, C.O. Sallum, E. Watson, E.D. Watt, A.T. Alexandrescu, Hydrogen exchange of monomeric alpha-synuclein shows unfolded structure persists at physiological temperature and is independent of molecular crowding in Escherichia coli, Protein science 17 (2008) 1434-1445.

78. C. Li, G.F. Wang, Y. Wang, R. Creager-Allen, E.A. Lutz, H. Scronce, K.M. Slade, R.A. Ruf, R.A. Mehl, G.J. Pielak, Protein ^{19}F NMR in Escherichia coli, Journal of the American chemical society 132 (2009) 321-327.

79. A.P. Schlesinger, Y. Wang, X. Tadeo, O. Millet, G.J. Pielak, Macromolecular crowding fails to fold a globular protein in cells, Journal of the American chemical society 133 8082-8085.

80. D. Sakakibara, A. Sasaki, T. Ikeya, J. Hamatsu, T. Hanashima, M. Mishima, M. Yoshimasu, N. Hayashi, T. Mikawa, M. Walchli, B.O. Smith, M. Shirakawa, P. Guntert, Y. Ito, Protein structure determination in living cells by in-cell NMR spectroscopy, Nature 458 (2009) 102-105.

81. K. Luby-Phelps, Cytoarchitecture and physical properties of cytoplasm: volume, viscosity, diffusion, intracellular surface area, International review of cytology 192 (2000) 189-221.

82. P. Selenko, Z. Serber, B. Gadea, J. Ruderman, G. Wagner, Quantitative NMR analysis of the protein G B1 domain in *Xenopus laevis* egg extracts and intact oocytes, Proceedings of the national academy of sciences of the United States of America 103 (2006) 11904-11909.

83. T. Sakai, H. Tochio, T. Tenno, Y. Ito, T. Kokubo, H. Hiroaki, M. Shirakawa, In-cell NMR spectroscopy of proteins inside *Xenopus laevis* oocytes, Journal of biomolecular NMR 36 (2006) 179-188.

84. J.F. Bodart, J.M. Wieruszeski, L. Amniai, A. Leroy, I. Landrieu, A. Rousseau-Lescuyer, J.P. Vilain, G. Lippens, NMR observation of Tau in *Xenopus* oocytes, Journal of magnetic resonance 192 (2008) 252-257.

85. T. Sakai, H. Tochio, K. Inomata, Y. Sasaki, T. Tenno, T. Tanaka, T. Kokubo, H. Hiroaki, M. Shirakawa, Fluoroscopic assessment of protein leakage during *Xenopus* oocytes in-cell NMR experiment by co-injected EGFP, Analytical biochemistry 371 (2007) 247-249.

86. P. Selenko, D.P. Frueh, S.J. Elsaesser, W. Haas, S.P. Gygi, G. Wagner, In situ observation of protein phosphorylation by high-resolution NMR spectroscopy, Nature structural & molecular biology 15 (2008) 321-329.

87. K. Inomata, A. Ohno, H. Tochio, S. Isogai, T. Tenno, I. Nakase, T. Takeuchi, S. Futaki, Y. Ito, H. Hiroaki, M. Shirakawa, High-resolution multi-dimensional NMR spectroscopy of proteins in human cells, Nature 458 (2009) 106-109.

88. Y. Ito, P. Selenko, Cellular structural biology, Current opinion in structural biology 20 (2010) 640-648.

89. G.J. Pielak, C. Li, A.C. Miklos, A.P. Schlesinger, K.M. Slade, G.F. Wang, I.G. Zigoneanu, Protein nuclear magnetic resonance under physiological conditions, Biochemistry 48 (2009) 226-234.

CHAPTER 2

Interaction of α-Synuclein and its A30P Variant with Vesicles of Composition Similar to Mitochondrial Membranes

Summary

α-Synuclein, an intrinsically-disordered protein associated with Parkinson's disease, interacts with mitochondria but the details of this interaction are unknown. Cardiolipin is the main anionic lipid in mitochondria where almost all of its acyl chains possess two double bonds. We probed the interaction of α-synuclein and its A30P variant with lipid vesicles by using fluorescence anisotropy and ^{19}F nuclear magnetic resonance. Both proteins interact strongly with large unilamellar vesicles of composition similar to that of the inner mitochondrial membrane, which contains cardiolipin, but have no affinity for vesicles mimicking the outer mitochondrial membrane, which lacks cardiolipin. The ^{19}F data show that the interaction involves α-synuclein's N-terminal region. These data indicate that the middle portion of the protein, which contains the KAKEGVVAAAE repeats, is involved in binding, probably via electrostatic interactions between the lysines and cardiolipin. However, the saturation of the cardiolipin acyl side chains also determines the strength of α-synuclein binding. Eliminating one double bond increases affinity, while complete saturation

dramatically decreases affinity. Increasing the temperature increases the binding of wild-type, but not the A30P variant. These data suggest that membrane packing density is important in determining α-synuclein affinity. This idea was confirmed by examining the anisotropy of 1,6-diphenyl-1,3,5-hexatriene in the presence of vesicles with or without the proteins. The results advance our understanding of α-synuclein's interaction with mitochondrial membranes.

2.1 Introduction

Parkinson's disease and other neurodegenerative disorders are characterized by cytoplasmic neuronal inclusions known as Lewy bodies [1-4]. α-Synuclein, a 140-amino acid intrinsically disordered protein, is the main component of Lewy bodies [5-8]. The protein (Figure 2.1 A) comprises a positively-charged N-terminal region (residues 1-60) with an imperfect consensus repeat KTKEGV involved in lipid binding, a hydrophobic middle segment known as the NAC region (Non Amyloid Component, residues 61-95), and a negatively-charged C-terminal region (residues 96-140) [9, 10].

The protein helps maintain SNARE-complex assembly at presynaptic vesicles through its C-terminus, while the N-terminus is anchored to the vesicle [11]. Its function is important during increased synaptic activity when the nerve terminals repeatedly release neurotransmitters, which requires the assembly and disassembly of the SNARE complex. The protein is also involved in aging, but the reason for its age-related loss of function is unknown [11].

α-Synuclein localizes not only to the presynaptic neural terminals but also to other subcellular compartments such as mitochondria [12, 13]. This

localization is associated with mitochondrial dysfunction [13-15] including impaired complex I function [12, 16], oxidative stress [17], and mitochondrial lipid abnormalities [16]. More specifically, a decrease in cardiolipin (CL) and a change in its acyl side chains were noted in mitochondria from the brains of mice lacking α-synuclein [16]. The side chain changes involve a reduction in polyunsaturated fatty acids [16, 18] and an increase in saturated fatty acids [16]. Since CL is a mitochondria-specific phospholipid, the implied importance of α-synuclein at the mitochondrial level is evident. Although the exact link between the loss of α-synuclein and the decrease in CL is unclear, the findings suggest that α-synuclein helps control intracellular transport of lipids [16].

The interaction of α-synuclein with vesicles of different lipid composition [19], phospholipid headgroups [20], sizes [21], and surfaces [22, 23] has been studied. Despite these efforts little is known about the interaction of α-synuclein with the mitochondrial membrane, the mechanism of α-synuclein transport through the outer mitochondrial membrane, and the localization of the protein in the inner mitochondrial membrane [17].

We used fluorescence anisotropy and high resolution nuclear magnetic resonance spectroscopy (NMR) to investigate the interaction of wild-type α-synuclein and one of its familial Parkinson's disease variants [24], A30P, with large unillamelar vesicles (LUVs) having lipid compositions similar to the inner and outer mitochondrial membranes. We evaluated the importance of CL as well as the effect of saturated and unsaturated CL acyl side chains on α-synuclein's interaction with LUVs that mimic the inner mitochondrial membrane. We also

investigated the effect of temperature on affinity, and using ^{19}F-labeled α-synuclein, we determined which region of the protein interacts with LUVs containing CL. The results advance our understanding of α-synuclein's interaction with mitochondrial membranes.

2.2 Materials and Methods

2.2.1 Expression, Purification, and Labeling of Human α-Synuclein and its A30P Variant

Wild-type α-synuclein, A30P α-synuclein, V3C α-synuclein and V3C;A30P α-synuclein were expressed from a T7-7 plasmid in *Escherichia coli* BL21-Gold(DE3) competent cells (Stratagene Cloning Systems, La Jolla, CA). The proteins were purified as described [25, 26].

The V3C mutation at position 3 was made by using a Stratagene site-directed mutagenesis kit. The cysteine was used to attach Alexa Fluor 488 (Invitrogen, Carlsbad, CA). For labeling, 12 mg of V3C α-synuclein were dissolved in sterile, degassed water to a final concentration of 2 mg/mL. Tris(2-carboxyethyl)phosphine and $NaHCO_3$ were added in a 10-fold molar excess over the protein. The mixture was incubated at room temperature with shaking for 30 min. Next, Alexa Fluor 488 C5-maleimide was added in a 10-fold molar excess over protein and the mixture incubated at room temperature with shaking for 2 h. The labeled protein was purified with gel filtration chromatography by using a Superdex 75 column eluted with 20% acetonitrile in phosphate buffered saline (NaCl 137 mM, KCl 2.7 mM, Na_2HPO_4 10 mM, KH_2PO_4 1.8 mM). The labeled protein was dialyzed against water.

The extinction coefficient of the dye at 494 nm (71,000 $M^{-1}cm^{-1}$) was used to quantify the labeled protein. The Lowry method (Pierce, Rockford, IL) was used to quantify the total protein. The degree of labeling was 84% for V3C α-synuclein and 99% for V3C;A30P α-synuclein. Aliquots containing 1 mg of labeled protein were lyophilized and stored at –80 °C.

For NMR experiments, wild-type and Y125F α-synuclein labeled with 3-fluoro-L-tyrosine were prepared as described [27].

2.2.2 Cell Culture and Mitochondria Isolation

Human epithelial carcinoma cells (HeLa) from ATCC were cultured in Dulbelcco's modified Eagle's medium (Invitrogen) supplemented with 10% fetal bovine serum, penicillin and streptomycin (100 µg/mL). The cultures were incubated at 37 °C in 5% CO_2. Mitochondria were isolated from HeLa cells (2 x 10^7 cells) by using a Mitochondria Isolation Kit for Cultured Cells (Pierce, Rockford, IL). Their activity was tested by assessing the cytochrome *c* oxidase activity with the Mitochondria Activity Assay Kit (BioChain Institute, Inc., Haywatd, CA).

2.2.3 Mitochondrial Import of α-Synuclein

Freshly isolated mitochondria were incubated with fluorescently-labeled α-synuclein in the presence of an energy mixture and transport buffer as described [28]. Trypsin was used to remove α-synuclein attached to the surface of mitochondria. Mito Tracker Red CMXRos (Invitrogen) was used to stain the active mitochondria after protein import and trypsinization. Fused silica and glass microscope slides were prepared as described [29]. Mitochondria containing α-

synuclein were allowed to attach to the poly-L-lysine coated slide for 30 min and then rinsed with minimal media. α-Synuclein import was tested using confocal microscopy on an inverted laser scanning microscope (Zeiss 510 Meta, Thornwood, NY) equipped with a 63 x, 1.4 NA, Plan-Apochromat, oil immersion objective.

2.2.4 Vesicle Preparation

Components were purchased from Avanti Polar Lipids, Inc. (Birmingham, AL) in chloroform, except cholesterol (CH, from ovine wool), which was dissolved in chloroform to a concentration of 1 mg/mL and stored at –20 ℃. The components were used without further purification.

Aliquots of the components, in chloroform, were mixed in glass vials and the solvent removed overnight in a vacuum concentrator. The dried mixtures were suspended in 1 mL of 50 mM sodium phosphate buffer, pH 7.4, to a final lipid concentration of 2 mM. The following phospholipids were used for preparing LUVs: CL (bovine heart), 1,2-dioleoyl-*sn*-glycero-3-phosphocholine (DOPC), 1,2-dioleoyl-*sn*-glycero-3-phosphoethanolamine (DOPE), 1',3'-bis[1,2-dimyristoyl-*sn*-glycero-3-phospho]-*sn*-glycerol (TM CL), and 1',3'-bis[1,2-dioleoyl-*sn*-glycero-3-phospho]-*sn*-glycerol (TO CL). Figure 2.1 B shows the structures of CLs.

Vesicles of composition DOPC:DOPE:CL:CH 2.0:1.3:1.0:0.6 molar ratio and DOPC:DOPE:CH 4.0:2.0:0.9, corresponding to inner and outer membrane of mitochondria [30], respectively, were prepared. LUVs with different ratios of CL (1.0, 0.8, 0.5, and 0) or different CL acid side chains (TM and TO) were also prepared.

LUVs were prepared by multiple extrusion [20, 31, 32] through a 0.1 μm polycarbonate membrane (Whatman Inc., Sanford, ME). For NMR experiments, the vesicles were prepared with the same protocol, but at a concentration of 4 mM. The dried mixture corresponding to the inner mitochondrial membrane was resuspended in 50 mM sodium phosphate buffer, pH 7.4, containing 10% D_2O. The final concentration of ^{19}F labeled protein in the NMR tube was 100 μM and the protein:lipid molar ratio was ~1:100. Protein in buffer alone was used as a reference.

2.2.5 Fluorescence Anisotropy of Labeled Proteins

The experiments were conducted on a FluoroLog®-322 spectrofluorometer (HORIBA Jobin Yvon Inc., Edison, NJ) with an excitation wavelength of 495 nm and an emission wavelength of 519 nm. Four hundred μL of protein (100 nM) in 50 mM sodium phosphate buffer, pH 7.4, were titrated with LUVs at 25 or 37 °C. Each point is the average of five measurements, and each condition was tested in triplicate. Control measurements using only LUVs or unlabeled wild-type α-synuclein in the same buffer were performed to assess background fluorescence, which was negligible. The anisotropy was calculated as described [33]. The dissociation constants (K_d) were calculated by fitting the data to a one site binding model (SigmaPlot 11.0).

2.2.6 DPH Fluorescence Anisotropy

1,6-Diphenyl-1,3,5-hexatriene (DPH) was incubated with LUVs containing TO, TM, or CL IM for one h at room temperature either in the presence or absence of proteins. The final molar lipid to DPH ratio was 300:1. Fluorescence

anisotropy was recorded at 25 °C by using an excitation wavelength of 360 nm and an emission wavelength of 440 nm. Fluorescence anisotropy was also measured at 37 °C for CL IM LUVs in the presence or absence of wild-type or A30P α-synuclein. The result for each condition represents the average of five measurements.

2.2.7 NMR

^{19}F spectra were acquired at 25 °C on a Varian Inova 600 MHz spectrometer equipped with a 5 mm triple resonance probe. The spectra comprised 2048 transients with a 30 kHz sweep width. The ^{19}F chemical shifts were referenced to trifluoroethanol at 0 ppm. The experiments were conducted in triplicate.

2.3 Results

2.3.1 In vitro Mitochondrial Import of α-Synuclein

Fluorescently-labeled α-synuclein localized in isolated mitochondria (Figure 2.2*A*). Mito Tracker Red CMXRos is an indicator of active mitochondria because its accumulation is related to membrane potential. The red fluorescence shows that mitochondria are active after protein import and trypsinization (Figure 2.2*B*). Co-localization of fluorescently-labeled protein and Mito Tracker Red indicates that the protein is localized in close proximity of the membranes, not in the matrix (Figure 2.2*D*). These findings agree with those of Devi et al. [15]. To better understand the distribution of α-synuclein in the inner and outer

membrane, we used lipid vesicles with a composition similar to these membranes.

2.3.2 Interaction with LUVs Having Lipid Compositions Similar to the Inner and Outer Mitochondrial Membrane

Mitochondria contain 25.3% phospholipid by mass [30]. In terms of phospholipid composition, the mitochondria comprise 40.8% phosphatidyl choline, 37.4% phosphatidyl ethanolamine, 19.1% CL, and ~3% phosphatidyl inositol. The major phospholipids of the outer membrane are phosphatidyl choline (55.2%), and phosphatidyl ethanolamine (25.3%). The major phospholipids of the inner membrane are phosphatidyl choline (44.5%), phosphatidyl ethanolamine (27.7%), and CL (21.5%). CL is essentially absent from the outer membrane [30].

Fluorescence anisotropy was used to quantify the interaction of fluorescently-labeled V3C α-synuclein and V3C;A30P α-synuclein with LUVs. Alexa Fluor 488 dye was chosen because of its high photostability [34]. Labeling at position 3 was selected because this region of the protein is highly dynamic, decreasing the possibility that the modification will disrupt the native conformation [35]. The average diameter of the LUVs, as determined by dynamic light scattering, is ~140 nm (Figure 2.3*A*-*D*), consistent with values for vesicles extruded through membranes with 100 nm pores [20, 31]. The vesicles were stable for at least three days if kept at 4 ℃ in 50 mM sodium phosphate buffer, pH 7.4. Nevertheless, the vesicles were used within 48 h. The presence or

absence of CL (Figure 2.3*A* and *B*) or CH (Figure 2.3*C* and *D*) does not affect the size of the vesicles.

First, we studied the interaction of fluorescently-labeled proteins with LUVs having a molar DOPC:DOPE:CH ratio of 4.0:2.0:0.90, which corresponds to the composition of the outer membrane. No change in the anisotropy was noted when titrating 100 nM protein with LUVs, suggesting no affinity of fluorescently labeled V3C or V3C;A30P α-synuclein for this type of vesicle (Figure 2.4 A and B).

LUVs with a molar ratio corresponding to the inner membrane (DOPC:DOPE:CL:CH of 2.0:1.3:1.0:0.60) gave strikingly different results; both the wild-type protein and the A30P variant bind with sub mM dissociation constants. As shown in Table 1, V3C α-synuclein binds slightly more strongly (K_d 130 μM) than the V3C;A30P variant (K_d 210 μM). Since only the inner membrane contains CL, these observations implicate CL in the binding of α-synuclein and are consistent with studies showing that α-synuclein interacts with vesicles containing anionic phospholipids [10, 20, 36, 37].

2.3.3 Importance of CL

α-Synuclein is mostly associated with the inner membrane of mitochondria in brains from patients with Parkinson's disease [12, 15]. Brains of mice lacking α-synuclein have reduced levels of only CL and phosphatidylglycerol (a CL precursor) [16]. Since CL is mitochondria-specific, we decided to investigate α-synuclein binding to LUVs containing different amounts of this phospholipid.

The data are shown in Figures 2.3, and the K_d values are compiled in Table 1. LUVs containing DOPC, DOPE, and CH in molar ratios corresponding to the inner mitochondrial membrane were prepared with 100%, 80%, 50%, and 0% CL, where 100% represents the normal amount in the inner membrane. For V3C α-synuclein, decreasing the CL by 20% causes less than a two-fold increase in K_d but halving the CL increases K_d by a factor of 6 (Table 1). No binding was noted when CL was absent (Figure 2.5 A). These findings show that CL is essential for the interaction between α-synuclein and the inner mitochondrial membrane.

We also studied the interaction of the A30P variant with these LUVs. The decrease in affinity is even stronger for the variant than it is for the wild-type protein (Figure 2.5 B).

2.3.4 Effect of the CL Acyl Group on Binding

Mitochondria from mice lacking α-synuclein have 51% more saturated fatty acids and 25% less n-6 polyunsaturated fatty acids, but the content of monounsaturated fatty acids is unchanged [16]. To investigate the effect of such changes on α-synuclein binding, LUVs with a molar ratio corresponding to the lipid composition of the inner membrane were prepared by using CL with a saturated acyl side chain (TM CL) and CL with one single double bond in the acyl chain (TO CL) (Figure 2.1 B).

The results are shown in Figure 2.6, and the K_d values are compiled in Table 1. The V3C variant binds LUVs with one double bond per side chain more strongly (K_d 67 μM) than those LUVs containing two double bonds(K_d 130 μM).

Complete saturation, however, abrogates binding. The affinity of A30P α-synuclein for LUVs containing one double bond per side chain (K_d 153 μM) is nearly the same as its affinity for LUVs with two (K_d 210 μM), but no binding was noted with only saturated side chains. We conclude that α-synuclein prefers the LUVs with unsaturated side chains, and that the affinity for LUVs with saturated acyl side chains is negligible.

2.3.5 Positional Information

Since V3C α-synuclein and V3C;A30P α-synuclein are both labeled with the dye at a single position (Figure 2.1 A), the fluorescence anisotropy studies provide information about overall protein binding but not positional information. ^{19}F NMR was used to test the effect of chain saturation and to determine if the specific regions of α-synuclein bind differently. ^{19}F is sensitive to its environment, such that small changes in the structure of a labeled region are easily detected.

α-Synuclein has four tyrosines, one at position 39 in the N-terminal region and the others near the C-terminus at the positions 125, 133, and 136 (Figure 2.1 A). The ^{19}F NMR spectrum of 3-fluoro-tyrosine-labeled wild-type α-synuclein in buffer alone exhibits only three resonances (Figure 2.7 A). As shown by Li et al. [27], who assigned all the resonances, the middle resonance is a composite from tyrosines 39 and 125. To avoid this problem, we used the Y125F variant to eliminate the overlap (Figure 2.7 B).

Spectra acquired in the presence of vesicles containing CL with two (CL), one (TO), and no (TM) double bonds are shown in Figure 2.7 C, D, and E, respectively. The resonances from positions 133 and 136 are unchanged by the

LUVs, but the resonance from position 39 decreases (Figure 2.7 C-E), indicating the interaction of the N-terminal region of the protein with the vesicles. The relative decrease of the position 39 resonance depends on the acyl side chain. The largest decrease occurs for the CL with two double bonds (TO CL) and the smallest for the completely saturated CL (TM CL), consistent with the order from the fluorescence anisotropy described above.

2.3.6 Temperature and Binding

Heat increases membrane fluidity. In Table 1 we compared the affinities at 25 °C (Figure 2.4 A and B) and 37 °C (Figure 2.8) of fluorescently-labeled V3C α-synuclein and V3C;A30P α-synuclein for LUVs with a composition corresponding to the inner membrane. The affinity of V3C α-synuclein is two fold greater (K_d 59 μM) at 37 °C than it is at 25 °C (K_d 134 μM), but the affinity of the V3C;A30P protein is unaffected.

2.3.7 DPH Fluorescence Anisotropy

The fluorescence anisotropy of DPH was used to examine the packing density of LUVs with different CL acyl side chains. The anisotropy depends on the type of phospholipid and its degree of saturation [38].

The data indicate that in buffer, at 25 °C, LUVs containing TO CL are as well packed as CL IM LUVs, but both are better packed than TM CL LUVs (Figure 2.9).α-Synuclein perturbs the membrane packing density. Wild-type and A30P α-synuclein reduce the anisotropy for all three types of LUVs. The decrease is comparable for wild-type and A30P α-synucleins. Studies conducted

at 37 ℃ also show a decrease in anisotropy for CL IM vesicles in the presence of both wild-type and A30P α-synuclein (Figure 2.9, inset).

2.4 Discussion

α-Synuclein interacts with isolated mitochondria from HeLa cells and is imported in the proximity of the inner membrane but it is not transported into the matrix.

α-Synuclein has no affinity for LUVs with the lipid composition of the outer mitochondrial membrane, which lacks CL. This observation is consistent with studies showing that α-synuclein enters mitochondria via the protein import channel [12] rather than through lipid interactions.

A significant affinity was noticed for both the wild-type protein and the A30P variant for LUVs with a composition similar to that of the inner mitochondrial membrane, with the V3C α-synuclein having slightly higher affinity (Figure 2.4). Vesicles with the composition of the inner mitochondrial membrane, but lacking CL, do not bind α-synuclein. Consistent with this conclusion, a decrease in CL reduces α-synuclein affinity (Figure 2.5 A and B), with the affinity of the A30P variant decreasing more than the affinity of the wild-type protein (Figure 2.5 B). These observations show the importance of CL in the inner mitochondrial membrane for α-synuclein localization. The increased affinity of α-synuclein for LUVs made from phospholipids with unsaturated side chains was confirmed [16]. However, in our study α-synuclein binds more strongly to the TO CL, which contains one double bond per acyl side chain compared to the CL, which contains two. To better understand the affinity of α-synucleins for CL

vesicles containing different fatty acids we investigated the vesicle packing density by using DPH fluorescence anisotropy.

The fluorescence anisotropy of DPH embedded in a LUV provides information about membrane fluidity, and hence the packing density of its acyl side chains. High packing density results in lower fluidity, and increased DPH anisotropy [39]. The data at 25 ℃ indicate that TO CL and CL IM vesicles are better packed than TM CL LUVs. That is, more water penetrates TM CL LUVs and fewer DPH molecules are inside the vesicles or are strongly interacting with saturated acyl side chains compared to TO CL and CL IM vesicles, reducing the fluorescence anisotropy. DPH fluorescence anisotropy decreases drastically when wild-type or A30P α-synucleins were added to LUVs containing TO, TM, or IM CL (Figure 2.9). The DPH fluorescence anisotropy data (Figure 2.9) correlate with binding constants (Table 1); stronger protein binding leads to decreased in DPH anisotropy. These observations suggest that α-synuclein-vesicle interactions destabilize the membrane [37].

Our ^{19}F NMR data suggest that only the N-terminal region interacts with the vesicles. Others have shown that this region interacts with phospholipid head groups forming an α-helix, while the C-terminus remains unstructured [20, 21, 36, 40]. The A30P variant has a lower affinity for anionic lipid vesicles compared to the wild-type protein [41-44]. We also observe a decrease in the affinity of A30P for all LUVs used compared to the wild-type protein (Table 1). These observations are consistent with the presence of proline at position 30, which interrupts the α-helix in the vesicle bound protein [37].

Increasing the temperature increases the fluidity of the vesicles, reducing their packing density. Binding of wild-type protein is stronger at 37 ℃ than it is at 25 ℃. The stronger binding at higher temperature suggests that the hydrophobic effect is important in α-synuclein membrane interaction. Taken together with the NMR and DPH data, it appears that the decrease in packing density at higher temperature exposes hydrophobic membrane surface, which interacts with hydrophobic residues on the α-helix formed. These findings are consistent with DPH data; wild-type α-synuclein induces a larger decrease in anisotropy compared to the A30P variant.

To our knowledge, this is the first study where fluorescence anisotropy and NMR were combined to investigate the affinity of α-synuclein for lipid vesicles with a composition similar to mitochondrial membranes. The data explain why α-synuclein has a high affinity for the inner membrane (it contains CL), show that the hydrophobic effect plays a role in binding, and indicates that the interactions involve the N-terminal region of the protein. These two techniques can also be used to monitor binding affinity of α-synuclein to isolated mitochondria and mitoplasts. Investigation of interaction between mitochondria and α-synucleins and the localization of the proteins in different sub-mitochondrial compartments should help elucidate the role of these proteins in the mitochondria dysfunction associated with neurodegenerative diseases.

2.5 Table and Figures

Table 2.1 Dissociation constants (μM) for fluorescently-labeled α-synucleins with LUVs.*

	OM	CL 100% (IM)	TO CL	TM CL	CL 80%	CL 50%	CL 0%	IM 37 ℃
V3C	-	130 ±20	67 ±3	3000 ±4000	210 ±20	850 ±120	-	59 ±3
V3C;A30P	-	210 ±20	153 ±7	-	680 ±150	1200 ±700	-	230 ±20

*Data were acquired at 25 ℃ unless otherwise specified; OM, outer membrane; IM, inner membrane; - , K_d could not be estimated.

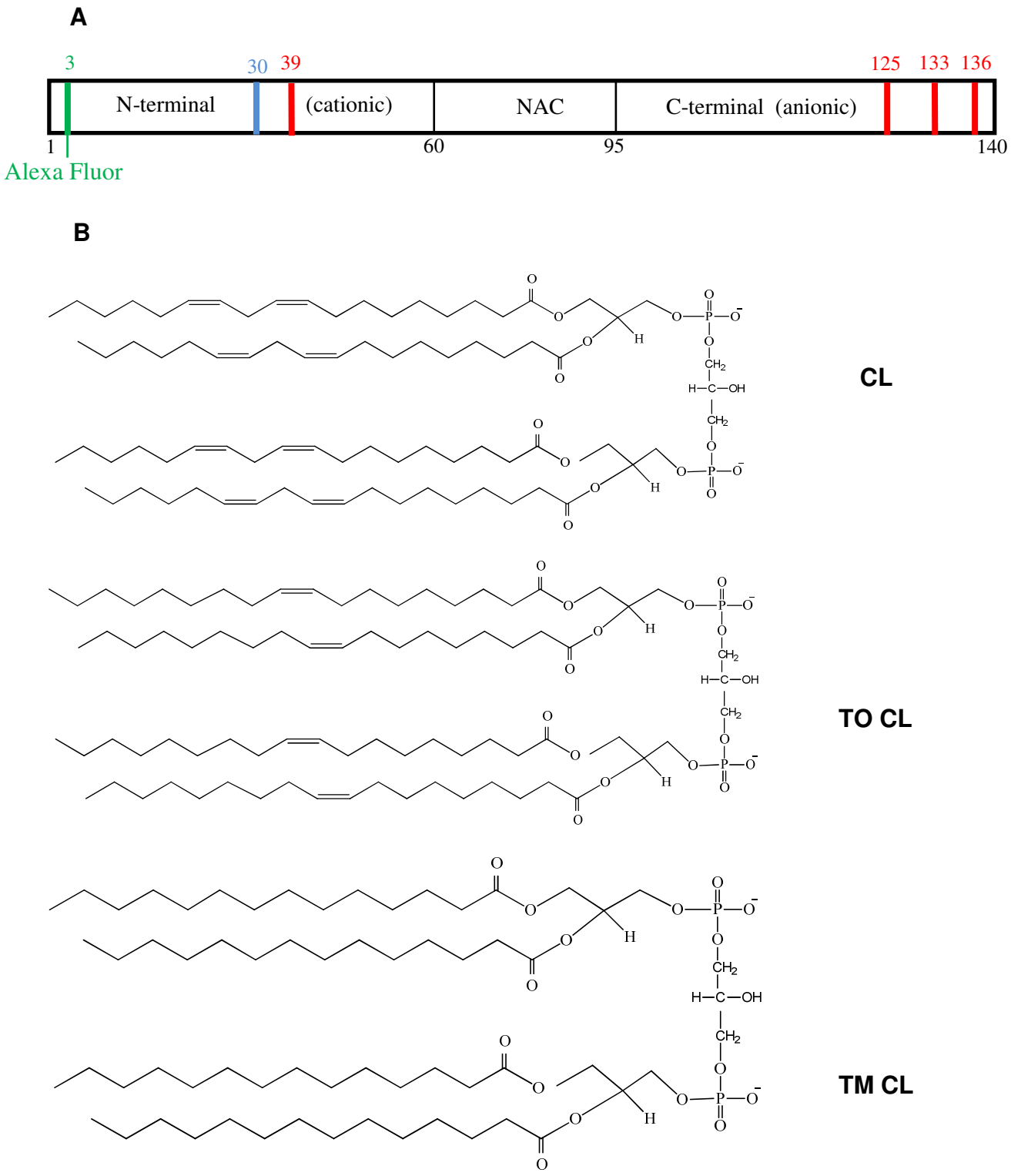

Figure 2.1 Schematic representation of α-synuclein and structural formulas of the CLs

Schematic representation of α-synuclein (A) showing the four tyrosines (red), the position labeled with dye (green), and the A30P point mutation (blue). (B) Structural formulas of the CLs used to prepare LUVs.

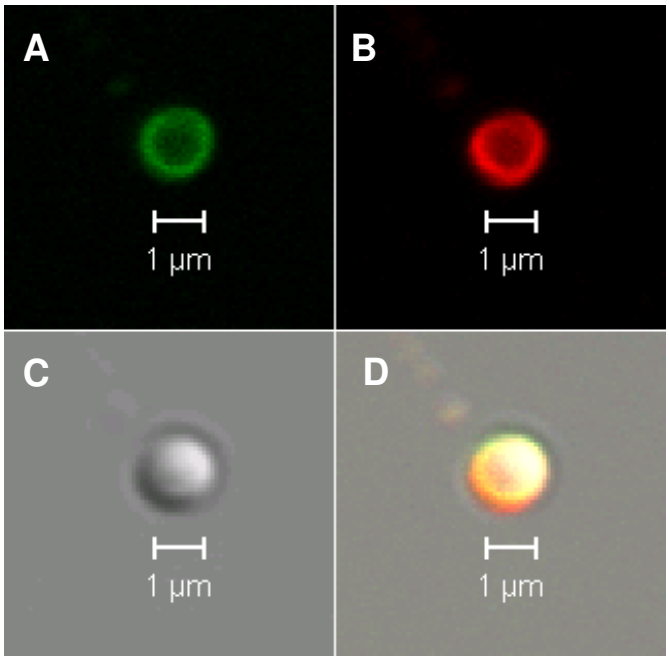

Figure 2.2 Confocal images of mitochondria incubated with α-synuclein

Isolated mitochondrion from HeLa cells incubated with fluorescently-labeled α-synuclein (A), and Mito Tracker Red (B), differential interference contrast (C), and the merged images (D).

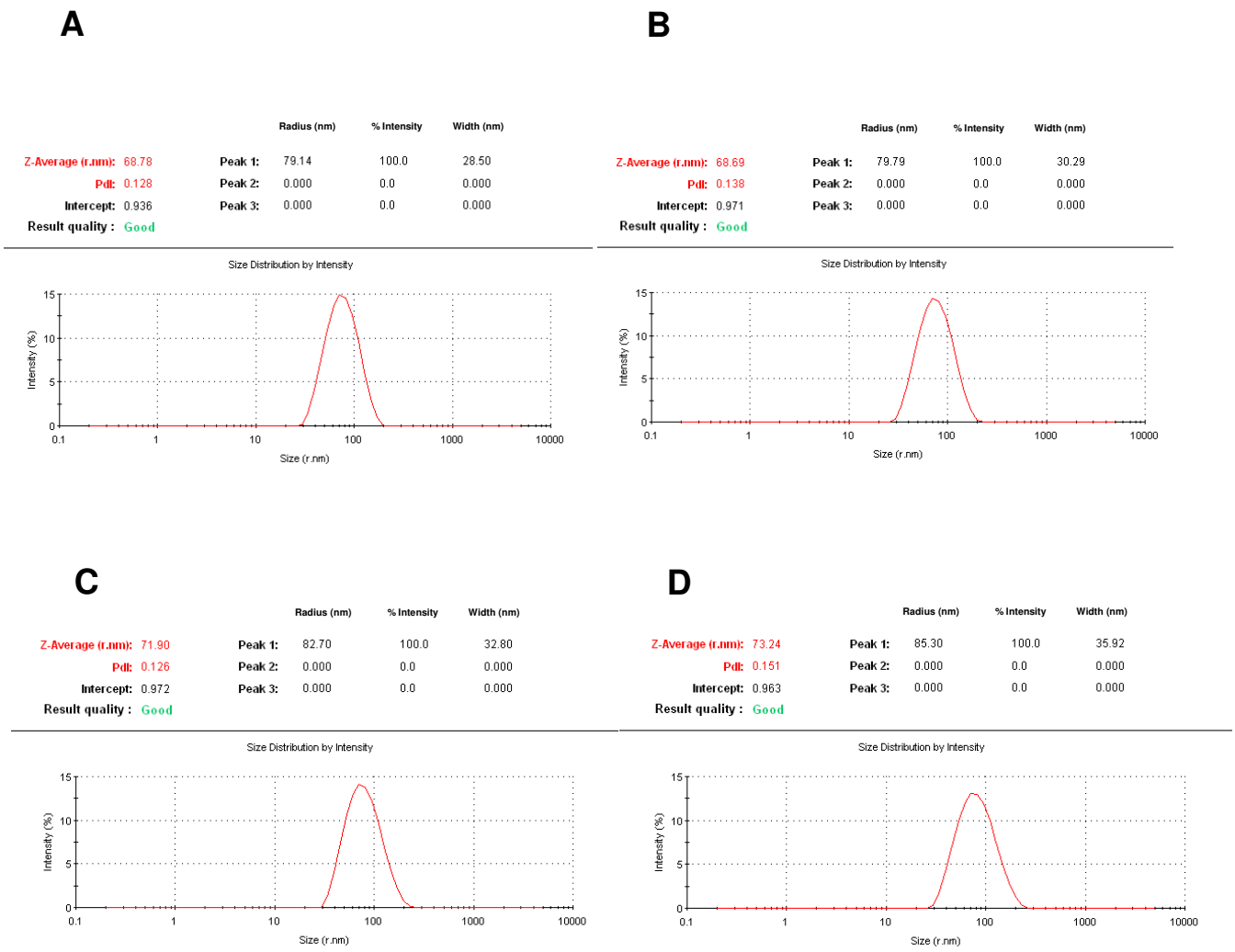

Figure 2.3 Size and polydispersity index of LUVs

Size and polydispersity index (PDI) of vesicles having a composition similar with mitochondrial inner membrane with CL (A) and without CL (B). Size and distribution of vesicles having a composition similar with mitochondrial outer membrane with CH (C) and without CH (D).

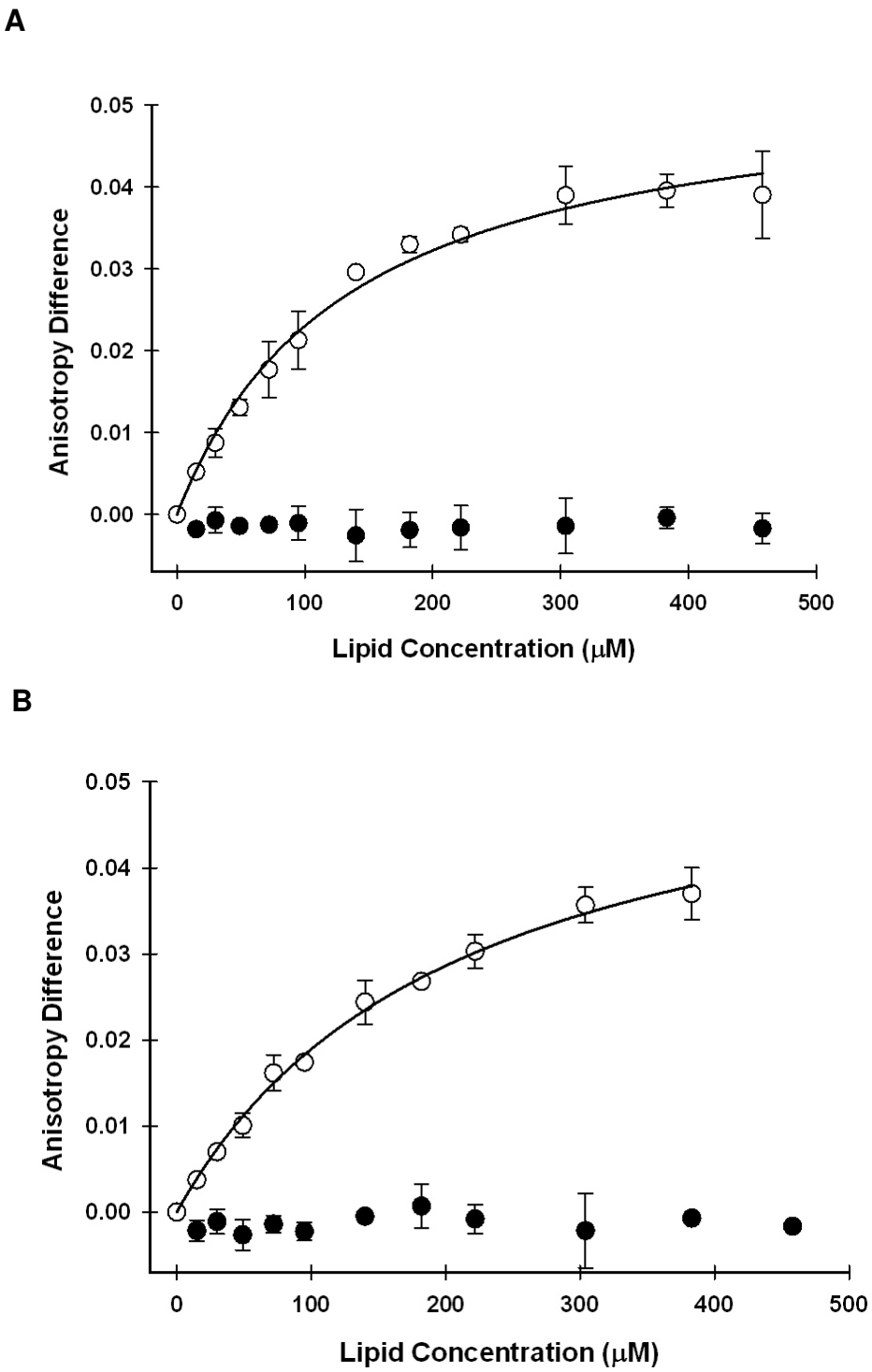

Figure 2.4 Interaction of α-synucleins with OM and IM LUVs

Interaction of fluorescently-labeled V3C α-synuclein (A) and V3C;A30P α-synuclein (B) with LUVs having a composition similar to that of the inner (○) and outer (●) membranes. Error bars represent the standard deviations from triplicate experiments.

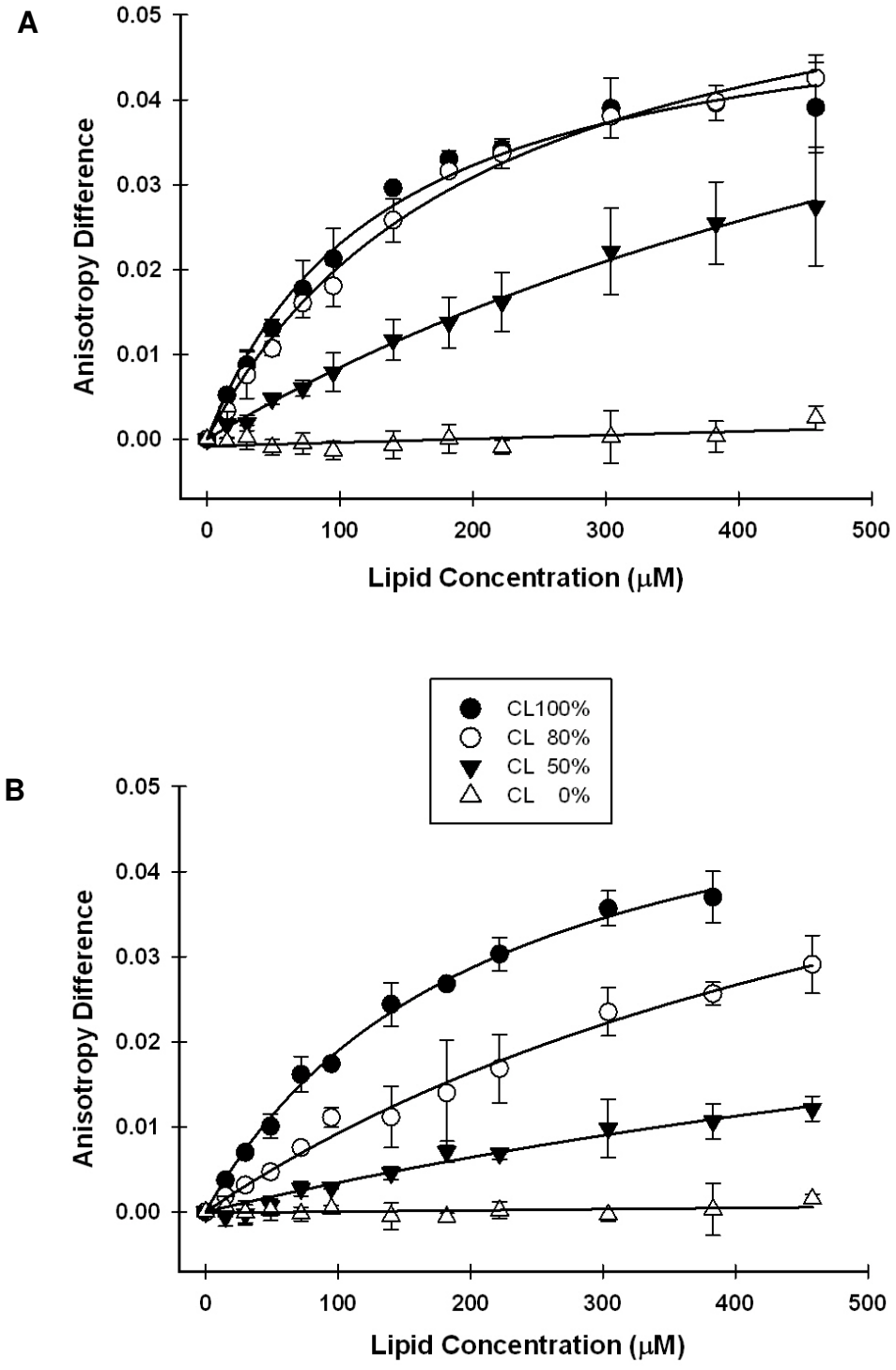

Figure 2.5 Interaction of α-synucleins with LUVs having different CL ratio

Differential binding affinity of fluorescently labeled - V3C α-synuclein (A) and - V3C;A30P α-synuclein (B) to LUVs having a composition similar to the inner membrane but varying amounts of CL. Error bars represent the standard deviations from triplicate experiments.

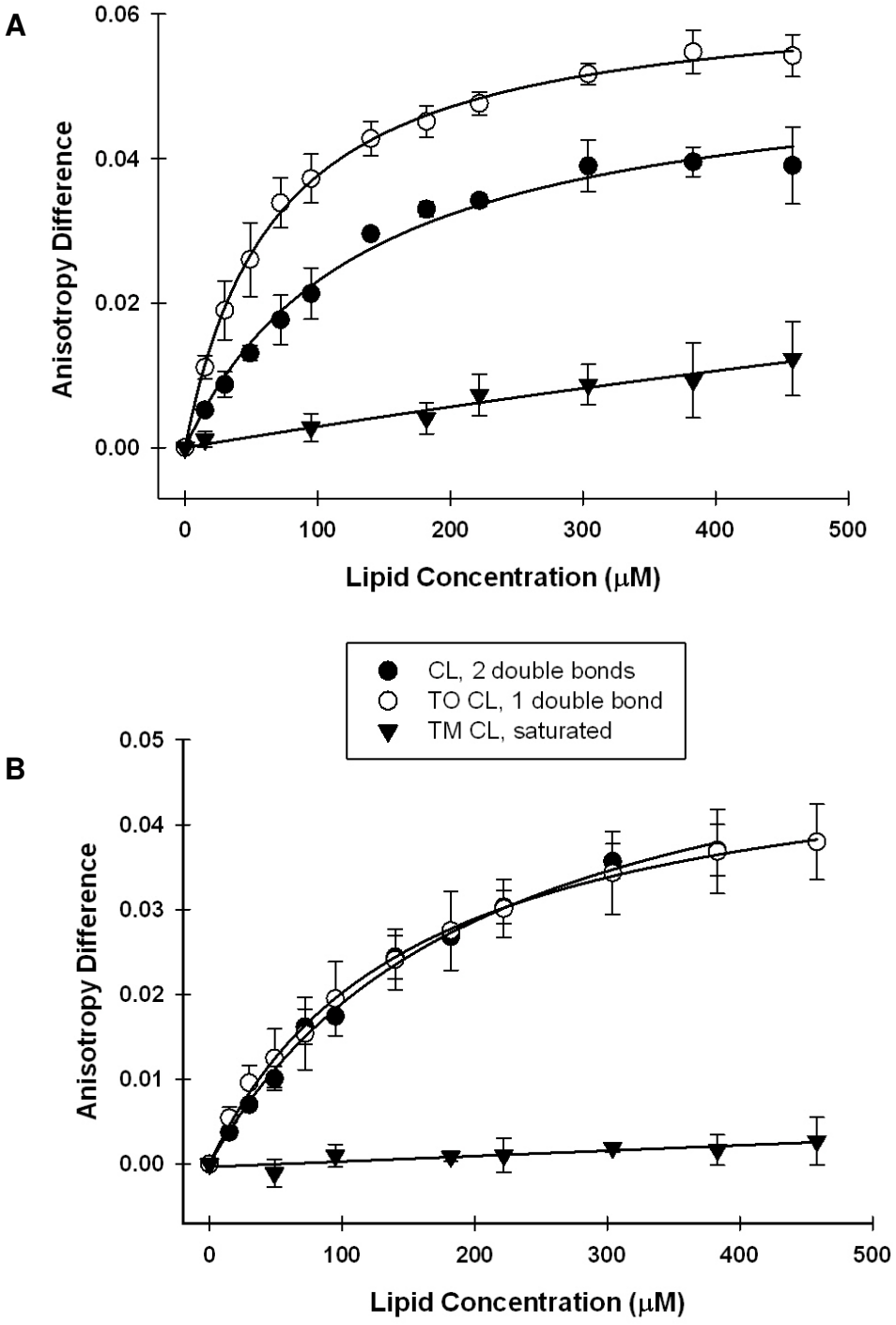

Figure 2.6 Interaction of α-synucleins with LUVs containing CLs with different side chains

Binding of fluorescently labeled - V3C α-synuclein (A) and - V3C;A30P α-synuclein (B) to LUVs with a composition similar with inner membrane but different degrees of side chain saturation. Error bars represent the standard deviations from triplicate experiments.

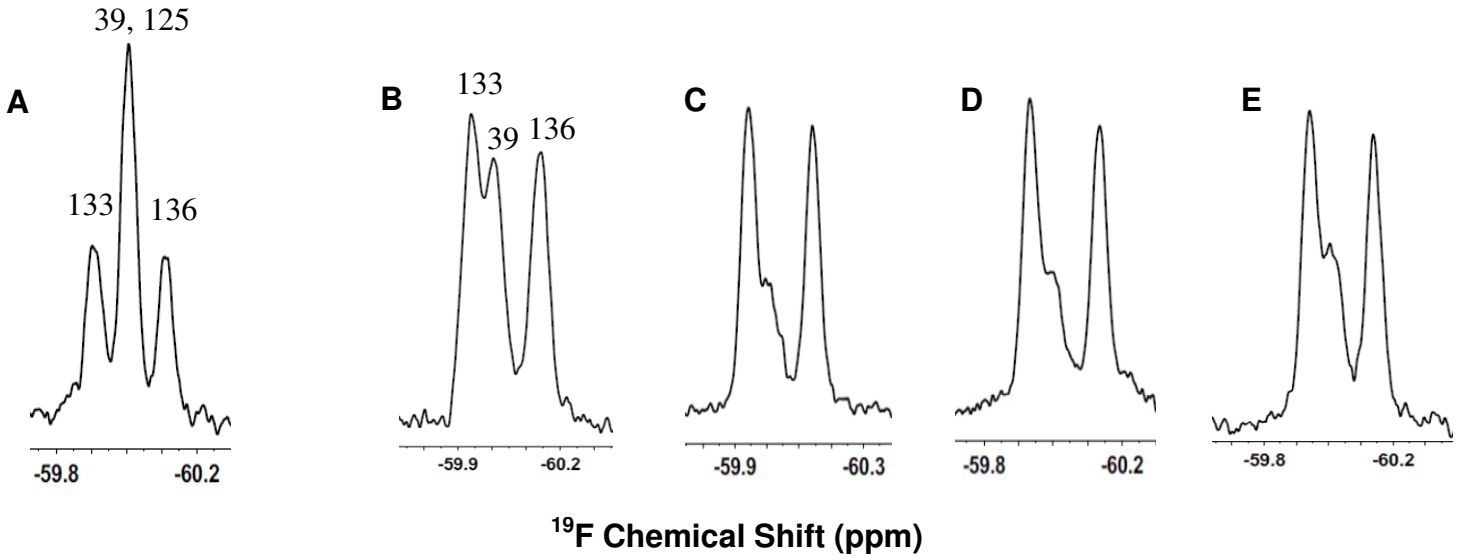

Figure 2.7 ^{19}F NMR spectra of α-synuclein interaction with LUVs containing CLs with different side chains

^{19}F NMR spectra of tyrosine labeled wild-type (A) and Y125F (B) α-synuclein in buffer and the labeled Y125F variant in the presence of LUVs containing 100% CL (C), TO CL (D), and TM CL (E). Assignments are shown above the resonances (*27*). The molar ratio of protein to lipid is ~1:100.

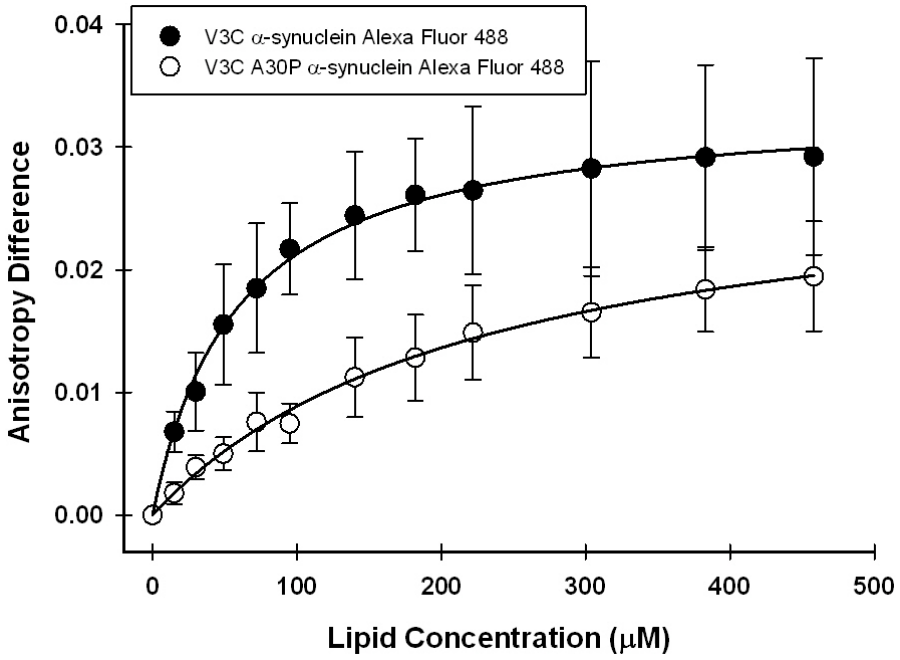

Figure 2.8 Interaction of α-synucleins with LUVs at 37 °C

Interaction of fluorescently-labeled-V3C α-synuclein and -V3C;A30P α-synuclein with LUVs having a composition similar to the inner membrane at 37 °C. Error bars represent the standard deviations from triplicate experiments.

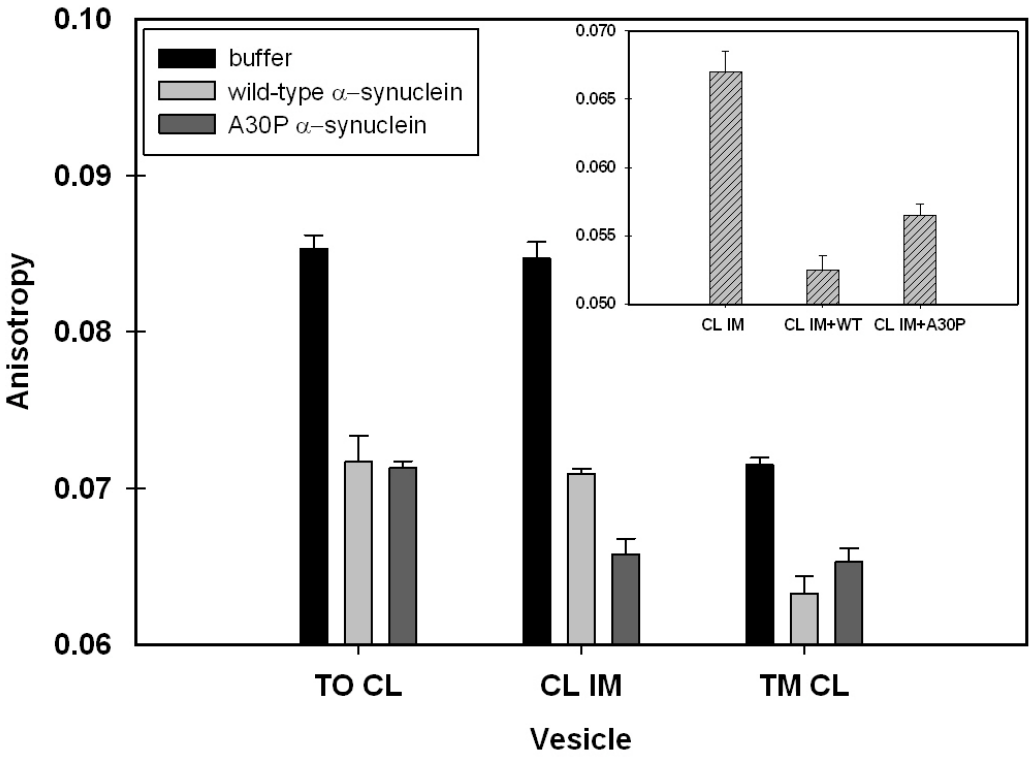

Figure 2.9 DPH anisotropy upon the interaction of α-synucleins with LUVs

DPH anisotropy upon the interaction of α-synucleins with LUVs having different CL acyl side chains at 25 ℃. The inset shows the anisotropy of CL IM in the presence and absence of α-synucleins at 37 ℃. Error bars represent the standard deviations from 5 experiments.

2.6 References

1. J.P. Anderson, D.E. Walker, J.M. Goldstein, R. de Laat, K. Banducci, R.J. Caccavello, R. Barbour, J. Huang, K. Kling, M. Lee, L. Diep, P.S. Keim, X. Shen, T. Chataway, M.G. Schlossmacher, P. Seubert, D. Schenk, S. Sinha, W.P. Gai, T.J. Chilcote, Phosphorylation of Ser-129 is the dominant pathological modification of alpha-synuclein in familial and sporadic Lewy body disease, The journal of biological chemistry 281 (2006) 29739-29752.

2. E. Junn, R.D. Ronchetti, M.M. Quezado, S.Y. Kim, M.M. Mouradian, Tissue transglutaminase-induced aggregation of alpha-synuclein: Implications for Lewy body formation in Parkinson's disease and dementia with Lewy bodies, Proceedings of the national academy of sciences of the united states of America 100 (2003) 2047-2052.

3. C. Liu, E. Fei, N. Jia, H. Wang, R. Tao, A. Iwata, N. Nukina, J. Zhou, G. Wang, Assembly of lysine 63-linked ubiquitin conjugates by phosphorylated alpha-synuclein implies Lewy body biogenesis, The journal of biological chemistry 282 (2007) 14558-14566.

4. K.C. Luk, C. Song, P. O'Brien, A. Stieber, J.R. Branch, K.R. Brunden, J.Q. Trojanowski, V.M. Lee, Exogenous alpha-synuclein fibrils seed the formation of Lewy body-like intracellular inclusions in cultured cells, Proceedings of the national academy of sciences of the united states of America 106 (2009) 20051-20056.

5. T.T. Ding, S.J. Lee, J.C. Rochet, P.T. Lansbury, Jr., Annular alpha-synuclein protofibrils are produced when spherical protofibrils are incubated in solution or bound to brain-derived membranes, Biochemistry 41 (2002) 10209-10217.

6. B.I. Giasson, J.E. Duda, I.V. Murray, Q. Chen, J.M. Souza, H.I. Hurtig, H. Ischiropoulos, J.Q. Trojanowski, V.M. Lee, Oxidative damage linked to neurodegeneration by selective alpha-synuclein nitration in synucleinopathy lesions, Science 290 (2000) 985-989.

7. J.C. Lee, R. Langen, P.A. Hummel, H.B. Gray, J.R. Winkler, Alpha-synuclein structures from fluorescence energy-transfer kinetics: implications for the role of the protein in Parkinson's disease, Proceedings of the national academy of sciences of the united states of America 101 (2004) 16466-16471.

8. M.G. Spillantini, R.A. Crowther, R. Jakes, M. Hasegawa, M. Goedert, Alpha-synuclein in filamentous inclusions of Lewy bodies from Parkinson's

disease and dementia with Lewy bodies, Proceedings of the national academy of sciences of the united states of America 95 (1998) 6469-6473.

9. V.N. Uversky, J. Li, A.L. Fink, Evidence for a partially folded intermediate in alpha-synuclein fibril formation, The journal of biological chemistry 276 (2001) 10737-10744.

10. M. Zhu, J. Li, A.L. Fink, The association of alpha-synuclein with membranes affects bilayer structure, stability, and fibril formation, The journal of biological chemistry 278 (2003) 40186-40197.

11. J. Burre, M. Sharma, T. Tsetsenis, V. Buchman, M.R. Etherton, T.C. Sudhof, Alpha-synuclein promotes SNARE-complex assembly *in vivo* and *in vitro*, Science 329 1663-1667.

12. L. Devi, V. Raghavendran, B.M. Prabhu, N.G. Avadhani, H.K. Anandatheerthavarada, Mitochondrial import and accumulation of alpha-synuclein impair complex I in human dopaminergic neuronal cultures and Parkinson disease brain, The journal of biological chemistry 283 (2008) 9089-9100.

13. N.B. Cole, D. Dieuliis, P. Leo, D.C. Mitchell, R.L. Nussbaum, Mitochondrial translocation of alpha-synuclein is promoted by intracellular acidification, Experimental cell research 314 (2008) 2076-2089.

14. M. Vila, D. Ramonet, C. Perier, Mitochondrial alterations in Parkinson's disease: new clues, Journal of neurochemistry 107 (2008) 317-328.

15. L. Devi, H.K. Anandatheerthavarada, Mitochondrial trafficking of APP and alpha-synuclein: Relevance to mitochondrial dysfunction in Alzheimer's and Parkinson's diseases, Biochimica et biophysica acta 1802 (2010) 11-19.

16. C.E. Ellis, E.J. Murphy, D.C. Mitchell, M.Y. Golovko, F. Scaglia, G.C. Barcelo-Coblijn, R.L. Nussbaum, Mitochondrial lipid abnormality and electron transport chain impairment in mice lacking alpha-synuclein, Molecular and cellular biology 25 (2005) 10190-10201.

17. M.S. Parihar, A. Parihar, M. Fujita, M. Hashimoto, P. Ghafourifar, Mitochondrial association of alpha-synuclein causes oxidative stress, Cellular and molecular life sciences 65 (2008) 1272-1284.

18. R. Sharon, I. Bar-Joseph, G.E. Mirick, C.N. Serhan, D.J. Selkoe, Altered fatty acid composition of dopaminergic neurons expressing alpha-

synuclein and human brains with alpha-synucleinopathies, The Journal of biological chemistry 278 (2003) 49874-49881.

19. G.F. Wang, C. Li, G.J. Pielak, ^{19}F NMR studies of alpha-synuclein-membrane interactions, Protein science 19 1686-1691.

20. E. Rhoades, T.F. Ramlall, W.W. Webb, D. Eliezer, Quantification of alpha-synuclein binding to lipid vesicles using fluorescence correlation spectroscopy, Biophysical journal 90 (2006) 4692-4700.

21. L. Kjaer, L. Giehm, T. Heimburg, D. Otzen, The influence of vesicle size and composition on alpha-synuclein structure and stability, Biophysical journal 96 (2009) 2857-2870.

22. A.C. Ferreon, Y. Gambin, E.A. Lemke, A.A. Deniz, Interplay of alpha-synuclein binding and conformational switching probed by single-molecule fluorescence, Proceedings of the national academy of sciences of the united states of America 106 (2009) 5645-5650.

23. C.C. Jao, B.G. Hegde, J. Chen, I.S. Haworth, R. Langen, Structure of membrane-bound alpha-synuclein from site-directed spin labeling and computational refinement, Proceedings of the national academy of sciences of the united states of America 105 (2008) 19666-19671.

24. R. Kruger, W. Kuhn, T. Muller, D. Woitalla, M. Graeber, S. Kosel, H. Przuntek, J.T. Epplen, L. Schols, O. Riess, Ala30Pro mutation in the gene encoding alpha-synuclein in Parkinson's disease, Nature genetics 18 (1998) 106-108.

25. B.C. McNulty, G.B. Young, G.J. Pielak, Macromolecular crowding in the *Escherichia coli* periplasm maintains alpha-synuclein disorder, Journal of molecular biology 355 (2006) 893-897.

26. R.A. Ruf, E.A. Lutz, I.G. Zigoneanu, G.J. Pielak, Alpha-Synuclein conformation affects its tyrosine-dependent oxidative aggregation, Biochemistry 47 (2008) 13604-13609.

27. C. Li, E.A. Lutz, K.M. Slade, R.A. Ruf, G.F. Wang, G.J. Pielak, 19F NMR studies of alpha-synuclein conformation and fibrillation, Biochemistry 48 (2009) 8578-8584.

28. S. Addya, H.K. Anandatheerthavarada, G. Biswas, S.V. Bhagwat, J. Mullick, N.G. Avadhani, Targeting of NH2-terminal-processed microsomal protein to mitochondria: a novel pathway for the biogenesis of hepatic mitochondrial P450MT2, The journal of cell biology 139 (1997) 589-599.

29. K.M. Slade, B.L. Steele, G.J. Pielak, N.L. Thompson, Quantifying green fluorescent protein diffusion in Escherichia coli by using continuous photobleaching with evanescent illumination, The journal of physical chemistry 113 (2009) 4837-4845.

30. A. Tzagoloff, Mitochondria, Plenum Press, New York, 1982.

31. W.S. Davidson, A. Jonas, D.F. Clayton, J.M. George, Stabilization of alpha-synuclein secondary structure upon binding to synthetic membranes, The journal of biological chemistry 273 (1998) 9443-9449.

32. M.E. Haque, T.J. McIntosh, B.R. Lentz, Influence of lipid composition on physical properties and peg-mediated fusion of curved and uncurved model membrane vesicles: "nature's own" fusogenic lipid bilayer, Biochemistry 40 (2001) 4340-4348.

33. M.E. Haque, L.L. Spremulli, C.J. Fecko, Identification of protein-protein and protein-ribosome interacting regions of the C-terminal tail of human mitochondrial inner membrane protein Oxa1L, The journal of biological chemistry 285 34991-34998.

34. K. Kamiya, J. Kobayashi, T. Yoshimura, K. Tsumoto, Confocal microscopic observation of fusion between baculovirus budded virus envelopes and single giant unilamellar vesicles, Biochimica et biophysica acta 1798 1625-1631.

35. C.W. Bertoncini, Y.S. Jung, C.O. Fernandez, W. Hoyer, C. Griesinger, T.M. Jovin, M. Zweckstetter, Release of long-range tertiary interactions potentiates aggregation of natively unstructured alpha-synuclein, Proceedings of the national academy of sciences of the united states of America 102 (2005) 1430-1435.

36. C.R. Bodner, A.S. Maltsev, C.M. Dobson, A. Bax, Differential phospholipid binding of alpha-synuclein variants implicated in Parkinson's disease revealed by solution NMR spectroscopy, Biochemistry 49 862-871.

37. M.J. Volles, P.T. Lansbury, Jr., Vesicle permeabilization by protofibrillar alpha-synuclein is sensitive to Parkinson's disease-linked mutations and occurs by a pore-like mechanism, Biochemistry 41 (2002) 4595-4602.

38. E. London, G.W. Feigenson, Convenient and Sensitive Fluorescence Assay for Phospholipid Vesicles Using Diphenylhexatriene, Analytical biochemistry 88 (1978) 203-211.

39. M. Shinitzky, Y. Barenholz, Fluidity parameters of lipid regions determined by fluorescence polarization, Biochimica et biophysica acta 515 (1978) 367-394.

40. D. Eliezer, E. Kutluay, R. Bussell, Jr., G. Browne, Conformational properties of alpha-synuclein in its free and lipid-associated states, Journal of molecular biology 307 (2001) 1061-1073.

41. E. Jo, J. McLaurin, C.M. Yip, P. St George-Hyslop, P.E. Fraser, alpha-Synuclein membrane interactions and lipid specificity, The journal of biological chemistry 275 (2000) 34328-34334.

42. M. Stockl, P. Fischer, E. Wanker, A. Herrmann, Alpha-synuclein selectively binds to anionic phospholipids embedded in liquid-disordered domains, Journal of molecular biology 375 (2008) 1394-1404.

43. E. Jo, N. Fuller, R.P. Rand, P. St George-Hyslop, P.E. Fraser, Defective membrane interactions of familial Parkinson's disease mutant A30P alpha-synuclein, Journal of molecular biology 315 (2002) 799-807.

44. D.P. Karpinar, M.B. Balija, S. Kugler, F. Opazo, N. Rezaei-Ghaleh, N. Wender, H.Y. Kim, G. Taschenberger, B.H. Falkenburger, H. Heise, A. Kumar, D. Riedel, L. Fichtner, A. Voigt, G.H. Braus, K. Giller, S. Becker, A. Herzig, M. Baldus, H. Jackle, S. Eimer, J.B. Schulz, C. Griesinger, M. Zweckstetter, Pre-fibrillar alpha-synuclein variants with impaired beta-structure increase neurotoxicity in Parkinson's disease models, The EMBO journal 28 (2009) 3256-3268.

CHAPTER 3

Interaction of Proteins and Peptides with Plasma Membrane Studied by Fluorine NMR

Summary

Fluorine NMR is a powerful tool for monitoring the insertion and conformation of cell-penetrating peptides upon interaction with cellular plasma membrane. To gain insight into the interaction of proteins and peptides with the membrane, α-synuclein and a modified α-synuclein with a cell-penetrating peptide covalently attached to its N-terminus were studied. By monitoring the decrease in the resonances of 3-fluoro-tyrosine labeled proteins, important information about the change in conformation of the protein in the presence of cells was noted. With α-synuclein, a decrease in the resonance from position 39 was noted indicating that only the N-terminus interacts with the plasma membrane. However, when the fusion construct was incubated with cells, a decrease in the resonance from the peptide region was noted while no change was noted in the resonances from α-synuclein region. Longer incubation, studied by using confocal fluorescence microscopy, reveals that the fusion construct translocates inside the cells but α-synuclein by itself did not cross the membrane in considerable amounts.

3.1 Introduction

Biological components have to be delivered to intracellular compartments in significant amounts to observe effects in the cytosol, nucleus, or other organelles. The greatest barrier to delivery is the cellular plasma membrane. A series of delivery systems has been developed to overcome this problem.

Cell-penetrating peptides cross the plasma membrane in an energy independent mode [1-3]. The peptide can be non-covalently attached to the cargo [4], overexpressed as fused biomolecule in bacteria (if the cargo is a protein) [5, 6], or bound through noncovalent (electrostatic and/or hydrophobic) interactions [7]. Several cell-penetrating peptides have been developed [5, 6]. One of the most popular peptide is the trans-acting activator of transcription (TAT) from the human immunodeficiency virus (HIV-1), which assures intracellular delivery of proteins [8], oligonucleotides [9, 10], liposomes [11], or nanoparticles [12]. TAT has a nuclear localization sequence that targets the fused proteins to the nucleus [13]. TAT fused to the N-terminus of α-synuclein was delivered to astrocytes [14] and PC12 [15] cells. Kim et al. [5] designed a cytoplasmic transduction peptide (CTP) derived from TAT, which delivers biomolecules to the cytoplasm rather than to the nucleus. Among the sequences tested, the eleven amino-acid sequence, YGR_2AR_6, proved most efficient in translocating β-galactosidase into several cell lines. After transduction, the peptide is cleaved by cytoplasmic enzymes, releasing its cargo. CTP has increased transduction potential compared with TAT [5].

Fluorine nuclear magnetic resonance spectroscopy (^{19}F NMR) has a high sensitivity to the environment and allows the monitoring of interactions via the decrease in ^{19}F signal intensity. Also, it is a powerful probe for in-cell and *in vivo* studies because there is no background. Fluorine NMR is a suitable technique for studying protein-ligand interactions [16], fibril formation [17], and protein interaction with lipid vesicles [18], or sodium dodecyl sulfate micelles [19]. ^{19}F NMR has also been used to study the interaction of peptides with small unilamellar vesicles, bicelles [20] and living cells [21].

Here, we used ^{19}F NMR to study the interaction of wild-type α-synuclein and a CTP-α-synuclein construct with the plasma membrane of Chinese hamster ovary (CHO-K1) cells. We also investigated the effect of incubation time of the fused construct with the cells and the penetration of the peptide into the membrane. Longer incubation resulted in translocation of the protein across plasma membrane. Intracellular localization of the fluorescently-labeled construct was studied by confocal imaging in CHO-K1, human epithelial carcinoma (HeLa) cells, and cultured primary murine neurons. The results advance our understanding on the interaction of proteins and peptides with the plasma membrane and prove that ^{19}F NMR is a valuable tool for probing these interactions.

3.2 Experimental Procedures

3.2.1 Site-directed Mutagenesis

The CTP-α-synuclein construct was created in two steps with a Stratagene site-directed mutagenesis kit. First, YGR_2A was inserted at the N-terminus of wild-type α-synuclein gene by using the following primers:

Forward 5'-3':

GCAGGAGATATACATATGTATGGCCGTCGTGCGGATGTATTCATGAAAGG

Reverse 5'-3':

CCTTTCATGAATACATCCGCACGACGGCCATACATATGTATATCTCCTGC

Second, the R_6 fragment was inserted using the following primers:

Forward 5'-3':

GTATGGCCGTCGTGCGCGTCGTCGTCGTCGTCGTGATGTATTCATGAAAGG

Reverse 5'-3':

CTTTCATGAATACATCACGACGACGACGACGACGCGCACGACGGCCATAC'

The insertions were confirmed with the sequencing primer:

5'-GGGAGACCACAACGGTTTCCCTCTAG-3'.

The V3C mutation was generated in the α-YGR_2AR_6 synuclein mutant by using the following primers:

Forward 5'-3':

CGTCGTCGTCGTCGTCGTGATTGCTTCATGAAAGGACTTTCAAAG

Reverse 5'-3':

CTTTGAAAGTCCTTTCATGAAGCAATCACGACGACGACGACGACG.

3.2.2 Expression and Purification of α-Synuclein Variants

V3C α-synuclein and V3C CTP-α-synuclein were expressed in *E. coli* and purified as described by McNulty et al. [22] with modifications. Briefly, the pT7-7 plasmids containing the wild-type, V3C, CTP or V3C CTP-α-synuclein genes were transformed into *E. coli* BL21-Gold(DE3) competent cells (Stratagene Cloning Systems, La Jolla, CA) and plated on Luria broth agar plates containing 100 μg/mL ampicillin (LB_{Amp}). A single colony was added to 50 mL of LB_{Amp} and the culture was grown in a rotary shaker (225 rpm) for 16-18 h at 37 ℃. The overnight culture was used to inoculate one liter of $LB_{Amp,}$ which was grown to an optical density at 600 nm of 0.6-0.8. The culture was induced with isopropyl-β-D-thiogalactopyranoside to a final concentration of 1 mM, followed by protein expression for 4 h and then centrifugation (Sorvall RC-5B, SS-34 rotor) at 4000 rpm for 30 min at 4 ℃. The cell pellet was resuspended in 20 mL of lysis buffer (10 mM Tris, pH 8.0, 1 mM phenylmethanesulfonylfluoride, 1 mM ethylenediaminetetraacetic acid). Dithiothreitol (final concentration 1 mM) was added to the buffer for V3C wild-type and V3C CTP-α-synucleins. The cells were sonicated, the lysate was boiled and centrifuged. The supernatant was subjected to 10 mg/mL streptomycin sulfate precipitation and the supernatant subjected to $(NH_4)_2SO_4$ precipitation (360 g/L). The pellet was resuspended in 20 mM Tris (pH 7.7) and dialyzed (SnakeSkin, MWCO 3500, Pierce) against the same buffer, overnight at 4 ℃. Next, the protein was purified by using anion exchange chromatography (AKTA FPLC UPC-900, Q-10 column, Amersham Pharmacia Biotech, Pittsburgh, PA) with a 1-M NaCl linear gradient at 4 ℃ followed by gel filtration chromatography (Superdex 75, Amersham Pharmacia Biotech). Protein

purity was assessed with sodium dodecyl sulfate polyacrylamide gel electrophoresis (SDS-PAGE, BioRad, Hercules, CA) with Coomassie Brilliant blue staining. The insertion of YGR_2AR_6 was confirmed by using matrix-assisted laser desorption/ionization mass spectrometry (MALDI-MS) of Lys C digested samples. Purified α-synuclein was lyophilized and stored at –80 °C. α-Synucleins labeled with 3-fluoro-tyrosine (3FY) were expressed and purified as described by Li et al. [17].

3.2.3 Alexa Fluor Labeling

Twelve mg of V3C α-synuclein or V3C CTP-α-synuclein were dissolved in sterile degassed water to a final concentration of 2 mg/mL. T*ris*(2-carboxyethyl)phosphine and $NaHCO_3$ were added to the mixture in a molar excess of 10:1 with respect to protein. The mixture was incubated at room temperature with shaking for 30 min. Next, Alexa Fluor 488 C5-maleimide (Invitrogen) was added in a ten-fold excess to α-synuclein. The mixture was incubated at room temperature with shaking for 2 h. The labeled α-synuclein was purified by gel filtration chromatography using Superdex 75 column and 20% acetonitrile with PBS as an eluent. The labeled protein was dialyzed against water, and the labeling efficiency was determined as described in the Alexa Fluor 488 C5-maleimide labeling protocol (Invitrogen). The absorbance at 494 nm along with the extinction coefficient of 71,000 $M^{-1}cm^{-1}$ for Alexa Fluor 488 was used to quantify the labeled α-synuclein. The Lowry method was used to quantify the total amount of protein (Lowry protein assay kit, Pierce). Aliquots of 1 mg labeled protein were lyophilized and stored at –80 °C.

3.2.4 Cell Culture

Chinese hamster ovary cells (CHO-K1) and human epithelial carcinoma cells (HeLa) were obtained from the UNC Lineberger Cancer Center. Cells were seeded in 6-well glass plates (Corning Life Sciences, Lowell, MA) at a density of ~$2x10^5$ cells/well with the cells in media (F-12 media for CHO-K1 cells and Dulbecco's modified Eagle's media for HeLa cells) supplemented with 10% fetal bovine serum (FBS), penicillin (100 units/mL), and streptomycin (100 µg/mL) at 37 ℃ in 5% CO_2. Primary murine sympathetic neurons dissected from the superior cervical ganglia were prepared as described by Deshmukh and Johnson [23] and then seeded at ~$2x10^4$ neurons/6-well collagen coated plate. The neurons were kept in AM50 media supplemented with 10% FBS, penicillin (100 units/mL), streptomycin (100 µg/mL), and neuronal growth factor at 37 ℃ in 5% CO_2.

3.2.5 Fluorine NMR

NMR spectra of 3FY-labeled α-synuclein were acquired at 37 ℃ on a Varian Inova 600 MHz NMR spectrometer at a frequency of 564.5 MHz using a 5 mm triple resonance probe (Varian 600 H-F(C,X)). The CHO-K1 cells were incubated with ^{19}F-labeled CTP-α-synuclein in F-12 media at 37 ℃ for different times. Aliquots from this mixture were mixed with equal volumes of 20% (w/v) Ficoll solution in F-12 media. The final sample contained 100 µM ^{19}F CTP-α-synuclein in F-12 media with ~$1.5x10^7$ cells/mL in 20% (w/v) Ficoll and 10% D_2O. The interaction of the CHO-K1 cells with ^{19}F-labeled wild-type α-synuclein and Y125F α-synuclein were studied in the same way. Cell viability was tested after

each NMR experiment by using the trypan blue exclusion assay. The viability was always greater than 90%.

3.2.6 Fluorescence Image Acquisition and Quantification

The cells were treated with fluorescently-labeled CTP-α-synuclein for 20 h. For imaging, four washing steps with PBS were performed after protein translocation. The cells were imaged in their complete media with a Zeiss confocal microscope equipped with LSM 5 software and a 40x oil objective. In addition, mitochondria were stained with Mito Tracker Red CMX Ros (Invitrogen) immediately prior to imaging. Fluorescence measurements were acquired with multichannel detection using 488 nm excitation (argon laser) for Alexa Fluor 488 labeled protein and 543 nm excitation (HeNe1 laser) for Mito Tracker Red. Untreated cells were tested under the same conditions to assess autofluorescence.

3.3 Results and Discussion

3.3.1 CTP-α-Synuclein Expression, Purification and Labeling

The fused construct (Figure 3.1) was expressed in *E. coli*. The CTP-α-synuclein expression level is ~2/3 that of the wild-type protein under the same conditions as assessed by comparing the chromatograms of the two proteins at 280 nm (Figure 3.2 *A*). The construct was pure as tested on SDS-PAGE (Figure 3.2 *B*). The CTP insertion was confirmed by matrix-assisted laser desorption/ionization mass spectroscopy analysis (Figure 3.3). V3C α-synuclein and V3C CTP-α-synuclein were labeled with Alexa Fluor 488 maleimide dye at

efficiencies of ~90% and ~80%, respectively. The single band on the SDS PAGE indicates that the labeled sample is pure (Figure 3.4).

3.3.2 Cell Suspensions for NMR Experiments

Studying the interaction of wild-type and CTP-α-synuclein with the plasma membrane with fluorine NMR requires that the cells remain suspended during data acquisition. CHO-K1 cells tend to settle quickly to the bottom of NMR tube because of their relatively large size (diameter ~20 μm). Settling of the cells and the ^{19}F-labeled protein or fused construct attached to their surface will remove the sample from the NMR detection zone, degrading the accuracy of data acquisition. A few trials were done to solve this problem.

A Shigemi NMR tube was used. Figure 3.5 shows a Shigemi tube loaded with α-synuclein in Hibernate E media (BrainBits, Springfield, IL). The main advantage of a Shigemi tube is that even if the cells settle, they will still be in the detection zone. Once cells settle, however, they are deprived of nutrients, and the pH can change in a short time thus decreasing cell viability. Hibernate E (BrainBits LLC, Springfield, IL) keeps the media at a pH that facilitates survival when cells are kept outside of their natural environment for a short time. Hibernate E was not useful for our experiment, because of the large amount of cells settling as shown by the low viability (<20%).

Several devices [24], gels [25], and natural biodegradable polymers [26] have been used to prolong cells viability during NMR experiments. Ficoll, a hydrophilic polysaccharide, was used to prevent settling of *Xenopus laevis*

oocytes during NMR data acquisition [27]. To our knowledge, there are no reports on using Ficoll to keep mammalian cells in suspension.

We tested the ability of Ficoll to keep CHO-K1 cells in suspension at 37 ℃ (Figure 3.6). After 3 h in the NMR tube, the cells settled in 10% (w/v) Ficoll and exhibited low viability. At 20% (w/v) the cells remained in suspension with a viability of 92%. At higher concentration, Ficoll may induce floatation of cells. We concluded that 20% (w/v) Ficoll is optimal for keeping CHO-K1 cells in the NMR detection zone.

3.3.3 Interaction of Wild-type and Y125F α-Synucleins with Plasma Membrane

^{19}F-labeled wild-type α-synuclein was incubated with the cells as described in the Experimental Procedure Section. A decrease in the intensity of the middle peak was noted in the presence of cells (Figure 3.7 *A*). This decrease is probably caused by restricted motion of the protein region that interacts with plasma membrane. The middle peak represents an overlap of the resonances from positions 39 and 125 [17]. We used Y125F α-synuclein to determine which of the two resonances changed upon interaction with the cells. For this variant, the middle peak corresponds only to the resonance from position 39. A significant decrease in the resonance from position 39 was noted upon incubating Y125F α-synuclein with the cells, while the resonances from positions 133 and 136 remained almost unchanged (Figure 3.7 *B*). No significant change in peaks intensity was noted when Y39F α-synuclein was used (Figure 3.9). Thus it appears that only the N-terminal region interacts with plasma membrane.

Control experiments were performed to check if the decrease noted is an artifact caused by experimental conditions. For instance, the decrease could be caused by a slight change in pH. To test this idea, we collected the data for the Y125F variant under the same conditions as those used for the sample containing the cells, but at pH ~6. No decrease in intensity was noted for the resonance at position 39 but there was a slight change in chemical shift (Figure 3.8 *A*). Fluorine NMR has a high sensitivity to the environment [28]. We also tested the effect of Ficoll. We kept the Y125F variant in 20% (w/v) Ficoll in media for 12 h. No change in the intensities was noted between the initial sample, and the final sample (Figure 3.8 *B*). We concluded that a slight change in the pH of media or the presence of Ficoll would not cause a decrease in the resonance at position 39, and the reduction is an effect of the protein interacting with the cells. However, if the cells were mixed with 20% (w/v) Ficoll first and then the protein was added, a broadening of the middle peak was noted perhaps as a result of the increased viscosity of Ficoll.

3.3.4 Interaction of CTP-α-Synuclein with the Plasma Membrane

^{19}F-labeled CTP-α-synuclein was used to study the early stage insertion of the CTP into the plasma membrane. CTP-α-synuclein has five tyrosines, one in the CTP at position -11, one at the position 39 in the N-terminal region of α-synuclein, and three in the C-terminal region (Figure 3.1). Figure 3.9*A* shows the spectrum of 3FY-labeled fusion protein in F-12 media containing 20% (w/v) Ficoll and 10% D_2O. A significant change was noted when CHO-K1 cells were added (Figure 3.10 *B*). After 1h, one resonance disappeared leaving a spectrum

resembling that of wild-type α-synuclein (Figure 3.10 *C*). The decrease and disappearance of resonance is attributed to the interaction of the CTP in the fused construct with the plasma membrane. In summary, most of the fusion construct bound to the cells in the first hour as shown by the disappearance of resonance at position 39.

Comparing the interaction of ^{19}F-labeled α-synuclein and ^{19}F-labeled CTP-α-synuclein with the plasma membrane suggests a model wherein α-synuclein's N-terminal region lies along the surface of the membrane. This is because only the region around position 39 interacts with the cells while the resonances from C-terminus remain unaffected suggesting that the C-terminal region is not in the proximity of membrane. No significant translocation of fluorescently-labeled protein was noted when wild-type α-synuclein was used as tested by confocal microscopy imaging. This observation indicates that the protein does not cross the plasma membrane, but rather only its N-terminus interacts with the cells. For CTP-α-synuclein, a different type of binding is proposed. The CTP inserts perpendicular to the cellular lipid bilayer while the α-synuclein portion does not interact with plasma membrane after 1h of incubation, as suggested by the observation that the resonance at position 39 is unaffected. Perhaps some of the fused construct penetrates the lipid bilayer in the first hour, but the amount was insufficient for detection.

We attempted to assign the Y-11 resonance in the fusion protein by using the 3FY-labeled Y-11F variant but the ^{19}F resonances from the remaining tyrosines were not well resolved (Figure 3.11). This may be due to intra- and

intermolecular interactions between the positively charged CTP and N-terminus α-synuclein and the negatively charged α-synuclein C-terminus (Figure 3.1). To confirm that the peptide is interacting with plasma membrane and to verify that CTP-α-synuclein is translocating into the cells, we used a different approach.

3.3.5 Translocation of CTP α-Synuclein in Cells

Translocation of CTP-α-synuclein into mammalian cells was tested by incubating the fluorescently-labeled construct with cells for 20 h. Three cell lines, CHO-K1, HeLa, and primary culture neurons, were tested. The CTP translocated α-synuclein into all the cell types (Figure 3.12). As shown in the left hand column of Figure 3.12, CTP targeted the cargo to the cytoplasm as previously shown [5]. Mitochondrial staining confirmed localization of the protein to the cytoplasm with no fluorescence present in the nucleus. Mitochondria have a uniform distribution in the cytosol, surrounding the nucleus. Some co-localization of α-synuclein and mitochondria was noted in all three cell lines, especially in the neuronal cell line. This observation agrees with the findings presented in Chapter 2, and with other studies suggesting interaction of α-synuclein with mitochondria and lipid vesicles [29-33]. Control experiments using fluorescently-labeled α-synuclein under the same conditions showed no significant intracellular fluorescence when the same settings of the microscope were used. This observation indicates that α-synuclein does not cross the plasma membrane in the absence of CTP. No autofluorescence was noted for the cells used. These data support our model that α-synuclein N-terminus is along to the membrane surface while CTP is inserted in the lipid bilayer of plasma membrane.

3.4 Conclusion

Fluorine NMR, combined with fluorescence microscopy, provides information on the interaction and change in conformation of α-synuclein and CTP-α-synuclein. This study proves the utility of ^{19}F NMR for investigating the interactions between proteins and plasma membrane. This technique can be a powerful tool for investigation of interactions and translocation of various carriers into the cells.

3.5 Figures

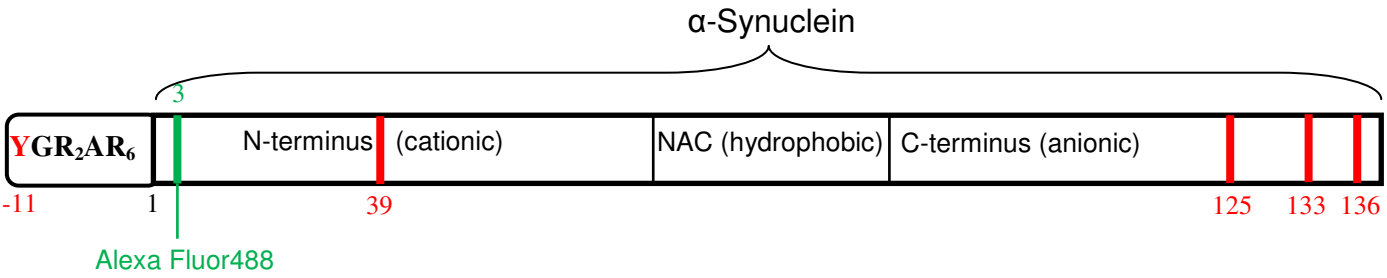

Figure 3.1 Schematic representation of CTP covalently attached to the N-terminus of α-synuclein

The red bars show the positions of tyrosines. The green bar shows the fluorescently-labeled position.

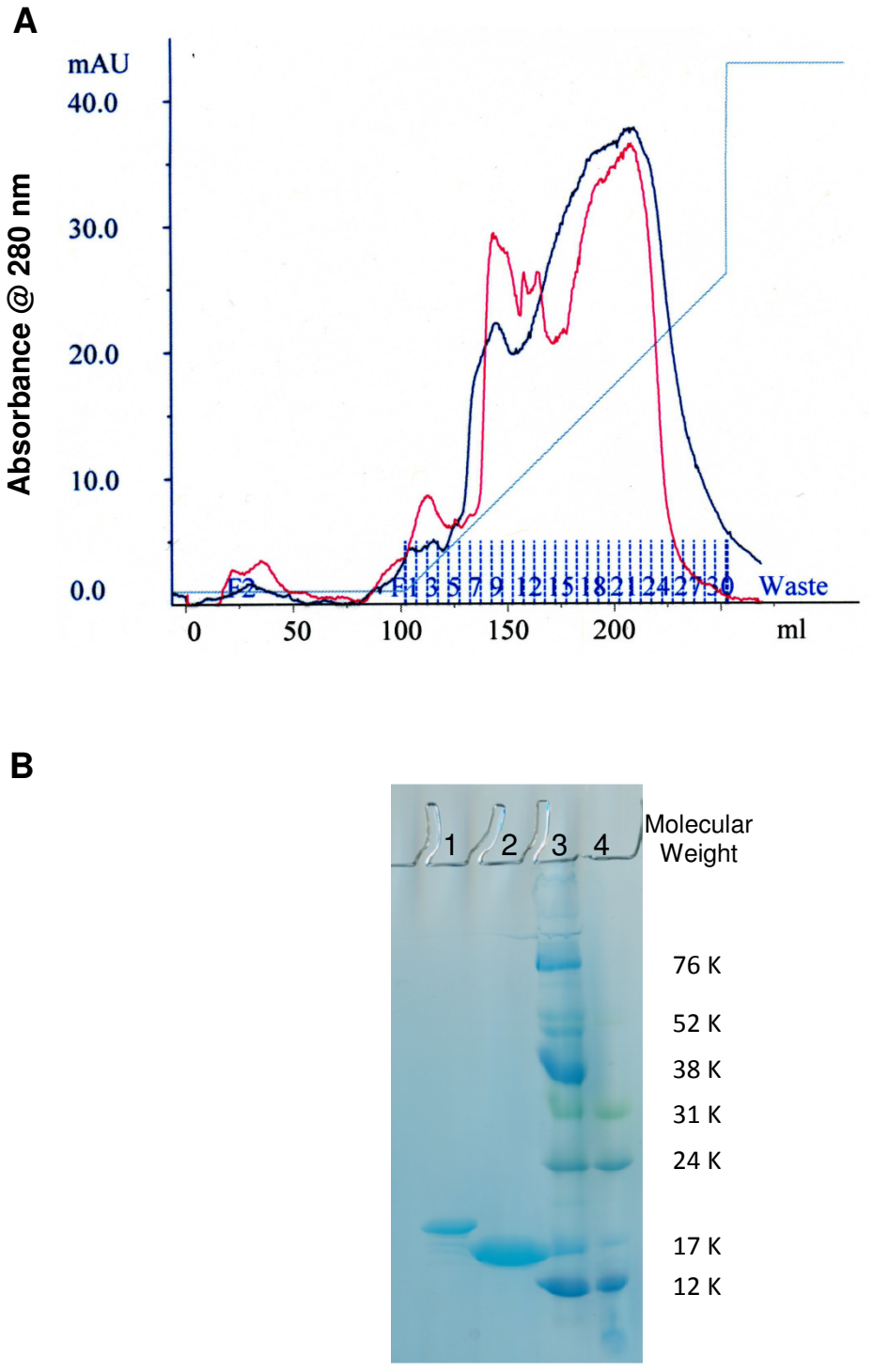

Figure 3.2 Chromatograms and SDS-PAGE of wild-type and CTP-α-synuclein

Chromatograms of α-synuclein (*A* red, fractions 7-9) and CTP-α-synuclein (*A* dark blue, fractions 5-9) elution from an anion exchange column and SDS-PAGE analysis (B) of CTP-α-synuclein (lane 1),α-synuclein (lane 2), and protein markers (lanes 3 and 4).

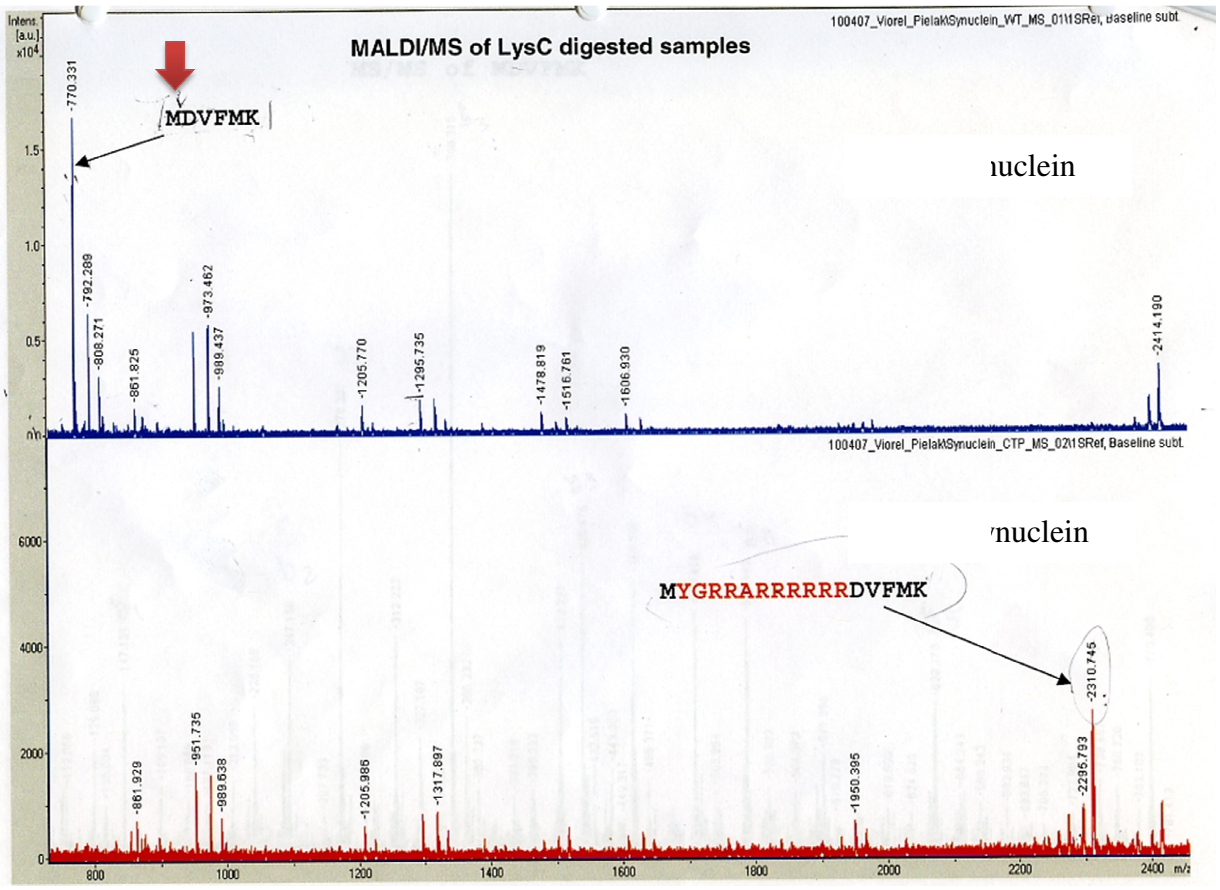

Figure 3.3 MALDI/MS of wild-type and CTP-α-synuclein

Matrix-assisted laser desorption/ionization mass spectroscopy analysis of wild-type α-synuclein (top) and CTP-α-synuclein (bottom). The CTP insertion is highlighted in red.

Figure 3.4 Purified CTP-α-synuclein

SDS-PAGE of purified, fluorescently-labeled V3C CTP-α-synuclein after size exclusion chromatography. The lanes represent the fractions eluted from FPLC.

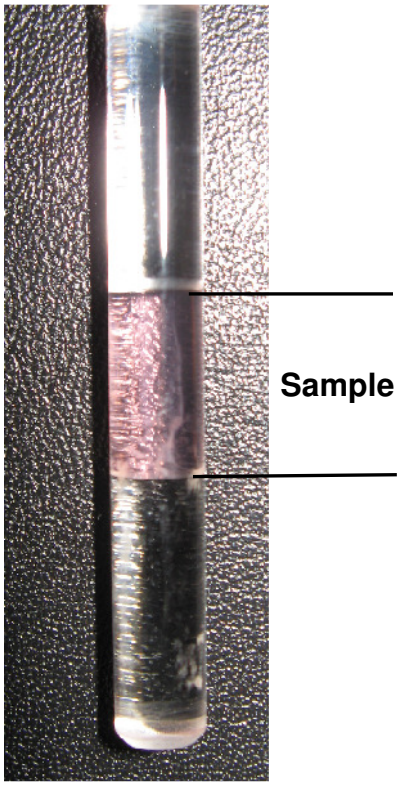

Figure 3.5 NMR sample

Shigemi tube containing 300 µL ^{15}N-enriched α-synuclein in Hibernate E (10% D_2O)

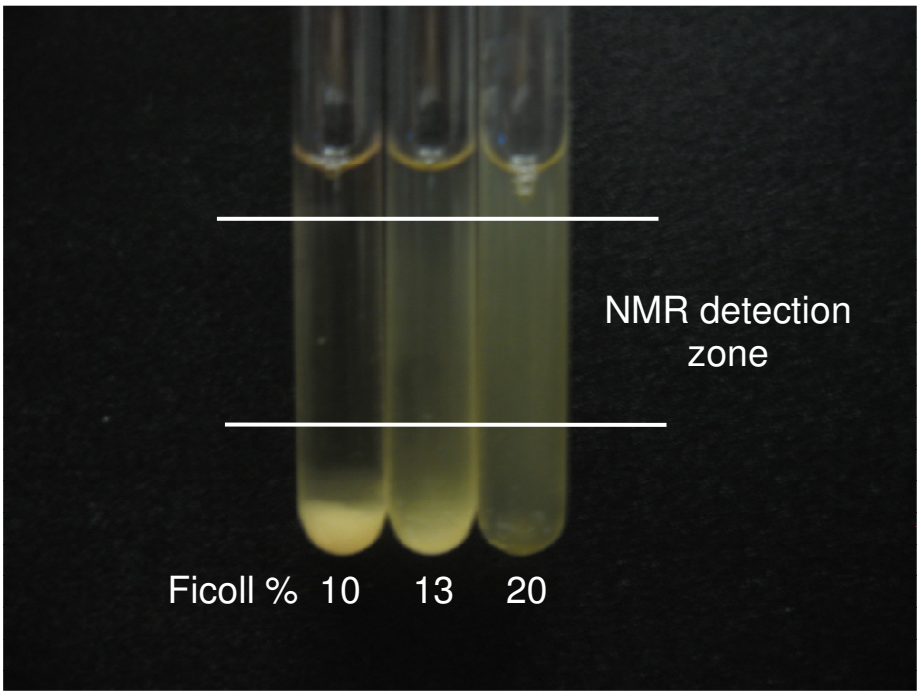

Figure 3.6 NMR tubes containing cells suspended in Ficoll

NMR tubes containing $6x10^6$ CHO-K1 cells in 300 µL of F-12 media containing 10% D_2O with various (w/v) concentrations of Ficoll at 37 ℃ after 3h. The cells viability was 92%.

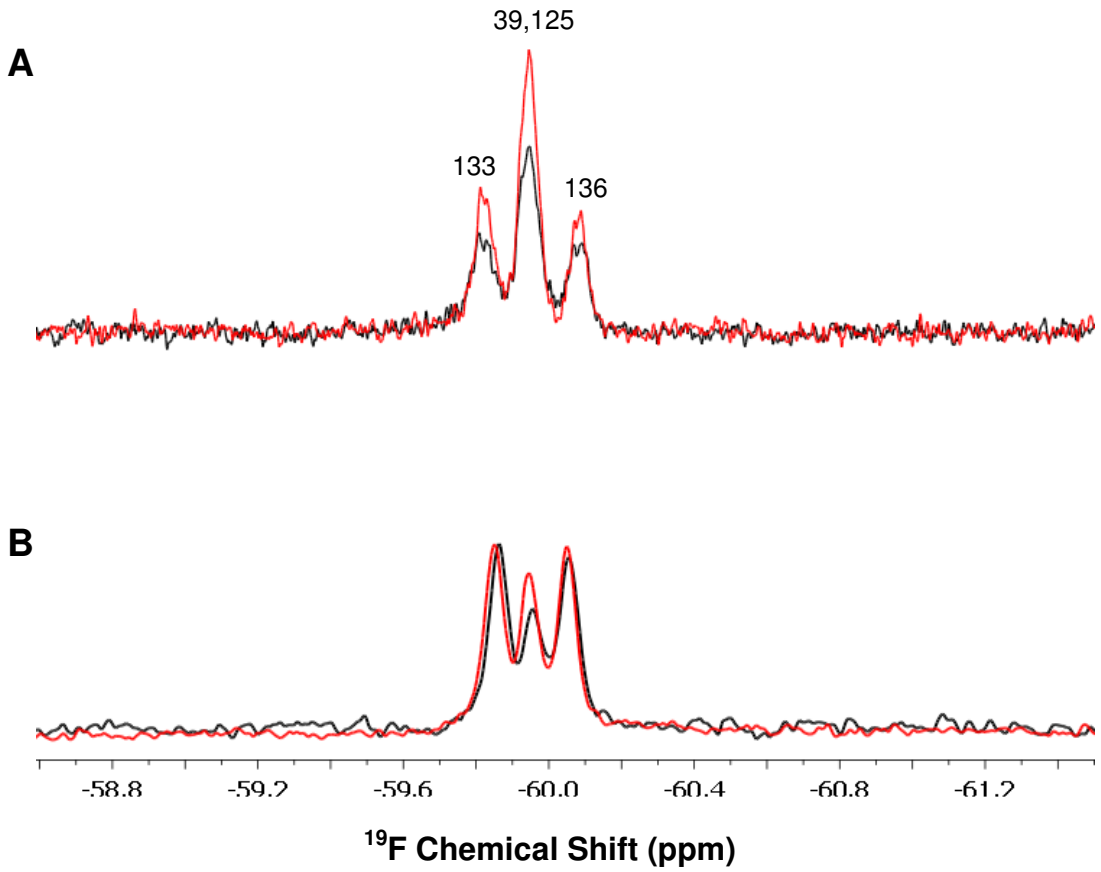

Figure 3.7 ^{19}F NMR spectra of wild-type and Y125F α-synuclein

(A) Interaction of ^{19}F-labeled wild-type α-synuclein and (B) ^{19} F-labeled Y125F α-synuclein with CHO-K1 cells in 20% (w/v) Ficoll. Red spectra were acquired in the absence of cells. The protein concentration was 100 μM. Residue assignments are shown above the spectra in panel A.

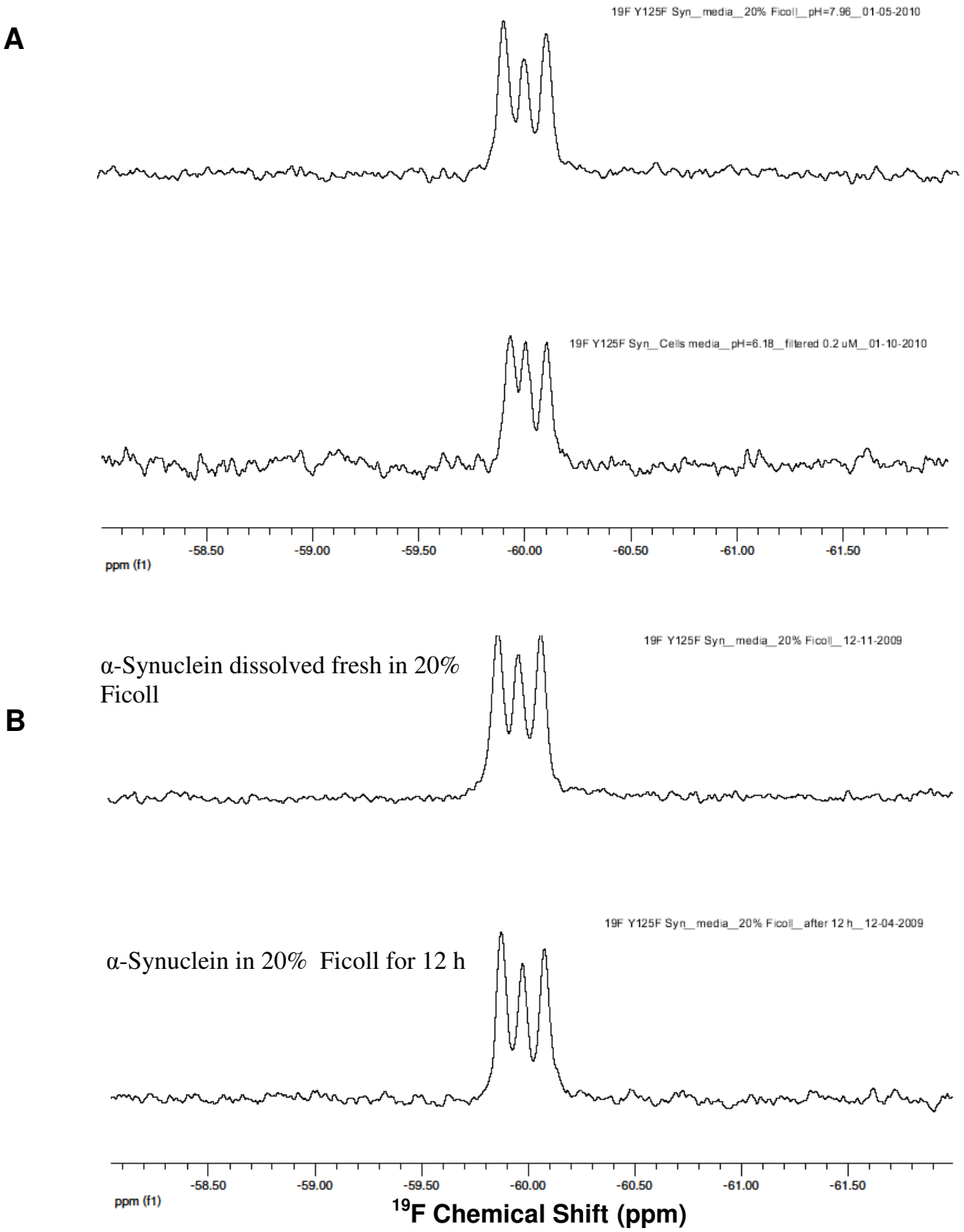

Figure 3.8 α-Synuclein in Ficoll - controls

(A) Effect of pH and (B) incubation time in Ficoll on the ^{19}F spectrum of Y125F α-synuclein.

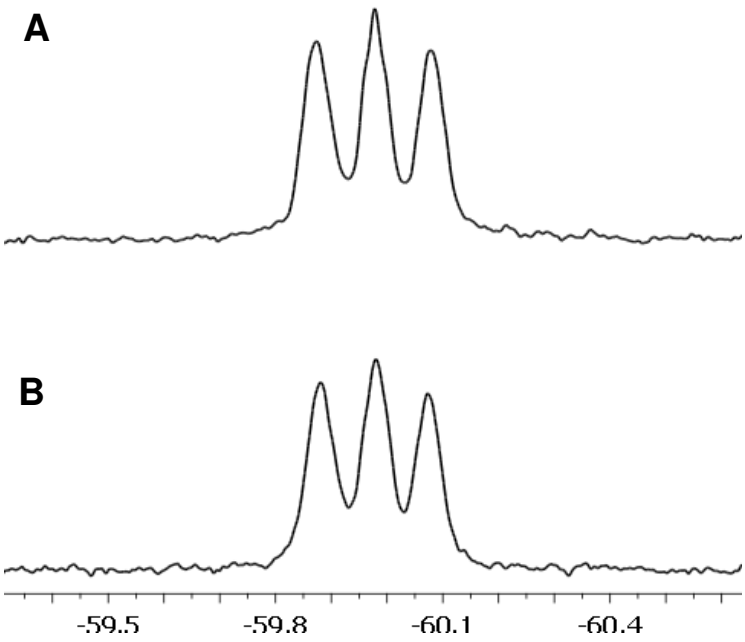

Figure 3.9 Interaction of ^{19}F-labeled Y39F α-synuclein with CHO-K1 cells

(A) protein only, (B) protein and cells.

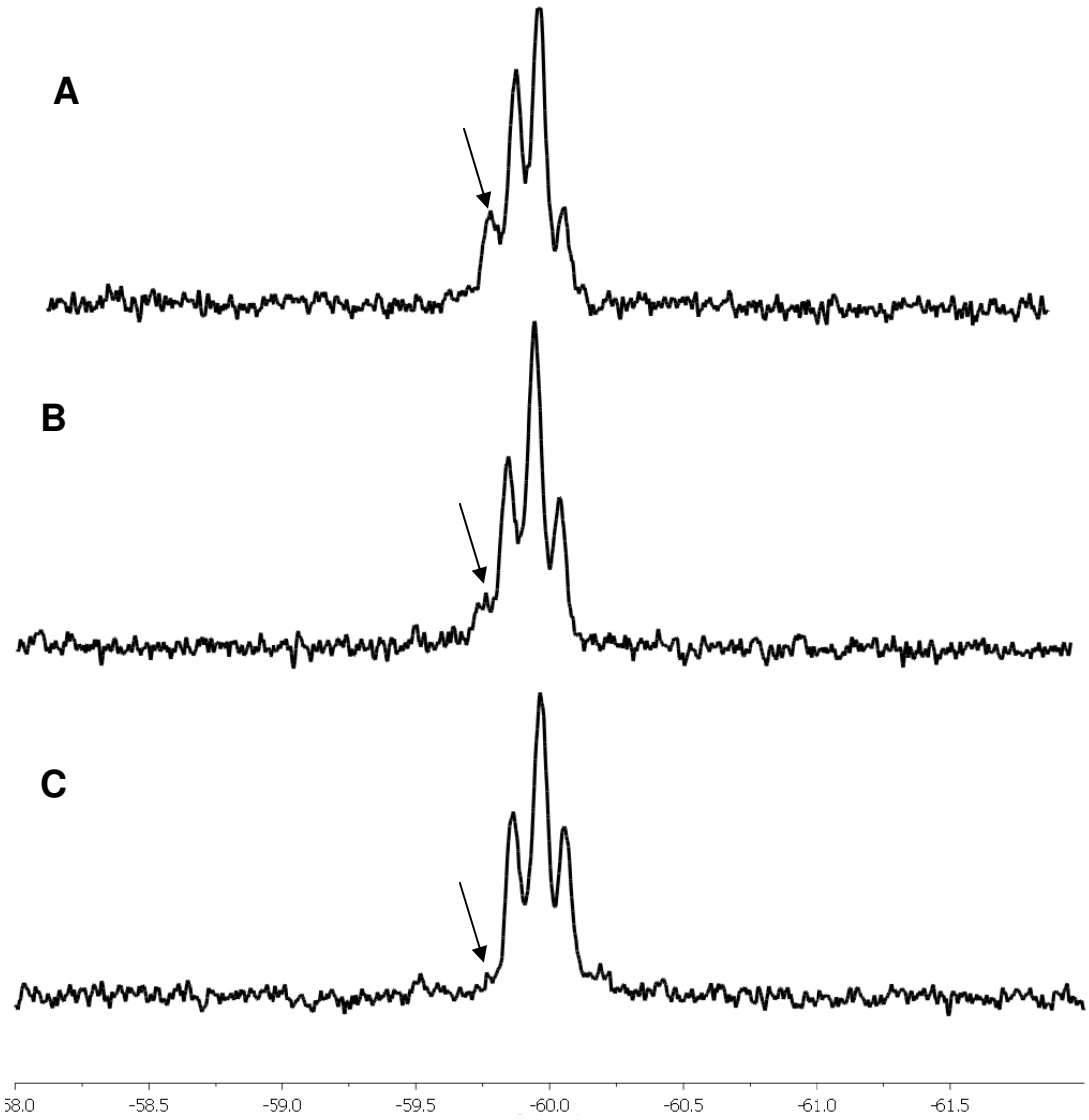

Figure 3.10 Interaction of ^{19}F-labeled CTP-α-synuclein with CHO-K1 cells

Interaction of ^{19}F-labeled CTP-α-synuclein with CHO-K1 cells as a function of time. (A) CTP-α-synuclein in media with 20% Ficoll, (B) CTP-α-synuclein and CHO-K1 cells in media with 20% (w/v) Ficoll, (C) CTP-α-synuclein with CHO-K1 cells in media with 20% Ficoll incubated at 37 ℃ for 1 h. The protein concentration was 100 μM. The arrow indicates the decrease in the resonance from Y-11.

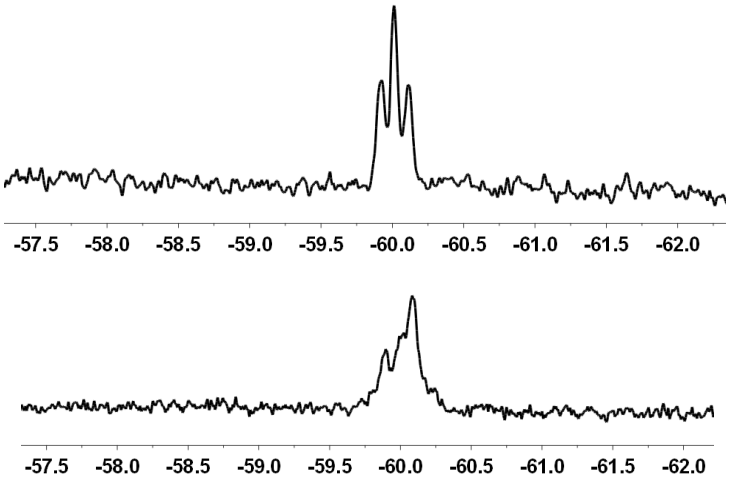

Figure 3.11 Attempted assignments of the Y-11 resonance in CTP-α-synuclein

The spectra were collected in 50 mM sodium phosphate buffer, pH 7.4 at 37 ℃. Top: 3FY labeled wild-type α-synuclein; Bottom: Y-11F CTP-α-synuclein.

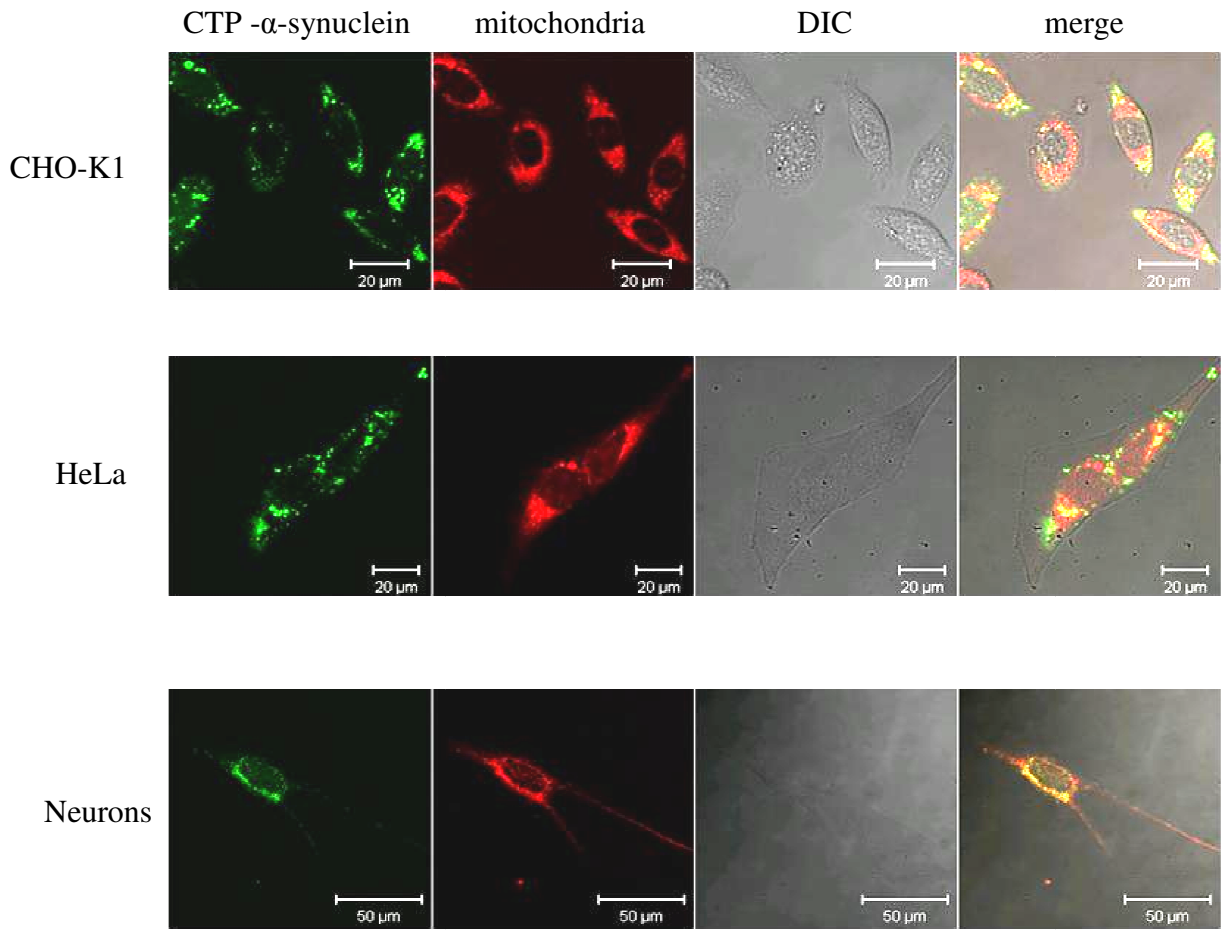

Figure 3.12 CTP mediated delivery of α-synuclein into cells

CTP mediated delivery of fluorescently-labeled α-synuclein into CHO-K1 cells, HeLa cells, and primary culture neurons. From left to right: Alexa Fluor 488 (green). Mito Tracker Red fluorescence (red), differential interference contrast, and merge of the three images.

3.6 References

1. S.T. Henriques, A. Quintas, L.A. Bagatolli, F. Homble, M.A. Castanho, Energy-independent translocation of cell-penetrating peptides occurs without formation of pores. A biophysical study with pep-1, Molecular membrane biology 24 (2007) 282-293.

2. V.P. Torchilin, TAT peptide-modified liposomes for intracellular delivery of drugs and DNA, Cellular & molecular biology letters 7 (2002) 265-267.

3. A. Lamaziere, C. Wolf, O. Lambert, G. Chassaing, G. Trugnan, J. Ayala-Sanmartin, The homeodomain derived peptide Penetratin induces curvature of fluid membrane domains, PloS one 3 (2008) e1938.

4. M. Pooga, U. Soomets, M. Hallbrink, A. Valkna, K. Saar, K. Rezaei, U. Kahl, J.X. Hao, X.J. Xu, Z. Wiesenfeld-Hallin, T. Hokfelt, T. Bartfai, U. Langel, Cell penetrating PNA constructs regulate galanin receptor levels and modify pain transmission *in vivo*, Nature biotechnology 16 (1998) 857-861.

5. D. Kim, C. Jeon, J.H. Kim, M.S. Kim, C.H. Yoon, I.S. Choi, S.H. Kim, Y.S. Bae, Cytoplasmic transduction peptide (CTP): new approach for the delivery of biomolecules into cytoplasm *in vitro* and *in vivo*, Experimental cell research 312 (2006) 1277-1288.

6. K. Inomata, A. Ohno, H. Tochio, S. Isogai, T. Tenno, I. Nakase, T. Takeuchi, S. Futaki, Y. Ito, H. Hiroaki, M. Shirakawa, High-resolution multi-dimensional NMR spectroscopy of proteins in human cells, Nature 458 (2009) 106-109.

7. M.C. Morris, J. Depollier, J. Mery, F. Heitz, G. Divita, A peptide carrier for the delivery of biologically active proteins into mammalian cells, Nature biotechnology 19 (2001) 1173-1176.

8. E. Kubo, N. Fatma, Y. Akagi, D.R. Beier, S.P. Singh, D.P. Singh, TAT-mediated PRDX6 protein transduction protects against eye lens epithelial cell death and delays lens opacity, American journal of physiology 294 (2008) C842-855.

9. A. Eguchi, T. Akuta, H. Okuyama, T. Senda, H. Yokoi, H. Inokuchi, S. Fujita, T. Hayakawa, K. Takeda, M. Hasegawa, M. Nakanishi, Protein transduction domain of HIV-1 Tat protein promotes efficient delivery of DNA into mammalian cells, The Journal of biological chemistry 276 (2001) 26204-26210.

10. A. Ziegler, J. Seelig, High affinity of the cell-penetrating peptide HIV-1 Tat-PTD for DNA, Biochemistry 46 (2007) 8138-8145.

11. V.P. Torchilin, R. Rammohan, V. Weissig, T.S. Levchenko, TAT peptide on the surface of liposomes affords their efficient intracellular delivery even at low temperature and in the presence of metabolic inhibitors, Proceedings of the national academy of sciences of the united states of america 98 (2001) 8786-8791.

12. C.C. Berry, J.M. de la Fuente, M. Mullin, S.W. Chu, A.S. Curtis, Nuclear localization of HIV-1 tat functionalized gold nanoparticles, IEEE transactions on nanobioscience 6 (2007) 262-269.

13. E. Vives, P. Brodin, B. Lebleu, A truncated HIV-1 Tat protein basic domain rapidly translocates through the plasma membrane and accumulates in the cell nucleus, The Journal of biological chemistry 272 (1997) 16010-16017.

14. H.S. Choi, S.H. Lee, S.Y. Kim, J.J. An, S.I. Hwang, D.W. Kim, K.Y. Yoo, M.H. Won, T.C. Kang, H.J. Kwon, J.H. Kang, S.W. Cho, O.S. Kwon, J.H. Choi, J. Park, W.S. Eum, S.Y. Choi, Transduced Tat-alpha-synuclein protects against oxidative stress *in vitro* and *in vivo*, Journal of biochemistry and molecular biology 39 (2006) 253-262.

15. D. Albani, E. Peverelli, R. Rametta, S. Batelli, L. Veschini, A. Negro, G. Forloni, Protective effect of TAT-delivered alpha-synuclein: relevance of the C-terminal domain and involvement of HSP70, FASEB Journal 18 (2004) 1713-1715.

16. L. Yu, P.J. Hajduk, J. Mack, E.T. Olejniczak, Structural studies of Bcl-xL/ligand complexes using ^{19}F NMR, Journal of biomolecular NMR 34 (2006) 221-227.

17. C. Li, E.A. Lutz, K.M. Slade, R.A. Ruf, G.F. Wang, G.J. Pielak, ^{19}F NMR studies of alpha-synuclein conformation and fibrillation, Biochemistry 48 (2009) 8578-8584.

18. G.F. Wang, C. Li, G.J. Pielak, ^{19}F NMR studies of alpha-synuclein-membrane interactions, Protein Science 19 1686-1691.

19. G.F. Wang, C. Li, G.J. Pielak, Probing the micelle-bound aggregation-prone state of alpha-synuclein with ^{19}F NMR spectroscopy, Chembiochem 11 1993-1996.

20. B.C. Buer, J. Chugh, H.M. Al-Hashimi, E.N. Marsh, Using fluorine nuclear magnetic resonance to probe the interaction of membrane-active peptides with the lipid bilayer, Biochemistry 49 (2010) 5760-5765.

21. E. Okamura, K. Ninomiya, S. Futaki, Y. Nagai, T. Kimura, C. Wakai, N. Matubayasi, Y. Sugiura, M. Nakahara, Real-time in-cell F-19 NMR study on uptake of fluorescent and nonfluorescent F-19-octaarginines into human Jurkat cells, Chemistry Letters 34 (2005) 1064-1065.

22. B.C. McNulty, A. Tripathy, G.B. Young, L.M. Charlton, J. Orans, G.J. Pielak, Temperature-induced reversible conformational change in the first 100 residues of alpha-synuclein, Protein science 15 (2006) 602-608.

23. M. Deshmukh, E.M. Johnson, Jr., Evidence of a novel event during neuronal death: development of competence-to-die in response to cytoplasmic cytochrome c, Neuron 21 (1998) 695-705.

24. N.G. Sharaf, C.O. Barnes, L.M. Charlton, G.B. Young, G.J. Pielak, A bioreactor for in-cell protein NMR, Journal of magnetic resonance 202 140-146.

25. F.Y. Hsu, S.W. Tsai, F.F. Wang, Y.J. Wang, The collagen-containing alginate/poly(L-lysine)/alginate microcapsules, Artificial cells, blood substitutes, and immobilization biotechnology 28 (2000) 147-154.

26. I. Ghidoni, T. Chlapanidas, M. Bucco, F. Crovato, M. Marazzi, D. Vigo, M.L. Torre, M. Faustini, Alginate cell encapsulation: new advances in reproduction and cartilage regenerative medicine, Cytotechnology 58 (2008) 49-56.

27. J.F. Bodart, J.M. Wieruszeski, L. Amniai, A. Leroy, I. Landrieu, A. Rousseau-Lescuyer, J.P. Vilain, G. Lippens, NMR observation of Tau in Xenopus oocytes, Journal of magnetic resonance 192 (2008) 252-257.

28. C.J. Deutsch, J.S. Taylor, Intracellular pH as measured by ^{19}F NMR, Annals of the New York academy of sciences 508 (1987) 33-47.

29. C.E. Ellis, E.J. Murphy, D.C. Mitchell, M.Y. Golovko, F. Scaglia, G.C. Barcelo-Coblijn, R.L. Nussbaum, Mitochondrial lipid abnormality and electron transport chain impairment in mice lacking alpha-synuclein, Molecular and cellular biology 25 (2005) 10190-10201.

30. M.S. Parihar, A. Parihar, M. Fujita, M. Hashimoto, P. Ghafourifar, Mitochondrial association of alpha-synuclein causes oxidative stress, Cellular and Molecular Life Sciences 65 (2008) 1272-1284.

31. L. Devi, H.K. Anandatheerthavarada, Mitochondrial trafficking of APP and alpha synuclein: Relevance to mitochondrial dysfunction in Alzheimer's and Parkinson's diseases, Biochimica et biophysica acta 1802 (2010) 11-19.

32. N.B. Cole, D. Dieuliis, P. Leo, D.C. Mitchell, R.L. Nussbaum, Mitochondrial translocation of alpha-synuclein is promoted by intracellular acidification, Experimental cell research 314 (2008) 2076-2089.

33. P.K. Auluck, G. Caraveo, S. Lindquist, Alpha-synuclein: membrane interactions and toxicity in Parkinson's disease, Annual review of cell and developmental biology 26 (2010) 211-233.

Chapter 4

Progress towards In-cell NMR of α-Synuclein Translocated into Mammalian Cells

Summary

The goal of this project was to understand how the crowded environment in mammalian cells affects the structure of α-synuclein and to gain insight into the protein's physiological role by using in-cell NMR. A series of delivery systems were used to translocate α-synuclein across the plasma membrane of higher eukaryotic cells. PEP-1, an amphipathic peptide, was used to form a noncovalent complex with α-synuclein and translocate the protein into cells. To assess translocation, valine 3 was modified to cysteine (V3C) by site-directed mutagenesis, and Alexa Fluor 488 C_5-maleimide dye was used to label α-synuclein at this site. Confocal laser microscopy and staining with Mito Tracker Red confirmed partial localization of α-synuclein at the mitochondrial level. α-Synuclein uptake was quantified by comparing the fluorescence of cell lysates on 10-20% gradient SDS-PAGE to standards. About 100 μM α-synuclein was present in a total of ~10^8 cells. A cytoplasmic transduction peptide covalently attached to the N-terminus of α-synuclein was also used to deliver α-synuclein.

This new biopolymer was also labeled, and confocal laser microscopy confirmed localization at mitochondrial level. Electroporation and two other proprietary reagents were used for delivery of α-synuclein, and translocation assessed by using confocal microscopy of live cells or fluorescence quantification on SDS-PAGE. Preliminary in-cell NMR studies conducted on α-synuclein delivered with PEP-1 shows that the protein's N-terminus was binding or cleaved inside of cells but the signal to noise ratio was very low so no firm conclusion could be drawn.

4.1 Introduction

In-cell NMR studies of natively disordered proteins are important because the size range detectable by NMR is larger for disordered proteins than it is for globular proteins. Also, relevant information about the intracellular behavior of these proteins may be revealed. The increased sensitivity arises from differences in global and local motions for globular and disordered proteins [1]. The properties of globular proteins do not change too much with experimental conditions but the properties of natively disordered proteins can vary significantly [2].

The first in-cell NMR study of an intrinsically disordered protein was reported by Dedmon et al. [3]. The protein, FlgM, regulates flagellar synthesis upon binding a transcription factor. The intracellular environment in *E. coli* causes the C-terminal half of FlgM to gain structure while the N-terminal half remains unstructured. Also, McNulty et al. used in-cell NMR to investigate the of α-synuclein in *E. coli* [4].

The ^{1}H-^{15}N NMR experiments of ^{15}N-enriched B1 domain of streptococcal protein G (GB1) in nucleated higher eukaryotic cells were conducted in *Xenopus laevis* oocytes [5]. The positions of the GB1 resonances remained the same in oocytes and in dilute solution, but a change in cross peak intensity was noted. It can be concluded that the crowded environment in cells does not affect the structure of GB1 but the resonances of amides involved in intramolecular hydrogen bonds are diminished. This observation is consistent with the idea that more dynamic parts of the protein are less affected by the increased viscosity in cells.

The first ^{1}H-^{15}N in-cell NMR spectra in mammalian cells were obtained in HeLa cells. Ubiquitin and ubiquitin derivatives were delivered to the cytosol by using covalently attached cell-penetrating peptides [6]. The ^{1}H-^{15}N heteronuclear multiple quantum coherence spectra showed that the peptide was cleaved by cytosolic enzymes. The ^{1}H-^{15}N intracellular spectrum of ubiquitin after peptide cleavage is similar with that of the protein in dilute solution only the resonances are broader.

The detection of proteins by NMR in higher eukaryotic cells may require the presence of fewer molecules of protein than in bacteria. This is expected because the cytosol of higher eukaryotic cells has a lower apparent viscosity than that of bacteria [7].

In-cell NMR of α-synuclein in higher eukaryotic cells may provide information about its structure, function, and intracellular behavior. However,

NMR is highly insensitive. Consequently, α-synuclein needs an efficient delivery system to reach detectable cytosolic concentrations.

Several types of delivery systems for protein translocation into cells have been developed. These systems include covalent [8-14] and non-covalent peptides [15-19], polymeric nanoparticles [20-22], liposomes [23, 24], electroporation [25, 26].

For this study, a series of delivery systems was used to translocate α-synuclein into CHO-K1 cells, HeLa cells, and neuronal cell lines. Specifically, we examined the peptides PEP-1 and CTP, PULSin reagent, electroporation, and the proprietary QQ reagent provided by Dr. Wang at Wayne State University.

Little is known about the intracellular structure and function of intrinsically disordered proteins, but these proteins are involved in signal transduction and are associated with protein-aggregation-based diseases, including several neurodegenerative disorders. The purpose of this study was to understand the effects of intracellular macromolecular crowding in mammalian cells on intrinsically disordered proteins, and more specifically on α-synuclein.

4.2 Materials and Methods

4.2.1 Substances and Materials

Trypsin and all tissue culture media and reagents were purchased from Invitrogen (Carlsbad, CA). PEP-1 was synthesized by Elim Biopharmaceuticals (Hayward, CA). PULSin was purchased from Polyplus-Transfection (New York, NY) and the electroporation reagents from Lonza Biologics Inc. (Portsmouth, NH). M-PER reagent was purchased from Pierce (Rockford, IL). Ampicillin,

streptomycin sulfate, $(NH_4)_2SO_4$ were purchased from Sigma (Sigma-Aldrich, St. Louis, Mo). Tris(2-carboxyethyl) phosphine hydrochloride (TCEP), phenylmethylsulphonyl fluoride (PMSF) were obtained from Pierce (Rockford, IL). Dithiothreitol (DTT) and isopropyl-beta-D-thiogalactopyranoside (IPTG) were acquired from Fisher Scientific (Fair Lawn, NJ) and ethylenediaminetetraacetic acid (EDTA) from Mallinckrodt (Raleigh, NC).

4.2.2 Site-directed Mutagenesis

The α-YGR_2AR_6 synuclein mutant (CTP-α-synuclein; Figure 3.1) was created in two steps with a Stratagene site-directed mutagenesis kit. First, YGR_2A was inserted at the N-terminus of the wild-type α-synuclein gene and then the R_6 fragment was added (Chapter 3). The V3C CTP-α-synuclein construct was created as mentioned in Chapter 3.

4.2.3 Expression and Purification of α-Synuclein Variants

α-Synuclein constructs were expressed in *E. coli* and purified following the procedure described by McNulty et al. [2] with modifications as described in Chapter 3.

4.2.4 Alexa Fluor Labeling

The V3C and V3C CTP-α-synuclein derivative were labeled with Alexa Fluor 488 C_5-maleimide dye as described in Chapter 3. The extinction coefficient at 494 nm, 71,000 $M^{-1}cm^{-1}$, for Alexa Fluor 488 was used to quantify the fluorescently-labeled protein, and the Lowry assay was used to quantify the total amount of protein. Aliquots of 1 mg labeled protein were lyophilized and stored at – 80 °C.

4.2.5 Cell Culture

The Chinese hamster ovary (CHO-K1) and human epithelial carcinoma (HeLa) cell lines were obtained from UNC Lineberger Cancer Center. Cells were seeded in 6-well plastic uncoated plates (Corning Life Sciences, Lowell, MA) at a density of ~$2x10^5$ cells/well in F-12 for CHO-K1 cells and Dulbecco's modified Eagle's medium, DMEM, for HeLa cells, each supplemented with 10% FBS, penicillin (100 units/mL), and streptomycin (100 µg/mL) at 37 ℃ in 5% CO_2.

Primary murine sympathetic neurons were dissected from the superior cervical ganglion as described by Deshmukh and Johnson [27], and seeded at ~$2x10^4$ neurons/6-well plate coated with collagen. The neurons were kept in AM50 media supplemented with 10% FBS, penicillin (100 units/mL), streptomycin (100 µg/mL), and neuronal growth factor at 37 ℃ in 5% CO_2. For fluorescence imaging, the cells were seeded using the same conditions but on plastic 6-well plates with glass bottoms (Corning).

4.2.6 Carriers for α-Synuclein Translocation into Mammalian Cells

4.2.6.1 PEP-1

Fluorescently-labeled α-synuclein was translocated into CHO-K1, HeLa cells, and neurons by forming a complex with the peptide, PEP-1. The peptide forms ~100 nm diameter complexes with the proteins (Figure 4.1). The protein (100 µg)/PEP-1 complexes with molar ratios 1:40, 1:20, 1:15, and 1:10, respectively, were studied. The complexes were formed in 200 µL PBS and then diluted to 600 µL with serum free media. The mixture was incubated for 30 min at 37 ℃. The cells were then treated with the complex as presented in Figure 4.2.

Cells at 60-80 % confluency were overlaid with α-synuclein/PEP-1 complex and incubated for 30 min at 37 ℃. One mL of media containing serum was added to each well and the cells were further incubated for 2 h. SDS-PAGE (BioRad, Hercules, CA) and standards of 0.10 and 0.010 mg/mL fluorescently-labeled α-synuclein were used to quantify the intracellular concentration of α-synuclein. As controls, cells treated with fluorescently-labeled protein alone (no PEP-1) and untreated cells (to check for autofluorescence) were tested under the same conditions. Next, the cells were washed twice with PBS and then incubated with trypsin/EDTA at 37 ℃ for 5-10 min. The cells were collected by centrifugation and washed with PBS. The cells were imaged and intracellular fluorescently-labeled protein was quantified on SDS-PAGE.

Intracellular degradation of α-synuclein was studied. Fluorescently-labeled protein in complex with PEP-1 (α-synuclein to PEP-1 molar ratio of 1:10) was incubated with the cells for 1 h under the same conditions as described above. The complex was removed and the cells were washed and detached by trypsinization at different times Trypsinized cells were then stored at -20℃. After 18 h the samples thawed, lysed and loaded on SDS-PAGE. Standards of 0.10 and 0.010 mg/mL of fluorescently-labeled protein were loaded on the gel as a reference for α-synuclein. Attempts to determine the in-cell NMR spectrum were conducted in CHO-K1 cells.

4.2.6.2 *Cytoplasmic Transduction Peptide (CTP)*

For CTP-α-synuclein (Figure 3.1), 100 μg/mL fluorescently-labeled CTP or 75 μM ^{19}F-labeled CTP-α-synuclein were overlaid onto CHO-K1 cells. The cells

were incubated at 37 ℃ and 5% CO_2 for 20 h. Confocal microscopy images were collected and attempts to determine the in-cell NMR spectrum of α-synuclein were conducted. Delivery of fluorescently-labeled CTP α-synuclein was also tested in HeLa cells and neurons.

4.2.6.3 *Cationic Amphiphile Molecule (PULSin)*

Samples of 4 µL of 1 mg/mL fluorescently-labeled α-synuclein were used. The ratios of protein to PULSin (Polyplus-Transfection, New York, NY) tested were 1:2, 1:3, and 1:4 (v/v). The CHO-K1 cells were incubated with the protein-PULSin complex for 5 h. Studies in the presence and absence of the lysosomal proteolysis inhibitor, NH_4Cl, were conducted. After washing with PBS and cell media, the cells were imaged and lysed using the M-PER reagent (Pierce). Comparative analysis of delivered protein in the presence or absence of NH_4Cl was studied on SDS-PAGE.

4.2.6.4 *Electroporation*

Electroporation of the cells was done by using the cell line nucleofector kits - R for HeLa cells and T for CHO-K1 cells (Lonza Biologics Inc.). The AMAXA instrument used for electroporation was provided by Lonza Inc. and a specialist from their technical team came to try to translocate α-synuclein and GFP to CHO-K1 and HeLa cells. It is company policy that the instrument can be used only by their team members till it is purchased. Their procedure is highly optimized for DNA transfection but not for protein translocation into the cells. Cells seeded at 70-80% confluency were detached by trypsinization and collected by centrifugation. About 10^6 cells were used for each experiment. The

cells were mixed with 5 µL of 1 mg/mL fluorescently-labeled α-synuclein or GFP and with 100 µL nucleofector solution. Optimization as a function of current intensity and time of electroporation was tried for both cell lines and for both proteins. In all cases, the cells were not kept in the nucleofector solution longer than 15 min. The pmaxGFP gene provided by Lonza was used as a control of electroporation. All the cells were seeded in 6-well plates in their media containing serum. The samples were analyzed on the second day after incubation at 37 ℃ and 5% CO_2.

4.2.6.5 *QQ Reagent*

The QQ reagent was used to translocate α-synuclein into CHO-K1, HeLa cells, and neurons. A mixture of 10% fluorescently-labeled α-synuclein and ^{15}N α-synuclein was used. The QQ reagent and the protein modification were done in Dr. Jianjun Wang's laboratory at Wayne State University [28]. The cells were treated with the QQ modified protein at a concentration of 1 mg/mL α-synuclein.

4.2.7 Fluorescence Image Acquisition and Quantification

For cell imaging, four washing steps with PBS were performed and then the cells were imaged in their complete media using a Zeiss confocal microscope equipped with LSM 5 software with a 40x oil objective. In addition, the cells were incubated with 50 nM Mito Tracker Red CMX Ros (Invitrogen) for 15 min immediately before imaging. Fluorescence imaging was performed using multichannel detection of excitation with an argon laser (488 nm) for Alexa Fluor 488 labeled protein and a HeNe1 laser (543 nm) for Mito Tracker Red detection. For intracellular protein quantification, cells were lysed using M-PER mammalian

protein extraction reagent following the protocol. Twenty five µL of the supernatant were loaded on 10-20% gradient SDS-PAGE (BioRad) for 55 min at 200 V, and the intracellular fluorescence was quantified with a VersaDoc MP imager (BioRad). Two known concentrations of fluorescently-labeled α-synuclein were used as standards. Cells incubated under the same conditions with fluorescently-labeled α-synuclein (no carrier) were used as a negative control. Cells untreated with the peptide, protein, or the complex were lysed to test for autofluorescence.

4.2.8 In-cell NMR

In-cell NMR experiments were conducted in CHO-K1 cells. The cells were seeded at a density of ~10^6 cells in a T75 flask (Corning, Edison, NJ). The cells at 70-80% confluency were overlaid with the PEP-1/^{19}F-labeled α-synuclein complex or with ^{19}F-labeled CTP-α-synuclein as described in the section on carriers for α-synuclein delivery. For the α-synuclein/PEP-1 complex, the concentration of α-synuclein was adjusted to correspond to that for experiments performed with fluorescently-labeled protein.

For CTP α-synuclein, a concentration of 75 mg/mL was used. After successive washings with PBS and cell media, the cells were trypsinized and resuspended in 20% Ficoll containing 10% D_2O as described in Chapter 3. The cells were placed in a 5-mm diameter NMR tube. A sample of 90:10 (v/v) 20% Ficoll in cell media to D_2O was used under the same conditions as a reference for shimming, pulse-width determination, and for determination of solvent-saturation frequency. The ^{19}F spectra were acquired at 37 ℃ as described in

Chapter 3. Data were processed by using MestReNova LITE (Mestrelab Research, Escondido, CA). NMR control experiments on the supernatant obtained after cell centrifugation and on the cell lysates were performed under the same conditions.

4.2.9 Cell Viability

Cell viability after each NMR experiment was tested by using the trypan blue exclusion assay.

4.3 Results and Discussion

4.3.1 Expression and Purification of α-Synuclein Variants

All α-synuclein variants were expressed in *E. coli* and purified as described under Materials and Methods. The protein yields varied between 28 and 60 mg of pure protein per L of culture. Several long term storage conditions were tested. Lyophilization followed by storage at –80 ℃ proved to be important for avoiding degradation.

4.3.2 Alexa Fluor Labeling

Labeling α-synuclein variants with Alexa Fluor 488 C_5-maleimide dye allows intracellular visualization and quantification of the proteins. The labeled biomolecules were successfully purified from excess free dye and other components of the reaction mixture. The labeling efficiency varied between 70 and 94%.

4.3.3 PEP-1 Mediated Delivery of α-Synuclein

Confocal micrographs show that α-synuclein was successfully translocated into all the three cell lines tested – CHO-K1, HeLa, and sympathetic neurons - by using the amphipathic peptide PEP-1 as a carrier (Figure 4.3, green). Mitochondria stained with Mito Tracker Red (Invitrogen) provide information about colocalization of the protein at the mitochondria level and distribution of the protein in the cytoplasm (Figure 4.3, red). Part of the protein is in the cytosol while some of the α-synuclein is associated with mitochondria. These findings are in agreement with those of Parihar et al. [29] and Cole [30] who demonstrated the presence of α-synuclein in mitochondria and with the data presented in Chapter 2. No significant fluorescence was observed in the nucleus.

Quantification of the intracellular fluorescently-labeled α-synuclein translocated into CHO-K1 and HeLa cells (Figure 4.4) showed that the amount of intracellular protein increases with increasing the amount of α-synuclein in the complex (Figure 4.4 *A*-*D*). A protein to PEP-1 molar ratio of 1:10 was found to be the best of those tested for the delivery of high amounts of α-synuclein into cells. About 100 μM α-synuclein was present in ~$2x10^7$ cells suspended in ~600 μL of media with 20% Ficoll. No significant intracellular fluorescence was noted when only the labeled protein was incubated with CHO-K1 or HeLa cells. Also, no internal fluorescence was noted for either cell line when the same settings of the microscope were used.

Intracellular degradation of α-synuclein translocated using PEP-1 was studied in CHO-K1 cells (Figure 4.5). α-Synuclein degrades inside the cells over time (Figure 4.5, bottom). Almost all the protein degraded after 4 h of incubation

at 37 ℃ when the cells were kept in their media. No intact protein was detected after 18 h but thick bands at the bottom of the gel corresponding to the free dye were observed. Degradation was reduced when the cells were kept in media containing the lysosomal proteolysis inhibitor, NH_4Cl (Figure 4.5, top). This observation indicates that the lysosome is important for intracellular degradation of α-synuclein, perhaps playing a physiological role in removing α-synuclein from the cells or brought to lysosome during import.

In-cell NMR studies of wild-type ^{19}F-labeled α-synuclein were conducted in CHO-K1 cells. The in-cell spectrum of ^{19}F-labeled α-synuclein is presented in Figure 4.6, top. The signal to noise ratio is poor, and the spectrum of the protein can barely be distinguished. Three peaks of almost equal size can be seen. The similarity of this spectrum with that of ^{19}F-labeled α-synuclein bound to the membranes suggests that the N-terminus of the protein binds to membranes inside the cells (Figure 3.7). The peaks are present around the same chemical shift as those from the ^{19}F-labeled α-synuclein in the media containing 20% Ficoll. An alternative explanation is that, as ^{19}F-labeled α-synuclein starts degrading inside the cells, the N-terminus region is cleaved and binds to the negatively charged membranes impeding the rotation of the tyrosine at the position 39 and consequently reducing the signal corresponding to this position. NMR control experiments were performed indicating that the signal is not coming from the protein that leaks from the cells (Figure 4.6, bottom).

In-cell NMR experiments in the presence and absence of NH_4Cl were conducted (Figure 4.7). The signal to noise ratio is poor because little α-synuclein

was translocated into the cells. However, the spectrum in the presence of lysosomal proteolysis inhibitor is similar with that of wild-type ^{19}F-labeled α-synuclein in dilute conditions. Even though the peaks are broader than those of the protein in 20% Ficoll or those corresponding to the protein bound to the plasma membrane (Figure 3.7), the middle peak corresponding to positions 39 and 125 is larger in the presence of lysosomal inhibitor supporting the supposition that the N-terminus may be cleaved in the absence of NH_4Cl.

All the NMR data were collected by using the hfdiff probe. Two different probes were tested for their sensitivity using a small ^{19}F molecule, 3-fluoro-tyrosine (Figure 4.8). The HFCX probe (S/N=100.1) gives ~2 times better signal than the hfdiff probe (S/N=46.3). The in-cell NMR experiments were repeated on the HFCX probe but the results were not reproducible. Cell viability after each NMR experiment was ~90% for all the experiments.

4.3.4 Delivery of α-Synuclein into Mammalian Cells by Using CTP

The cytoplasmic transduction peptide containing the 11 amino acid insertion, YGR_2AR_6, at the N-terminus of α-synuclein (Figure 3.1) was used to target the protein to the cytoplasm of three cell lines – CHO-K1, HeLa, and primary culture neurons. The V3C CTP α-synuclein was labeled with Alexa Fluor 488 maleimide dye with a labeling efficiency of 70-78%. Upon translocation, the CTP α-synuclein is cleaved by specific cytosolic enzymes and the protein is released [30]. Confocal micrographs show intracellular localization of α-synuclein in all the three cell lines tested (Figure 4.9). Some of the protein is localized in the mitochondria as we noted for α-synuclein translocated by using PEP-1

(Figure 4.3). However, no fluorescence was present in the nucleus. The CTP α-synuclein was incubated with the cells for 20 h because CTP is efficient in translocating significant amounts of cargo into the cytosol only after long periods of incubation [30]. During this time some of the delivered protein starts to degrade. The SDS-PAGE gels show almost no protein present in cells.

In-cell NMR experiments were attempted in CHO-K1 cells. Because of the cationic nature of the CTP, the cleaved peptide is supposed to interact with the negatively charged phospholipids in the intracellular membranes. Consequently, the peptide is not free to tumble and the resonances from the NMR active nuclei present in the peptide cannot interfere with the resonances from the protein [6]. After the incubation with ^{19}F-labeled CTP α-synuclein, 2x10^7 cells were placed in a NMR tube in media containing 20% Ficoll and 10% D_2O as described in Chapter 3. No signal was detected in cells or in the cell lysates perhaps because not enough α-synuclein was delivered into the cells.

4.3.5 Translocation of α-Synuclein by Using PULSin

PULSin is a commercially available reagent that contains a proprietary cationic amphiphile [31, 32]. It facilitates delivery of anionic proteins and antibodies into the cells. Different v/v ratios of 1 mg/mL fluorescently-labeled α-synuclein and PULSin were incubated with CHO-K1 cells in the presence and absence of NH_4Cl. Intracellular fluorescence was observed in all the cases by microscopic observation. The cell micrographs were not recorded by using confocal imaging. Instead, the cells were lysed to determine if significant amounts of α-synuclein were translocated into the cells. As seen in Figure 4.10,

fluorescently-labeled α-synuclein is present only in the cells kept in media containing lysosomal proteolysis inhibitor.

My experiments using PEP-1 showed that the lysosome is important for α-synuclein degradation. The results using PULSin confirm this conclusion.

The in-cell NMR experiments with ^{19}F-labeled α-synuclein were not attempted because an insignificant amount of intracellular fluorescence was noted in cells and also because of the high cost of PULSin.

4.3.6 Electroporation

Translocation of α-synuclein into CHO-K1 and HeLa cells was assessed using electroporation. The team from Lonza assisted me with the use of the instrument. The advantage of electroporation is that the protein can be delivered to the cells and no peptide cleavage or decaging is necessary in the cytosol. This allows easy detection of the NMR signal in cells without interference from the delivery reagent. The translocation of the protein takes place through pores formed in the plasma membrane because of the electric current applied. The exposure time and intensity of the current depends on the type of cells and the amount of protein to be translocated. In our case, the disadvantages of electroporation are the large amount of α-synuclein needed and the low cell viability that results from applying the current.

Fluorescently-labeled α-synuclein was translocated into CHO-K1 and HeLa cells and the cells were allowed to recover in their media for ~24 h after which they were imaged. No fluorescent SDS-PAGE band corresponding to α-synuclein was noted after almost 24 h. Instead, the presence of various bands of

different intensities at the bottom of the gel indicates that the α-synuclein was degraded and only the free dye remained (Figure 4.11). Fluorescence was noted in all the cells and for all the conditions tested. As a general trend, more fluorescence was present but fewer cells were observed by increasing the current. This trend was noted on SDS-PAGE, too. The parameters and the programs used for translocation were optimized at Lonza, but the information was not disclosed. Delivery of GFP by using electroporation was tried in the same cell lines but the experiments were not successful perhaps because of the high molecular weight of GFP (~27 kDa) as compared to α-synuclein (~14 kDa). The vector containing the GFP gene was used as control for electroporation and the cells became fluorescent the second day indicating that GFP was expressed in the cells as a result of gene translocation.

4.3.7 QQ Reagent as a Carrier

QQ reagent is a proprietary mixture of components and the sample containing our protein of interest was prepared in Dr. Wang's laboratory at Wayne State University [28]. A mixture of 10% fluorescently-labeled and 90% ^{15}N-enriched α-synuclein was used. The translocation of α-synuclein was tried in CHO-K1, HeLa, and primary culture neurons. As seen in Figure 4.12 no significant fluorescence is present inside the cells. Instead, most of the protein appears to be on top or surrounding the cells. In our case, QQ reagent is not an appropriate reagent for the delivery of α-synuclein to the cells.

4.4 Conclusion

Protein function may be affected as a result of intracellular macromolecular crowding or upon binding to different cellular components. Understanding the intracellular factors that play a role in the protein's behavior are important for studying intracellular protein-protein interactions, protein-drug interactions, protein diffusion and stability. α-Synuclein was successfully translocated into the cytoplasm of CHO-K1, HeLa, and primary culture neurons by using two peptides (PEP-1 and CTP) as carriers, electroporation, and the PULSin reagent. The amount of translocated protein increases with increasing protein concentration in the PEP-1/α-synuclein complex for CHO-K1 and HeLa cells. CTP, electroporation and PULSin successfully translocated α-synuclein into CHO-K1 and HeLa cells but either the protein was degraded during time or not enough α-synuclein was present in cells to conduct in-cell NMR experiments. Some of the protein is localized in the mitochondria with more mitochondrial localization in sympathetic neurons. In-cell NMR experiments performed on cells with protein translocated by using PEP-1, reveal that the protein was delivered to the cells but not in high enough amounts to be able to record an acceptable spectrum.

4.5 Future Directions

Significant amounts of α-synuclein have to be delivered into the cells for the protein to be detected using NMR. For the PEP-1/α-synuclein complex, one way to improve the translocation would be to repeat the procedure up to four times allowing the cells to recover in their media between treatments.

For CTP-α-synuclein, the aforementioned procedures can also improve protein translocation. In addition, treatment of the cells with pyrenebutyrate prior to their treatment with CTP should increase the α-synuclein concentration. Pyrenebutyrate creates pores in the plasma membranes allowing the protein to pass into the cytoplasm. Similar findings were reported for the translocation of cationic peptides [6, 33, 34].

Electroporation is another technique capable of delivering proteins inside the cells. The electroporation time and the intensity of the current are specific for each protein and require optimization. For that, it is more convenient to have the electroporator in the laboratory to be able to perform those trials.

For all the delivery systems used, it is important to mention as a limitation the high cost of the reagents or peptide used necessary to conduct in-cell NMR experiments. High number of cells containing important quantities of translocated protein is needed because of the low sensitivity of NMR.

Another relevant aspect is studying and understanding the interactions and intracellular behavior of α-synuclein variants, A30P and A53T, which may reveal important information about Parkinson's disease.

4.6 Figures

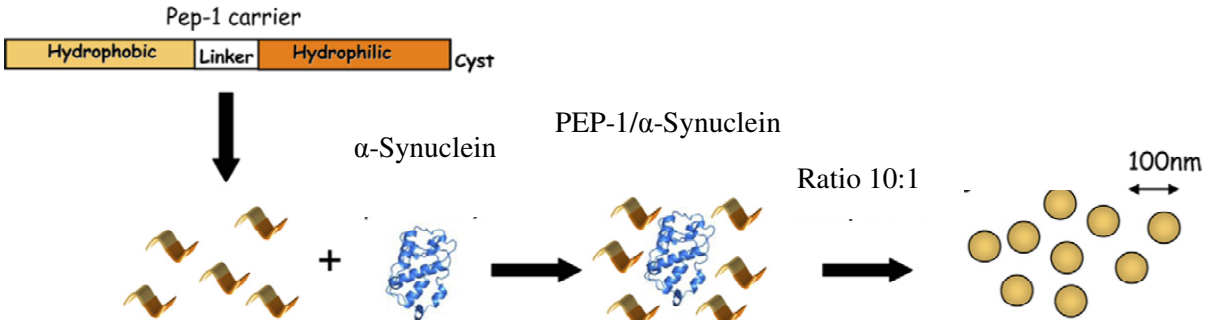

Adapted from M.A. Munoz-Morris et al. [16]

Figure 4.1 Schematic representation of the PEP-1/α-synuclein complex

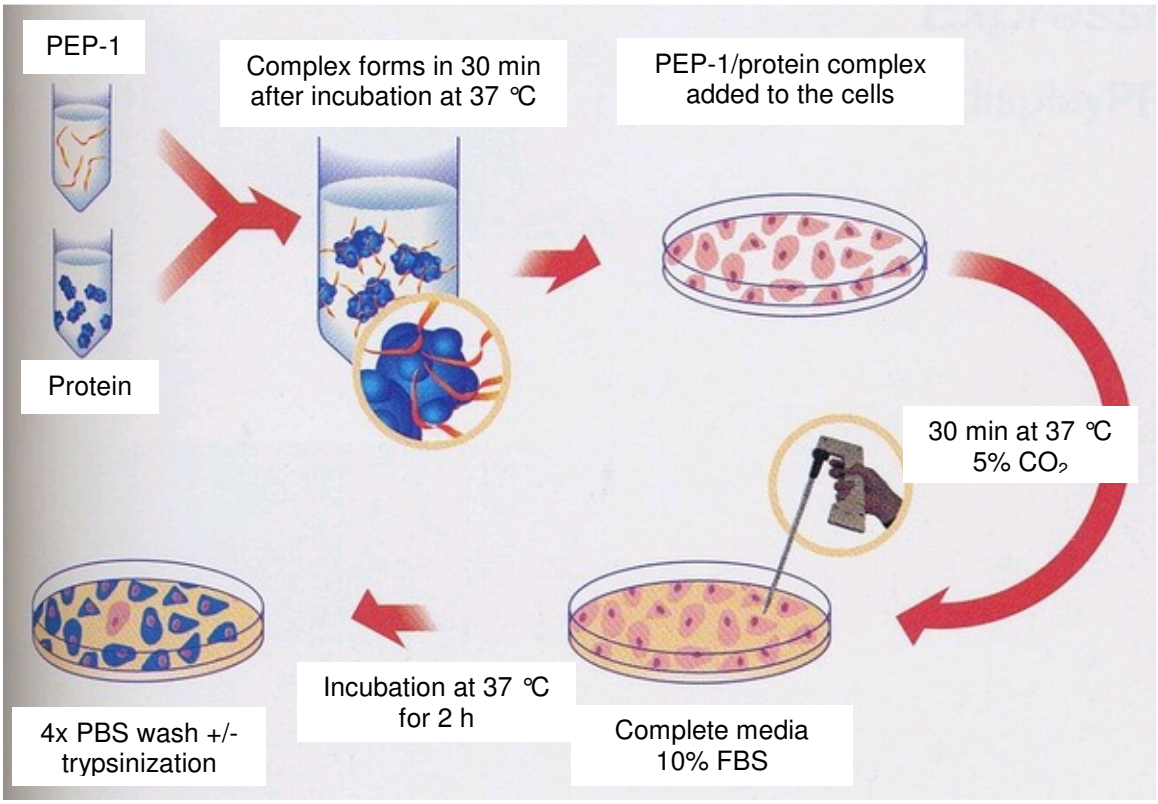

Adapted from: http://www.activemotif.com/documents/82.pdf

Figure 4.2 Schematic representation of α-synuclein translocation into higher eukaryotic cells using the PEP-1 peptide as a carrier

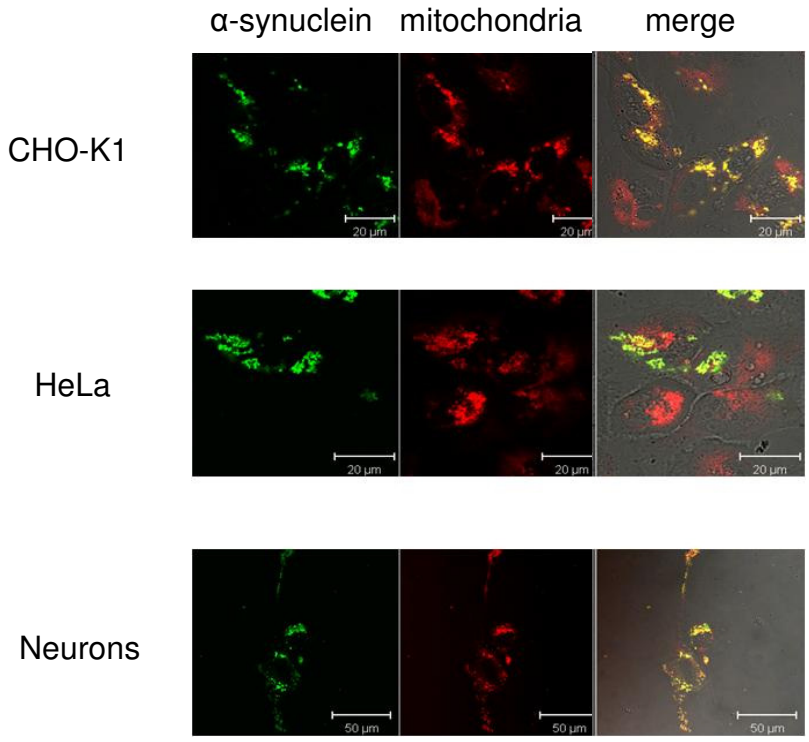

Figure 4.3 Translocation of CTP-α-synuclein into cells

Intracellular localization of α-synuclein after incubation of cells with fluorescently-labeled α-synuclein/PEP-1 complex at 37 ℃ for 2 h. The cells were also incubated with 50 nM Mitotraker Red at 37 ℃ for 15 min before imaging.

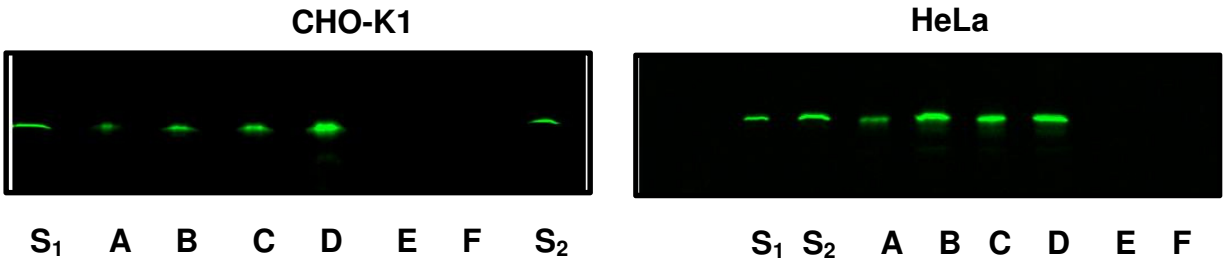

Figure 4.4 Cell lysates after translocation of PEP-1/α-synuclein complex

SDS-PAGE of cell lysates after translocation of fluoerescently-labeled α-synuclein into CHO-K1 and HeLa cell lines. Lanes A, B, C, and D represent protein to PEP-1 molar ratios of 1:40, 1:20, 1:15, and 1:10, respectively, S1 and S2 are standards (0.10 and 0.010 mg/mL, respectively) fluorescently-labeled α-synuclein, E cell lysates after translocation of fluorescently-labeled α-synuclein without PEP-1. F cells alone, to check for autofluorescence.

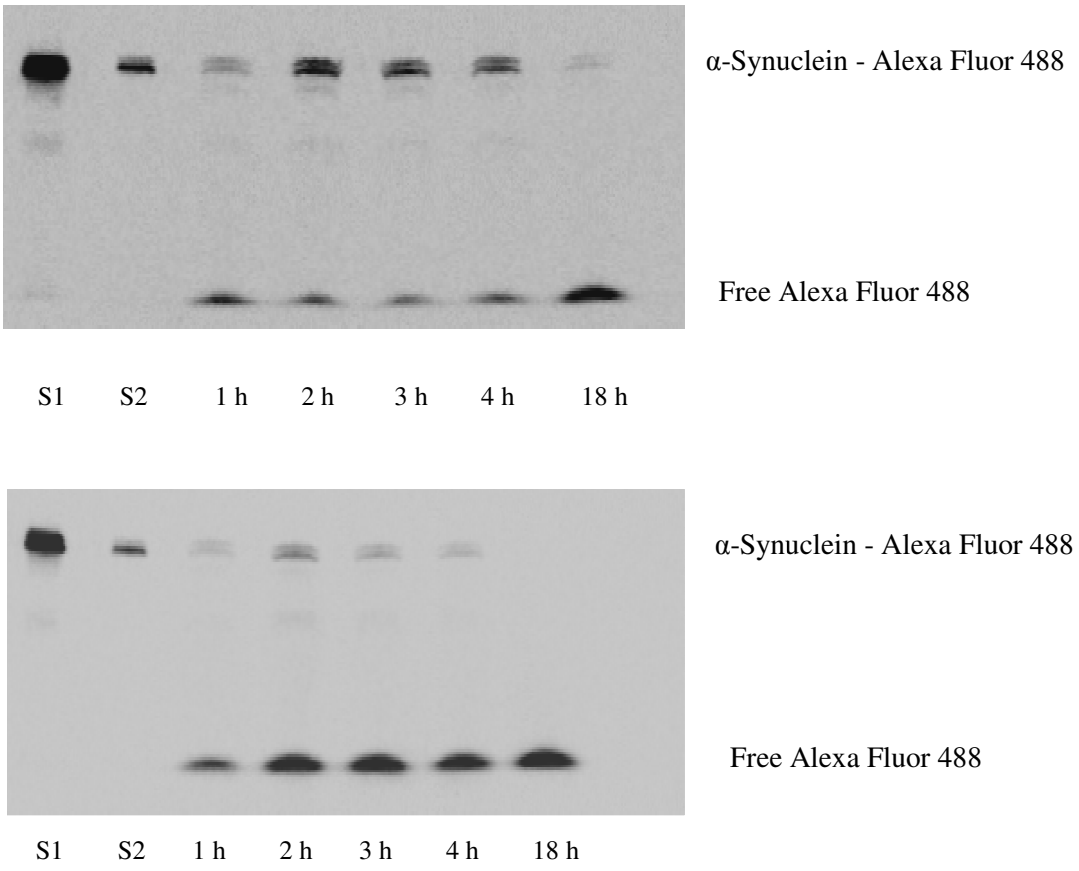

Figure 4.5 Intracellular degradation of α-synuclein

SDS-PAGE of cell lysates shows intracellular degradation of fluorescently-labeled α-synuclein after incubation of CHO-K1 cells for different times in the presence (top) or absence (bottom) of NH_4Cl. S_1 and S_2 are standards of 0.10 and 0.010 mg/mL, respectively.

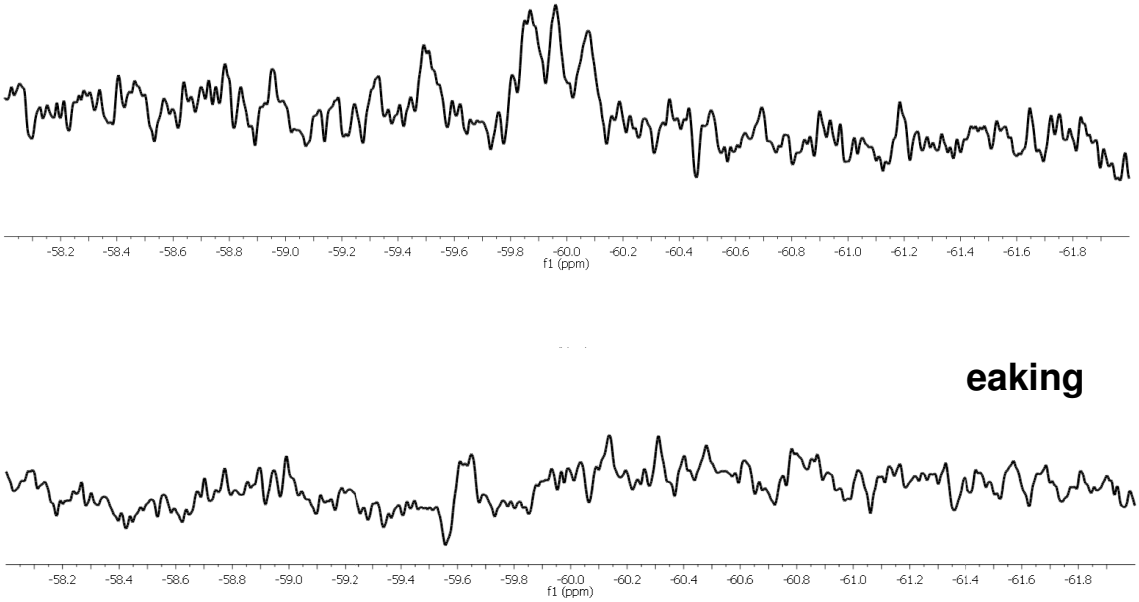

Figure 4.6 In-cell NMR of wild-type α-synuclein

CHO-K1 cells (top) and the supernatant after the experiment (bottom).

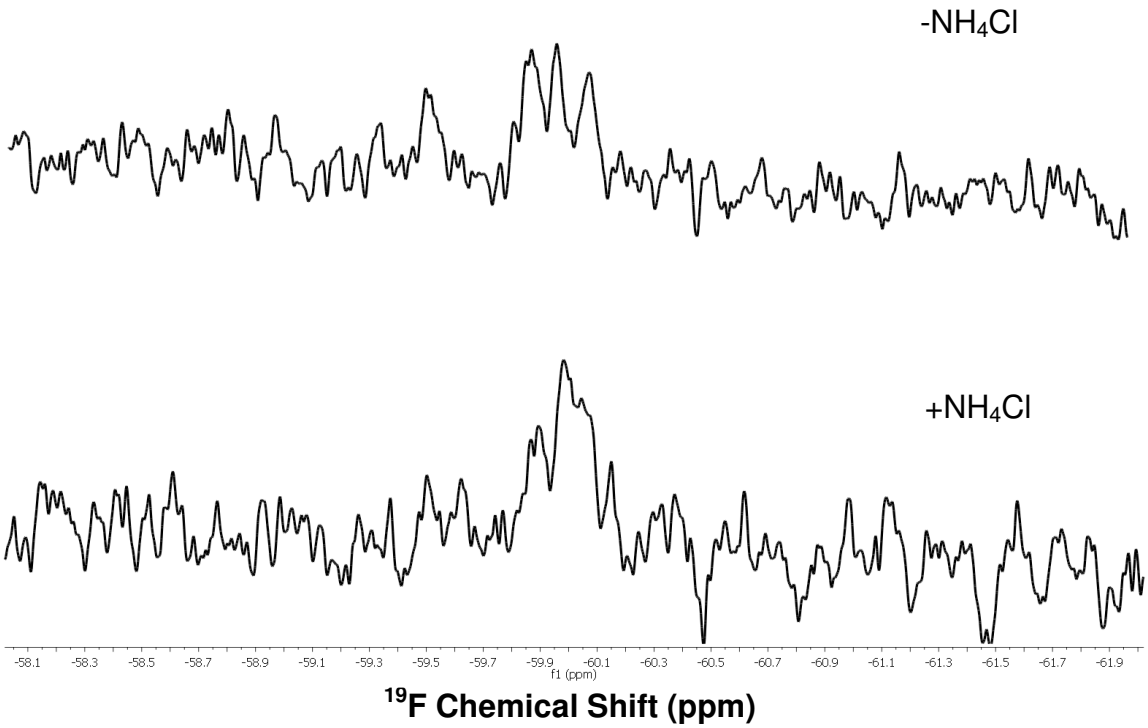

Figure 4.7 In-cell NMR of wild-type α-synuclein with and without NH_4Cl

CHO-K1 cells without (top) and with (bottom) the lysosomal proteolysis inhibitor, NH_4Cl.

NMR Probe: HFCX

S/N = 100.1

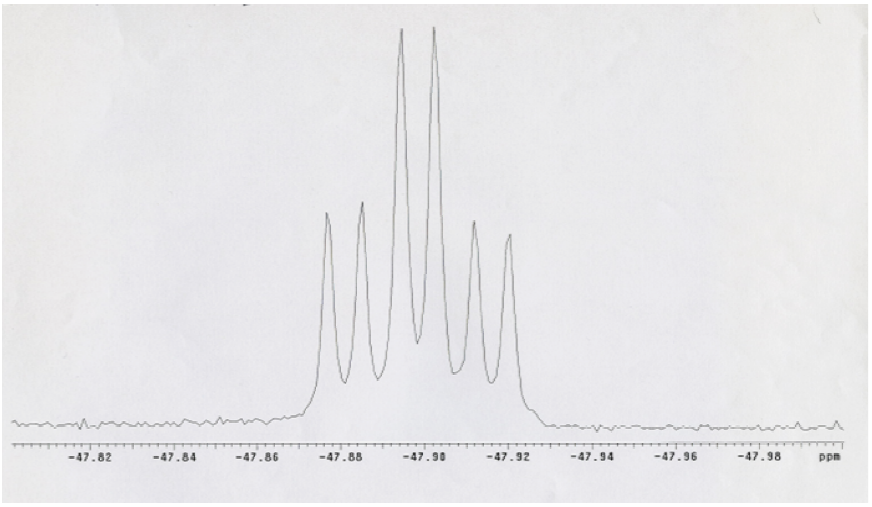

NMR Probe: hfdiff

S/N = 46.3

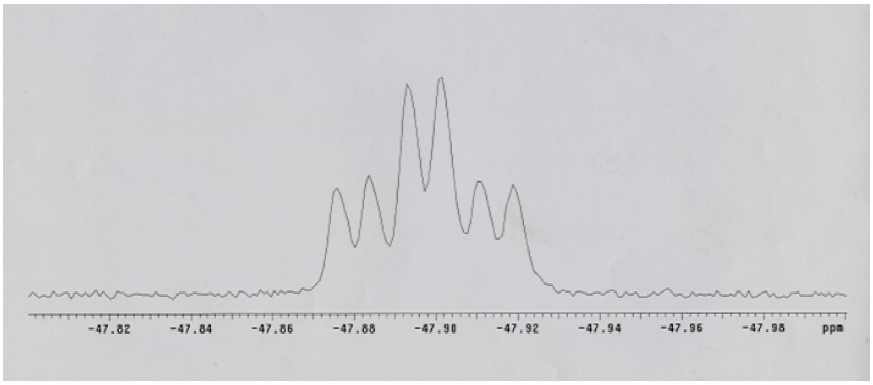

Figure 4.8 The sensitivity of two NMR probes tested using 3-fluoro-L-tyrosine

The HFCX (top) has better sensitivity than the hfdiff (bottom).

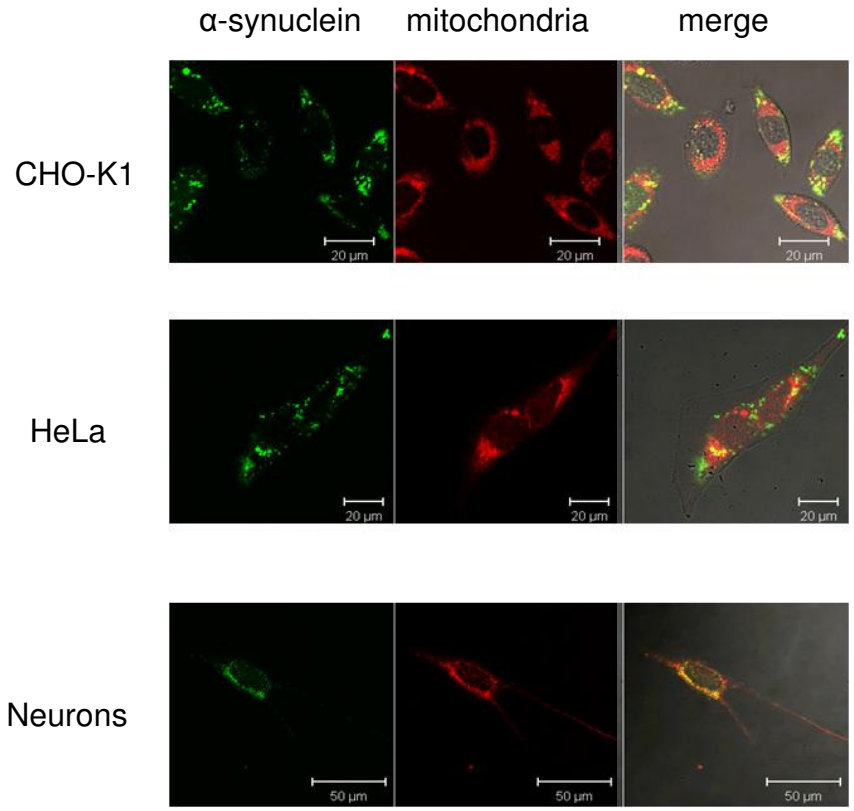

Figure 4.9 Translocation of CTP-α-synuclein into cells

Intracellular localization of α-synuclein after incubation of the cells with fluorescently-labeled CTP α- synuclein at 37 ℃ for 20 h. The cells were also incubated with 50 nM Mitotraker Red at 37 ℃ for 15 min before imaging.

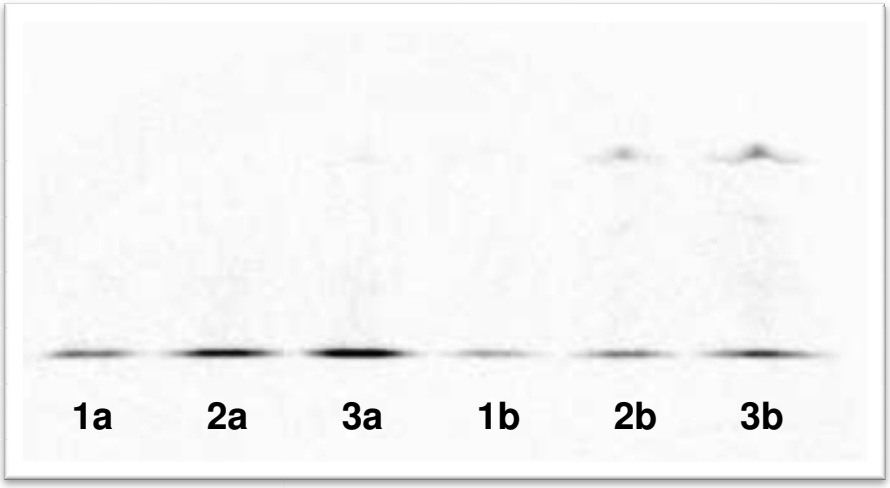

Figure 4.10 SDS-PAGE of cell lysates containing PULS-in/ α-synuclein with and without NH_4Cl

SDS-PAGE of CHO-K1 cells after incubation of fluorescently-labeled α-synuclein with PULSin for 5h at 37 ℃. For lanes 1, 2, and 3 the following volumes of reagent were used: 8, 12, and 16 µL, corresponding to 3, 4, and 6 µg protein. For lanes "a" no NH_4Cl was used and for lanes "b" 25 mM NH_4Cl was present in the cells media.

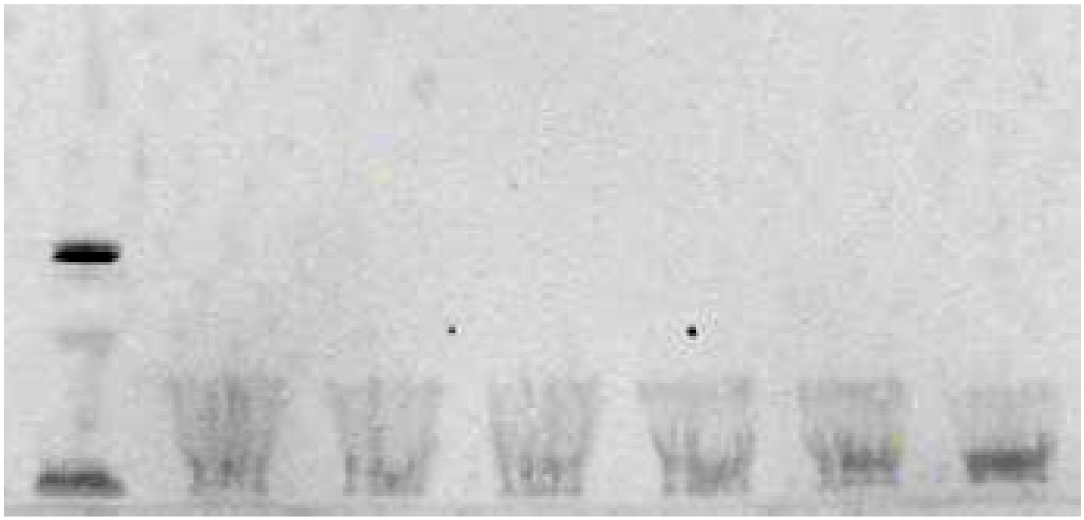

Figure 4.11 SDS-PAGE of cell lysates after translocation of α-synuclein into CHO-K1 cells by electroporation

The first column is the fluorescently-labeled protein without the cells. Program # 1-6 represents different conditions for electroporation time and intensity. The experimental conditions were not disclosed by Lonza, the company that provided as the instrument.

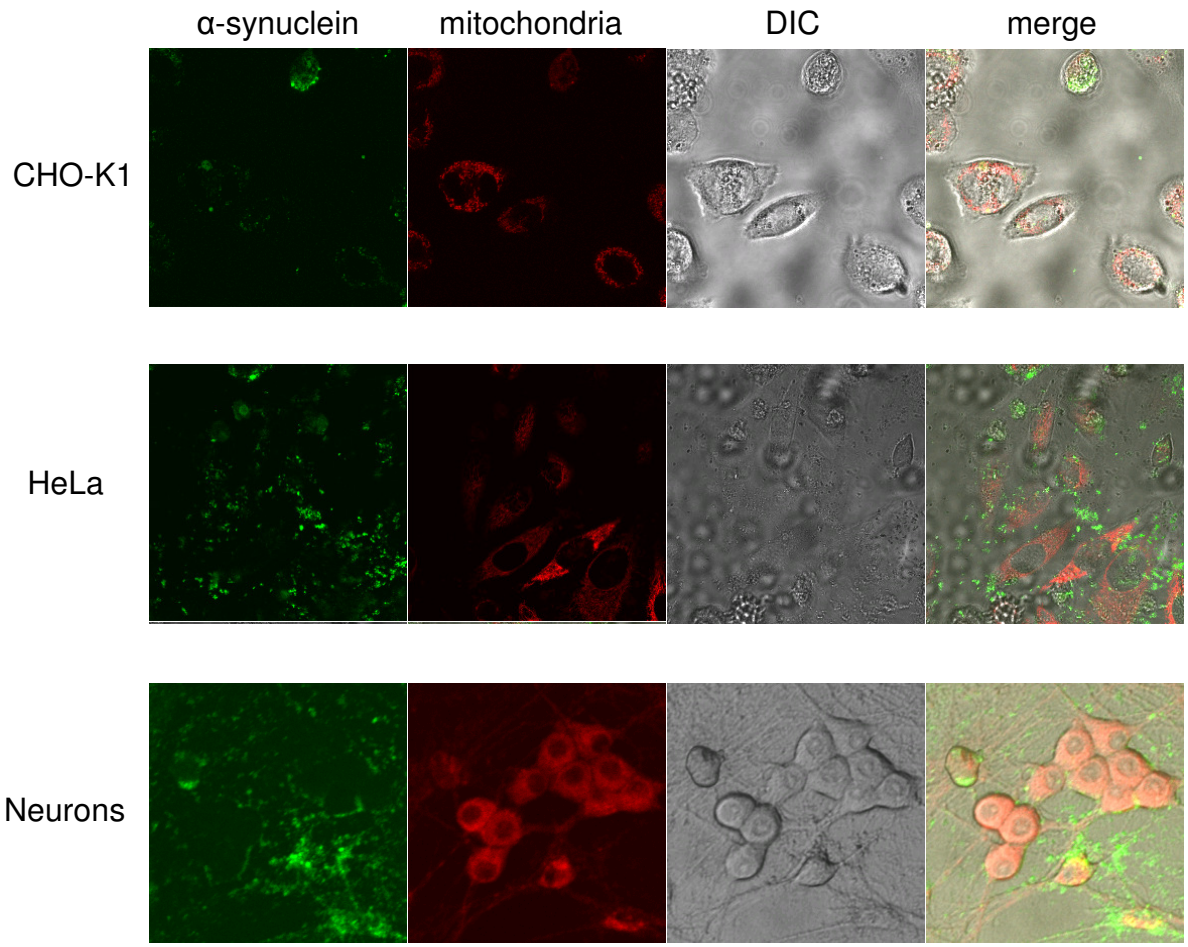

Figure 4.12 Distribution of QQ modified α-synuclein upon interaction with the cells

Distribution of α-synuclein after incubation of the cells with QQ modified protein at 37 ℃ for 3 h. The sample contains 10% fluorescently-labeled α-synuclein and 90% ^{15}N-enriched wild-type α-synuclein. The cells were also incubated with 50 nM Mitotraker Red at 37 ℃ for 15 min before imaging. DIC - differential interference contrast microscopy.

4.7 References

1. C. Li, L.M. Charlton, A. Lakkavaram, C. Seagle, G. Wang, G.B. Young, J.M. Macdonald, G.J. Pielak, Differential dynamical effects of macromolecular crowding on an intrinsically disordered protein and a globular protein: implications for in-cell NMR spectroscopy, Journal of the American chemical society 130 (2008) 6310-6311.

2. B.C. McNulty, A. Tripathy, G.B. Young, L.M. Charlton, J. Orans, G.J. Pielak, Temperature-induced reversible conformational change in the first 100 residues of alpha-synuclein, Protein science 15 (2006) 602-608.

3. M.M. Dedmon, C.N. Patel, G.B. Young, G.J. Pielak, FlgM gains structure in living cells, Proceedings of the national academy of sciences of USA 99 (2002) 12681-12684.

4. B.C. McNulty, G.B. Young, G.J. Pielak, Macromolecular crowding in the *Escherichia coli* periplasm maintains alpha-synuclein disorder, Journal of molecular biology 355 (2006) 893-897.

5. P. Selenko, Z. Serber, B. Gadea, J. Ruderman, G. Wagner, Quantitative NMR analysis of the protein G B1 domain in *Xenopus laevis* egg extracts and intact oocytes, Proceedings of the national academy of sciences of USA 103 (2006) 11904-11909.

6. K. Inomata, A. Ohno, H. Tochio, S. Isogai, T. Tenno, I. Nakase, T. Takeuchi, S. Futaki, Y. Ito, H. Hiroaki, M. Shirakawa, High-resolution multi-dimensional NMR spectroscopy of proteins in human cells, Nature 458 (2009) 106-109.

7. K. Luby-Phelps, Cytoarchitecture and physical properties of cytoplasm: Volume, viscosity. diffusion, intracellular surface area, International Review of cytology - a survey of cell biology, 192 (2000) 189-221.

8. K.M. Wagstaff, D.A. Jans, Protein transduction: cell penetrating peptides and their therapeutic applications, Current medicinal chemistry 13 (2006) 1371-1387.

9. D. Kim, C. Jeon, J.H. Kim, M.S. Kim, C.H. Yoon, I.S. Choi, S.H. Kim, Y.S. Bae, Cytoplasmic transduction peptide (CTP): new approach for the delivery of biomolecules into cytoplasm *in vitro* and *in vivo*, Experimental cell research 312 (2006) 1277-1288.

10. G.P. Dietz, M. Bahr, Delivery of bioactive molecules into the cell: the Trojan horse approach, Molecular and cellular neurosciences 27 (2004) 85-131.

11. H.S. Choi, S.H. Lee, S.Y. Kim, J.J. An, S.I. Hwang, D.W. Kim, K.Y. Yoo, M.H. Won, T.C. Kang, H.J. Kwon, J.H. Kang, S.W. Cho, O.S. Kwon, J.H. Choi, J. Park, W.S. Eum, S.Y. Choi, Transduced Tat-alpha-synuclein protects against oxidative stress *in vitro* and *in vivo*, Journal of biochemistry and molecular biology 39 (2006) 253-262.

12. D. Albani, E. Peverelli, R. Rametta, S. Batelli, L. Veschini, A. Negro, G. Forloni, Protective effect of TAT-delivered alpha-synuclein: relevance of the C-terminal domain and involvement of HSP70, FASEB journal 18 (2004) 1713-1715.

13. S. Deshayes, M.C. Morris, G. Divita, F. Heitz, Cell-penetrating peptides: tools for intracellular delivery of therapeutics, Cellular and molecular life sciences 62 (2005) 1839-1849.

14. H.S. Choi, J.J. An, S.Y. Kim, S.H. Lee, D.W. Kim, K.Y. Yoo, M.H. Won, T.C. Kang, H.J. Kwon, J.H. Kang, S.W. Cho, O.S. Kwon, J. Park, W.S. Eum, S.Y. Choi, PEP-1-SOD fusion protein efficiently protects against paraquat-induced dopaminergic neuron damage in a Parkinson disease mouse model, Free radical biology & medicine 41 (2006) 1058-1068.

15. M.C. Morris, J. Depollier, J. Mery, F. Heitz, G. Divita, A peptide carrier for the delivery of biologically active proteins into mammalian cells, Nature biotechnology 19 (2001) 1173-1176.

16. M.A. Munoz-Morris, F. Heitz, G. Divita, M.C. Morris, The peptide carrier Pep-1 forms biologically efficient nanoparticle complexes, Biochemical and biophysical research communication 355 (2007) 877-882.

17. S.T. Henriques, J. Costa, M.A. Castanho, Translocation of beta-galactosidase mediated by the cell-penetrating peptide pep-1 into lipid vesicles and human HeLa cells is driven by membrane electrostatic potential, Biochemistry 44 (2005) 10189-10198.

18. S. Deshayes, A. Heitz, M.C. Morris, P. Charnet, G. Divita, F. Heitz, Insight into the mechanism of internalization of the cell-penetrating carrier peptide Pep-1 through conformational analysis, Biochemistry 43 (2004) 1449-1457.

19. J.J. An, Y.P. Lee, S.Y. Kim, S.H. Lee, M.J. Lee, M.S. Jeong, D.W. Kim, S.H. Jang, K.Y. Yoo, M.H. Won, T.C. Kang, O.S. Kwon, S.W. Cho, K.S. Lee, J. Park, W.S. Eum, S.Y. Choi, Transduced human PEP-1-heat shock protein 27 efficiently protects against brain ischemic insult, The FEBS journal 275 (2008) 1296-1308.

20. S.S. Bale, S.J. Kwon, D.A. Shah, A. Banerjee, J.S. Dordick, R.S. Kane, Nanoparticle-mediated cytoplasmic delivery of proteins to target cellular machinery, ACS nano 4 (2010) 1493-1500.

21. Y. Liu, H. Wang, K. Kamei, M. Yan, K.J. Chen, Q. Yuan, L. Shi, Y. Lu, H.R. Tseng, Delivery of intact transcription factor by using self-assembled supramolecular nanoparticles, Angewandte chemie 50 (2011) 3058-3062.

22. J. Wang, S. Tian, R.A. Petros, M.E. Napier, J.M. Desimone, The complex role of multivalency in nanoparticles targeting the transferrin receptor for cancer therapies, Journal of the American chemical society 132 11306-11313.

23. S. Martins, B. Sarmento, D.C. Ferreira, E.B. Souto, Lipid-based colloidal carriers for peptide and protein delivery--liposomes versus lipid nanoparticles, International journal of nanomedicine 2 (2007) 595-607.

24. S. Meyenburg, H. Lilie, S. Panzner, R. Rudolph, Fibrin encapsulated liposomes as protein delivery system. Studies on the in vitro release behavior, Journal of control release 69 (2000) 159-168.

25. S. Baron, J. Poast, D. Rizzo, E. McFarland, E. Kieff, Electroporation of antibodies, DNA, and other macromolecules into cells: a highly efficient method, Journal of immunological methods 242 (2000) 115-126.

26. A.A. Deora, F. Diaz, R. Schreiner, E. Rodriguez-Boulan, Efficient electroporation of DNA and protein into confluent and differentiated epithelial cells in culture, Traffic 8 (2007) 1304-1312.

27. M. Deshmukh, E.M. Johnson, Jr., Evidence of a novel event during neuronal death: development of competence-to-die in response to cytoplasmic cytochrome c, Neuron 21 (1998) 695-705.

28. Q. Li, Y. Huang, N. Xiao, V. Murray, J. Chen, J. Wang, Real time investigation of protein folding, structure, and dynamics in living cells, Methods in cell biology 90 (2008) 287-325.

29. M.S. Parihar, A. Parihar, M. Fujita, M. Hashimoto, P. Ghafourifar, Mitochondrial association of alpha-synuclein causes oxidative stress, Cellular and molecular life sciences 65 (2008) 1272-1284.

30. N.B. Cole, D. Dieuliis, P. Leo, D.C. Mitchell, R.L. Nussbaum, Mitochondrial translocation of alpha-synuclein is promoted by intracellular acidification, Experimental cellular research 314 (2008) 2076-2089.

31. C.O. Weill, S. Biri, A. Adib, P. Erbacher, A practical approach for intracellular protein delivery, Cytotechnology 56 (2008) 41-48.

32. C.O. Weill, S. Biri, P. Erbacher, Cationic lipid-mediated intracellular delivery of antibodies into live cells, BioTechniques 44 (2008) Pvii-Pxi.

33. A.R. Nelson, L. Borland, N.L. Allbritton, C.E. Sims, Myristoyl-based transport of peptides into living cells, Biochemistry 46 (2007) 14771-14781.

34. T. Takeuchi, M. Kosuge, A. Tadokoro, Y. Sugiura, M. Nishi, M. Kawata, N. Sakai, S. Matile, S. Futaki, Direct and rapid cytosolic delivery using cell-penetrating peptides mediated by pyrenebutyrate, ACS chemical biology 1 (2006) 299-303.